SKI Report 98:27

IGSCC Crack Propagation Rate Measurement in BWR Environments

Executive Summary of a Round Robin Study

Peter L. Andresen

ISSN 1104-1374
ISRN SKI-R--98/27--SE

SKI
STATENS KÄRNKRAFTINSPEKTION
Swedish Nuclear Power Inspectorate

SKI Report 98:27

IGSCC Crack Propagation Rate Measurement in BWR Environments

Executive Summary of a Round Robin Study

Peter L. Andresen

GE Corporate Research and Development
P O Box 8, Schenectady, NY 12301, USA

SKI Project Number 95118

Summary

Five of the world's best laboratories at performing stress corrosion crack growth studies – ABB Atom AB, AEA Technology, GE Corporate Research & Development Center, Studsvik Material AB, and VTT Manufacturing Technology – were selected to participate in a round robin to evaluate the quality and reproducibility of testing conditions and resulting stress corrosion crack growth rates in sensitized type 304 stainless steel in 288 °C water. The test specifications were designed to make the material, test conditions and test procedures as identical as possible. Heat treated, machined and fatigue pre-cracked specimens were provided to all laboratories, and detailed test procedures prescribed the use of active loading, reversed dc potential drop crack monitoring, a common reference electrode supplied to all laboratories by GE CRD (to be used along side each laboratory's own reference electrode), and highly specified water chemistry conditions. A companion task performed by GE CRD involved direct evaluation of all reference electrodes to permit detailed comparison of their response under identical geometrical placement, thermal, and water chemistry conditions.

The ability of each laboratory to achieve optimal testing conditions varied (e.g., temperature and load stability, resolution of dc potential drop crack monitoring, purity of the autoclave outlet water, etc.), although all laboratories achieved an impressive standard of testing control. The most significant laboratory-to-laboratory differences were associated with their ability to achieve high purity autoclave outlet water, reproduce accurate measurements of corrosion potential on the test specimen, and provide high resolution crack following using reversed dc potential drop.

However, the most notable outcome of the program is the consistent observation by all laboratories that initiating and sustaining stress corrosion crack growth at constant load in sensitized type 304 stainless steel is difficult, despite the use of a moderately high stress intensity (30 MPa$\sqrt{m}$, higher in some instances), and high dissolved oxygen (up to 2000 ppb O_2) and corrosion potential (up to $\approx$ +200 mV_{she}) conditions. Concerns for specimen machining and pre-cracking were identified, although these factors were not the sole cause of difficulty in initiating and sustaining stress corrosion cracking. It was shown that many phases of specimen preparation and testing can have a large influence on the measured SCC response. Even under the best test conditions it is critical to ensure that a complete transition is made from the transgranular fatigue pre-crack to an intergranular stress corrosion crack. Retarded or completely stalled crack growth was best addressed by imposing very gentle unloading cycles to re-initiate and sustain crack growth. When sufficiently gentle, unloading cycles play a critical role in sustaining reproducible crack advance without greatly biasing the observed growth rate. They also aid in maintaining a straight crack front, which is important to ensure a uniform stress intensity along the crack front and ensure crack length accuracy when using dc potential drop.

While comparatively little of the total testing time successfully produced meaningful crack growth rates, the data exhibit the expected high crack growth rates in high dissolved oxygen environments. This is an important conclusion, as U.S. industry efforts have shown that a remarkably different growth rate is predicted based on statistical analyses of a broader collection of scattered crack growth rate data in sensitized type 304 stainless steel. The scatter in the data clearly dilutes all trends in SCC response, as the correlation, e.g., with corrosion potential (all other effects normalized in the correlation model) is quite weak ($R^2 < 0.1$) – in addition to the dependence on crack growth being shallow. The origin of the weak correlation, shallow dependence, and poor agreement with other sets of well-controlled data is a myriad of experimental and interpretational complexities and flaws, so that the mean of such data is the mean of the flaws, not the mean of the true SCC response. The complexities and flaws include a combination of testing issues and the occasional tendency for stress corrosion cracking to retard for a variety of artificial (e.g., from minor test perturbations) and real reasons. Substantial improvements in testing procedures, diligence in initiating and sustaining stress corrosion cracking, and careful interpretation of existing data are essential.

In focusing on a single stress intensity and high dissolved oxygen / corrosion potential conditions, this program obviously does not address the broad range of important stress corrosion cracking dependencies on stress intensity, corrosion potential, aqueous impurities, temperature, degree of sensitization, irradiation, material type, etc. However, it invaluably elucidates the complexities involved in generating and interpreting stress corrosion cracking data. It also underscores the crucial overall role of developing a fundamental understanding of SCC and a recognition of the common elements or "linkages" among SCC susceptible materials. These are necessary because of the sophistication required to generate high quality SCC data, and the number and complexity of the interactions among important variables.

Table of contents

Introduction and program objectives

Stress corrosion cracking of light water reactor structural materials has occurred throughout the four-decade history of their operation. Perhaps the most important early example is stress corrosion cracking of sensitized type 304 stainless steel in welded components, a problem that persists to this day. While SCC has enveloped a much broader array of materials and conditions – including nickel alloys and weld metals, low alloy steels, and irradiated materials – the importance of SCC in stainless steels has led to the development of the largest body of crack growth rate data of any of these materials.

Despite a three-decade emphasis on measurement of stress corrosion crack growth rates, the available data show a remarkably high degree of scatter and inconsistency, extending, e.g., over about a 1000X range under similar test conditions. As the origins of this scatter have been examined more closely, many concerns have arisen over experimental technique, quality and stability of test conditions, measurement of critical parameters like corrosion potential, procedures for pre-cracking and transitioning to stress corrosion cracking, proper calculation / interpretation of crack growth rates from measured data, etc.

The primary objective of this Round Robin program was to evaluate the state-of-the-art in experimental measurement of stress corrosion crack growth rates using the most highly qualified laboratories, ubiquitous material, and standardized test conditions. As described in detail in subsequent sections, the Round Robin specified conditions that were as identical as possible, including supplying the laboratories with specimens that were heat treated, machined, and pre-cracked in the same manner, and with a common reference electrode so that the quality and reference potential of the electrode could be separated from the positioning and measurement techniques employed by each laboratory. The specific test conditions and procedures were chosen to be realistic while also enhancing the likelihood of achieving reproducible crack growth rates by using relatively high dissolved oxygen concentrations that produce high corrosion potentials and stress corrosion crack growth rates.

Material, test procedures and controls

Test protocol specified in the RFP

The type 304 stainless steel specimens were prepared under a separate contract and supplied to all laboratories. The material was solution annealed at 1050 °C for 30 minutes, water quenched, then sensitized at 621 °C for 24 hours. All specimens were taken from the same heat and block of material, whose ladle (KTH check) composition is listed below.

Table 1 – Composition of Type 304 Stainless Steel (Wt. %)

Element	Cr	Ni	C	Mn	Mo	Si	Cu
Ladle	17.80	9.40	0.048	1.80	0.43	0.26	0.19
Analysis	17.99	9.26	0.048& 0.042	1.82	0.77	0.23	0.18
Element	Co	N	P	S	V	Nb	Al
Ladle	0.11	0.065	0.033	0.005	0.09	0.060	0.002
Analysis	0.22	--	0.030	0.005	0.11	0.05	0.003

The measurement of EPR was performed by VTT and reported as $I_r/I_a = 5.7\%$ and $P_a = 2.7$. The ASTM grain size was 2.5. The specimen was a standard 25 mm CT specimen with hemispherical side grooves of 5% of thickness on each side. The following test protocol was specified in the Request For Proposal:

Comparative Study Of Reference Electrodes.
The purpose of this test is to study discrepancies in corrosion potential measurements between several laboratories in order to either eliminate or calibrate the differences. Toward this end, all laboratories shall operate their test loop with their usual electrodes and with a standard electrode which will be supplied and used by all labs. In addition, a separate study by GE CRD will simultaneously monitor multiple reference electrodes supplied by each laboratory in high purity water under both oxygenated and deaerated conditions.

General test conditions – issues and comparisons

Most critical issues and concerns were anticipated in the design of this program, which identified precise requirements regarding techniques and conditions for stress corrosion crack growth rate testing, as summarized previously. When viewed from an historical perspective, all laboratories were successful in meeting a high testing standard, achieving a level of testing control and experimental quality commensurate with their selection as participants in this program.

However, in several areas there were notable differences in the ability of specific laboratories to achieve the best possible test conditions and stability, crack length resolution, corrosion potential measurement, etc. This section highlights the common strengths and occasional difficulties experienced in achieving optimal test controls and capabilities, and discusses the repercussions of such differences. A summary of the issues that arose during stress corrosion testing – including specimen machining, pre-cracking, accomplishing the transition to intergranular cracking, difficulties in achieving and sustaining crack growth at constant load, etc. are discussed in the section on stress corrosion crack growth results.

General Test Controls and Stability.

The parameters addressed in this section include test temperature, water pressure, and applied loading, all of which should be well defined and stable vs. time from "natural" fluctuations (stability of controllers, variations in room temperature, etc.) and "upset" conditions (e.g., problems with continuity of ac power, cooling water, etc.).

In most systems, the pressurization of water necessary to maintain it as liquid at elevated temperatures directly translates, by its action on the loading linkage, to a tare load on the specimen. Thus, the drift vs. time and the ≈ 1 Hz pulsation from the high pressure pump affect the loads applied to the specimen. The effect of pressure fluctuations is directly related to the size of the loading linkage that passes through the autoclave pressure seal. For a 19.05 mm diameter bar, a typical operating pressure of 10.3 MPa (1500 psi) produces 2950 N (663 pounds) load on the specimen. There is no evidence that any of the laboratories had problems in the latter area, as all use pulse dampeners to minimize this type of pressure surge.

Table 2 – Estimated Pressure Fluctuation During SCC Testing Peak-to-Peak Variation in MPa (psi)

	Short Term Fluctuation	Long Term Fluctuation
ABB	*not reported*	*not reported*
AEA Tech	0.18 (26)	0.18 (26)
GE CRD	0.14 (20)	0.14 (20)
Studsvik*	0.05 - 0.08 (7 - 12)	0.15 - 0.5 (22 - 73)*
VTT	0.15 (22)	2.5 (365)

* The control software corrects for long term drift in pressure

Similar concerns exist for the testing machine, which can impose undesired load fluctuations from thermal effects on the load cell, electronic noise, instabilities in the closed loop control system, and complete unloading (or overloading) when power spikes or outages occur. Most laboratories used servo-hydraulic testing machines, which have the advantage of being capable of fast response, e.g., for fatigue loading at 5 - 20 Hz. They are

prone to greater noise as well as susceptible to rapid unloading or overloading with power spikes or outages. However, the experience of most labs was reasonably good with servohydraulic testing machines, although almost every laboratory reported a problem with unexpected unloading which often caused a significant change in crack growth rate (e.g., see the Studsvik Test #2, Figure B.2.9 at 3250 hours, "Event" 0.48). Servo-electric testing machines, used in two tests at GE CRD, are less noisy and will maintain load following a power spike or outage; however, they are limited to ≈ 1 Hz operation, and during extended power outages, thermal contraction as the autoclave cools can cause overload of the specimen. ABB used gas pressurized bellows on 3 of the 12 CT specimens, but there is no information on the loading stability vs. time of this system.

Table 3 – Estimated Loading Fluctuation and Outages During SCC Testing
Peak-to-Peak Variation: Number of Complete Unloadings

Lab	Fluctuation	# of Unloads
ABB	*not reported*	*not reported*
AEA Tech	135N (30 lbs)	1 (in Test #1)
GE CRD	50N (11 lbs)	2 (all in Test #3)
Studsvik	40N (9 lbs)	3 (all in Test #2)
VTT	40N (9 lbs)	1 (in Test #2)

Fluctuations in test temperature of 1 °C are unlikely to affect stress corrosion crack growth rates; however, larger variations, while not markedly affecting growth rates, may tend to cause crack arrest or contribute to increased noise and decreased resolution in the crack length measurements. There were some differences among laboratories in temperature control as shown in the table below; however, there is no direct evidence that this produced an undesirable effect on SCC growth rate response.

Table 4 – Temperature Fluctuation During SCC Testing

Lab	Fluctuation
ABB	6 C, Peak to peak
AEA Tech	5.5 C, Peak to peak
GE CRD	0.4 C, Peak to peak
Studsvik	0.4 C, Peak to peak
VTT	1.5 C, Peak to peak

Water Chemistry.
Water chemistry has a dominant influence on stress corrosion cracking, and the challenges of meeting adequate water chemistry standards has grown dramatically as BWR water purity has improved from a U.S. fleet average of over 0.4 to nearly 0.1 μS/cm in the last 15 years. Achieving an autoclave outlet conductivity of 0.4 μS/cm in laboratories is challenging enough, but outlet conductivities below 0.1 μS/cm are much more difficult.

Assuming theoretical ionic purity inlet water (0.055 μS/cm), the contributions to autoclave outlet conductivity include breakdown of undissociated species (which don't affect inlet conductivity) and impurities released in autoclave systems. Common undissociated species include bacteria, organics, and some inorganic compounds. Species typically released from the autoclave include chromate (from Cr-bearing alloys in oxidizing water), fluoride (e.g., from Teflon insulation and seals), chloride (e.g., from reference electrodes), sulfur (from metals and lubricants), etc.

All laboratories participating in the Round Robin achieved very good water chemistry. Indeed, it appears that the largest contribution to the outlet conductivity was not associated with inlet water purity problems or "contaminants" from the autoclave system, but resulted from chromate that is released from all Cr-bearing materials exposed to oxygenated high temperature water. All laboratories were able to hold outlet conductivity at or below 0.12 μS/cm in 200 ppb O_2 (especially toward the end of the test), although at 2000 ppb O_2 the outlet conductivity ranged from >0.45 μS/cm (early in test) to long term values of ≈ 0.15 μS/cm for some labs, to <0.07 μS/cm for one lab.

Table 5 – Conductivity for Tests in 288 °C Water (μS/cm)

	Inlet	Outlet			
		200 ppb O_2 Pure Water	500 ppb O_2 Pure Water	500 ppb O_2 25 ppb SO_4	2000 ppb O_2 Pure Water
ABB	0.125	0.125	0.15	0.34	0.4 → 0.15
AEA Tech	0.056	0.11 → 0.08		0.29 → 0.26	
GE CRD	0.055	0.063	0.065	0.24	0.070
Studsvik	0.056	0.08		0.26	
VTT	0.073	0.2 → 0.08		0.4	0.45 → 0.15

Because of temperature fluctuations, gas mixing controls, and consumption of dissolved oxygen in the autoclave system, maintaining a constant dissolved oxygen can be difficult. The table below summarizes the short term and long term stability in the outlet dissolved oxygen level for each laboratory.

Table 6 – Stability of Outlet Dissolved Oxygen (ppb)
Short term / long term, peak-to-peak variation

	200 ppb O_2	500 ppb O_2	2000 ppb O_2
ABB	50 / 50	70 / 100	70 / 140
AEA Tech	40 / 80	40 / 125	--
GE CRD	8 / 15	15 / 30	50 / 150
Studsvik	13 / 50	50 / 200	--
VTT	25 / 100	40 / 125	275 / 300

Reversing dc potential drop – Resolution and Accuracy.

Reversing dc potential drop has become the preeminent technique for measuring crack length in conducting materials. In most designs, a constant current is passed through the specimen and the potential drop is measured. In many iron and nickel base austenitic specimens, roughly 50 to 500 μV of potential is generated when 1 to 10A of current is applied. Because the potentials are low – especially when you consider that high resolution requires stable measurements to <10 nV – it is necessary to eliminate sources of voltage from thermo-electric effects, bi-metallic junctions, etc. The most common approach is to reverse the current periodically and subtract the –current reading from the +current reading, which (in theory) eliminates all but the desired signal. High resolution digital voltmeters (DVM) provide superb rejection of ac noise induced by heaters, etc.

Accuracy and resolution are controlled by the DVM, the stability of the constant current supply (especially with changes in room temperature), autoclave temperature changes, the algorithms that convert from measured potential to crack length, evenness of the crack front, other factors that influence the specimen resistance beside crack advance (i.e., temperature, drifts in the resistivity of the metal from aging, creation of electrical shorting paths in the wake of the crack from asperities that touch (especially during unloading and/or if environmental conditions become sufficiently reducing to change from oxide to metal stability), etc.)

While many factors can be dominant in some circumstances, perhaps the most consistently troublesome is crack front unevenness. In CT (and other) specimens, there is a concentration of current flux lines near the crack tip, and this produces highly non-linear effects if there are regions of the crack front that have advanced less than the remainder of the front, or if islands of uncracked metal remain in the wake of the crack. If 5% of the crack front is pinned at the transgranular fatigue pre-crack, potential drop will not be greatly in error as the majority of the crack front advances. When the crack (i.e., all but the 5% of the crack front that is pinned) has advanced, e.g., 1 mm, the error in the potential drop reading can be considerable (e.g., it might register only 0.25 mm of advance). After 10 mm of advance, dc potential drop might register only 1 mm of advance. When post-test comparisons with the fracture surface are made, it is common to compute the average crack depth and apply a fixed correction factor to all test data, despite the fact that the actual correction factor is continuously varying throughout the test. Of course, since the evolution of the crack front is much more complex – and unknown – during a test, there is no way to back-correct data with confidence.

All laboratories had well designed reversing dc potential drop systems – indeed, this was a requirement for their selection. While a detailed characterization of their individual accuracy and resolution is difficult without the raw data files, approximate values are given below:

Table 7 – Estimated Typical Values of Crack Length Resolution & Accuracy
The correction factor = (actual avg. crack depth) / (indicated depth by potential drop)

Lab	Crack length resolution μm (peak-to-peak noise)	Correction factor on crack growth increment
ABB	20 - 30	1.10X → 2.7X, avg = 1.73X
AEA Tech	10 - 20	1.17
GE CRD	2 - 5	1.21X*, 1.01X, 0.94X*
Studsvik	2 - 5	0.27X**, 1.10X, 1.43X
VTT	5 - 10	1.02X, 1.09X, 1.11X

* somewhat uneven crack front from machining and/or pre-cracking
** correction factor based on very small crack increment

Corrosion potential measurements: issues and comparisons

This is an important element of the Round Robin, as evidenced in the requirement that every laboratory use two reference electrodes (their own, and a common electrode supplied by GE CRD) to measure the corrosion potential of the CT specimen. A separate task was also performed at GE CRD to compare in a single autoclave the response of all of the reference electrodes used in the Round Robin.

Corrosion potentials in single autoclave comparison

In this comparison study, reference electrodes provided by each laboratory were installed in a 4 liter stainless steel autoclave at GE CRD and exposed in 288 °C high purity water containing 300 ppb O_2 or 150 ppb H_2. The corrosion potentials of type 304 stainless steel and Pt electrodes were measured against each reference electrode using a Keithley 616 electrometer and a Keithley 705 scanner. The reference electrodes were arranged symmetrically around the Pt and stainless steel electrodes. The measured values were converted to the standard hydrogen electrode (SHE) scale on the basis of the conversion potentials at 288 °C supplied with each reference electrode as normally used by the laboratory.

Table 8 – Table of Conversion Values for Reference Electrodes

Laboratory & Reference Electrode	Ref. Potential
ABB Internal Pure H_2O Ag/AgCl	+139 mV_{she}
AEA External 0.1N KCl Ag/AgCl	-23 mV_{she}
GE CRD $Cu/Cu_2O/ZrO_2$	-275 mV_{she}
Studsvik Ext 0.01N KCl Ag/AgCl	+16 mV_{she}
VTT $Ni/NiO/ZrO_2$	-582 mV_{she}

The type 304 stainless steel electrode was pre-oxidized in 288 °C water containing 200 ppb O_2 for 3 weeks before corrosion potential measurements were made. The Pt electrode was platinized ("blacked") in chloroplatinic acid, which produces a very high surface area catalytic coating, and yields somewhat higher and more reproducible corrosion potentials in solutions containing oxygen than polished ("bright") Pt. Figures 1 and 2 show the corrosion potential behavior of the type 304 stainless steel and Pt electrodes, respectively, as measured against the various reference electrodes.

Several problems were identified before and during testing, such as leaks or shorts that developed in some reference electrodes. Since all high temperature aqueous reference electrodes are custom fabricated devices, occasional reliability problems are not surprising, nor are they the focus of the Round Robin measurements. However, they did complicate the comparison process.

The only test condition where a known, "correct" potential exists is on the Pt electrode in the 150 ppb H_2 environment (although the stainless steel response should be similar); this value is ≈ -535 mV_{she}. Comparisons of these potentials are given in the table below. In 150 ppb H_2 the Studsvik electrode measured a Pt potential much lower than the thermodynamic value, by ≈ 120 mV. After testing, the reference electrode was measured at room temperature to verify KCl concentration, and it showed an increase in its reference potential, indicative of possible dilution of the KCl electrolyte. However, Studsvik believes that there may have been some contribution from the temperature of the external reference reaction, which may have been above room temperature (the conversions are 16, 34 and 52 mV_{she} at 25, 35 and 45 °C). The GECRD, VTT, and ABB electrodes responded very well in 150 ppb H_2, giving ≈ -550 mV_{she} for the Pt and type 304 stainless steel electrodes. The AEA electrode was not functioning during this time period.

Table 9 – Corrosion Potentials of Pt and 304 SS in NWC and HWC
Single Autoclave Comparison Test at GE CRD

Laboratory and Reference Electrode	Pt 150 ppb H_2	Pt 300 ppb O_2	Stainless Steel 150 ppb H_2	Stainless Steel 300 ppb O_2
ABB Int. Pure H_2O AgCl	-526 mV_{she}	193 mV_{she}	-533 mV_{she}	64 mV_{she}
AEA Ext. 0.1N AgCl	61 mV_{she} *	261 mV_{she}	54 mV_{she} *	131 mV_{she}
GE CRD $Cu/Cu_2O/ZrO_2$	-543 mV_{she}	303 mV_{she}	-555 mV_{she}	173 mV_{she}
Studsvik Ext 0.01N AgCl	-643 mV_{she}	200 mV_{she}	-652 mV_{she}	66 mV_{she}
VTT $Ni/NiO/ZrO_2$	-550 mV_{she}	95 mV_{she} *	-522 mV_{she}	-52 mV_{she}

* not available or uncertain because of possible or known reference electrode failure

In 300 ppb O_2 the comparison revealed a difference of 110 mV among reference electrodes. The highest corrosion potentials on both stainless steel and Pt were observed using the GE

CRD $Cu/Cu_2O/ZrO_2$ reference electrode. While the issue of which reference electrode is most thermodynamic and stable is a complex one, for now we will assume that the GE CRD $Cu/Cu_2O/ZrO_2$ gives correct readings.

AEA External 0.1 M KCl Ag/AgCl Reference Electrode.
The AEA external 0.1 M KCl Ag/AgCl electrode gave the next highest corrosion potentials (after the GE CRD reference electrode), although after switching to 150 ppb H_2 after ≈ 6 days, it quickly failed, giving potentials that were 500 mV too high.

Studsvik External 0.01 M KCl Ag/AgCl Reference Electrode.
In 300 ppb O_2, the corrosion potentials measured by the Studsvik external 0.01 M KCl Ag/AgCl electrode were ≈ 120 mV below the GE CRD electrode. Since in 150 ppb H_2 the Studsvik electrode gave potentials that were markedly too low (by about the same 120 mV as observed in 300 ppb O_2), it's possible that some loss of KCl electrolyte may have occurred. However, on returning to 300 ppb O_2 at about 33 days, the Studsvik electrode gave potentials that were ≈ 30 to 40 mV below what it showed earlier in the test. Since the GE CRD electrode also showed potentials that were lower by about this amount, both on stainless steel and Pt, perhaps small changes occurred in the dissolved gas chemistry, not in the KCl electrolyte concentration.

ABB Internal Pure H_2O Ag/AgCl Reference Electrode.
The ABB internal pure H_2O Ag/AgCl electrode exhibited a more complex behavior. In 300 ppb O_2 it was 120 mV lower than the GE CRD electrode, but in 150 ppb H_2 it was ≈ 20 mV lower. One can only infer that its reference reaction is influence by dissolved gas (either oxygen or hydrogen; it's not clear which one because its "she" conversion factor was empirically established). This is consistent with the ability of dissolved gases to readily permeate its Teflon body at high temperature. On changing back to 300 ppb O_2, the ABB electrode measured almost the same potential as it had early in the test.

VTT $Ni/NiO/ZrO_2$ Membrane Reference Electrode.
more than 500 mV too low early in the test. After repair of the electrode (shown at about 21 days), its potentials were close to correct in 150 ppb H_2, but later it produced potentials that were quite low in 300 ppb O_2 later in the test. This apparently does not represent a fundamental problem in its reference potential or a sensitivity to dissolved gases, but simply a problem with the seal in this case.

Summary of Single Autoclave Corrosion Potential Measurements.
In a limited program of this type it is impossible to identify and characterize the origins of all of the problems that give rise to different reference half-cell potentials. Under the 150 ppb H_2 conditions, the Pt electrode acts thermodynamically (reversibly), so the correct corrosion potential is known. Under these conditions, the GE CRD, ABB, and (repaired) VTT electrode were quite close to thermodynamic. Comparison to the AEA electrode under these conditions is not possible, because of seal and corrosion problems. Under the 300 ppb

O_2 conditions, there is no such simple approach for determining what corrosion potential represents the thermodynamic value; however, the GE CRD was very consistent in its potentials, and there is no obvious mechanism for its reference potential to shift with the dissolved gas concentration. Clearly more work in this crucial area is merited.

Corrosion potentials during SCC testing

A review of the corrosion potential data obtained during the SCC tests at each laboratory shows many of the same concerns observed in the comparison test described above, and some additional ones. In addition to using their own reference electrode, each laboratory measured the corrosion potential of the CT specimen (and, in some cases, of a Pt electrode) against the GE CRD electrode. In some cases the placement of the reference electrodes in the autoclave proved to be an issue, because either one or both of the electrodes had to be located at some distance from the CT specimen. All laboratories also measured corrosion potential while the dc potential drop system was operating to determine whether it had an effect on the potential of the CT specimen. A summary of the characteristics of the corrosion potential measurements is shown below in Table 10.

Table 10 – Characteristics of Corosion Potential Measurements

	ABB	AEA *1	GE CRD	Studsvik	VTT *1
measured on CT or Coupon	Coupon *2	CT	CT	CT	CT
electrical isolation	Yes *3	Yes *3	Yes *4	Yes	Yes
location of their RE	*not reported*	≈8 cm *1	4 cm	1.5, 5 *5	≈8 cm *1
location of GE CRD RE	*not reported*	≈8 cm *1	4 cm	3, 1 *5	≈8 cm *1
influence of dcpd on CP	± 1100 mV	<5 mV	<1 mV	<1 mV	<2 mV

n/a = information not available RE = reference electrode *1 location estimated from reports

*2 ABB also measured the potential of a CT specimen vs. their reference

*3 ABB & AEA used oxidized zircaloy pins, which may not be as reliable as ZrO_2 insulators

*4 GE CRD electrically isolated the loading linkage, not the CT

*5 1.5 & 3 cm for specimen SKI 26, and 5 & 1 cm for SKI 40 & SKI 6

ABB Corrosion Potentials.

orrosion potential measurements at ABB were performed primarily in a side stream autoclave using separate stainless steel coupons; the same water flowed through all autoclaves, and thus it was nominally identical, although flow rates and temperatures varied somewhat. These measurements confirmed what was observed in the electrode comparisons at GE CRD, i.e., that in oxygenated water the corrosion potential of stainless steel was lower for the ABB reference electrode. However, an ABB reference electrode was also placed in one SCC autoclave and it measured a corrosion potential that was ≈ 70 mV higher than on the stainless steel coupon in the side stream autoclave (vs. an ABB reference),

indicating a difference between the CT and the side stream autoclaves. If this 70 mV difference is interpreted as a consistent bias, and is added to the measurements vs. the GE CRD electrode in the side stream autoclave, the resulting values would be very close to those measured at GE CRD. The exact physical placement of the reference electrodes (in either the side-stream or CT autoclave) was not identified, but since both the stainless steel coupon and CT specimen were electrically isolated, the 70 mV offset between the two corrosion potential measurements appears to result from differences in the positioning of the reference electrodes (coupled with potential fields in the solution that are often the origin of such positioning sensitivity).

When the corrosion potentials were measured on the CT specimens while the dc potential drop system was active, ABB found a very large interaction of about ± 1.1 V. Because of the high resistivity of the water, much of this polarization was associated with iR drop in solution, although the CT specimens were certainly polarized to some extent. The origin of this problem is likely ionic current leakage between the seal body and the wires that supply the reversed dc current to the CT specimens, because the voltage drop in these wires between the seal and the CT specimen is typically ≈ 1 V.

AEA Technology Corrosion Potentials.

In the discussion of the first SCC test (SKI specimen #21), the corrosion potential of the stainless steel CT specimen vs. the GE CRD reference electrode was ≈ 80 mV_{she}, although there had been jumps from 40, to 60, to 80 mV_{she} associated with some test perturbations at ≈ 285 and 600 hours. An AEA external 0.1N KCl Ag/AgCl reference electrode was installed during the first test, but it developed a leak and thereafter showed a systematic error, and eventually failed. The second SCC test (SKI specimen #35) was initiated in 150 ppb H_2 and the Pt corrosion potential was measured vs. the two reference electrodes. The measurement using the GE CRD $Cu/Cu_2O/ZrO_2$ reference was -499 mV_{she}, compared to -558 mV_{she} for the AEA external 0.1N KCl Ag/AgCl reference. Both electrodes were ≈ 30 mV off the theoretical potential of -535 mV_{she} for Pt. On checking, the $Cu/Cu_2O/ZrO_2$ electrode was found to be leaking from its seal, perhaps induced by the test perturbations and thermal cycling; it was returned to GE CRD for repair. In its place a second external Ag/AgCl electrode was installed. During SCC testing, the corrosion potentials measured with the two reference electrodes drifted vs. time and relative to each other. Ag/AgCl #1 gave a corrosion potential on the stainless steel CT specimen of ≈ 75 mV_{she} early in the test, and settled to a value of ≈ 30 mV_{she} throughout most of the test. Ag/AgCl #2 gave high potentials early in the test of ≈ 95 mV_{she}, but steadily drifted downward to ≈ -20 mV_{she}. At the end of the test the water chemistry was returned to 150 ppb H_2, and the corrosion potential of Pt as measured by Ag/AgCl #1 returned to its initial reading of -558 mV_{she}, while the Pt potential vs. Ag/AgCl #2 had dropped to -677 mV_{she}, indicative of leakage (dilution) of the electrolyte.

GE CRD Corrosion Potentials.

The GE CRD $Cu/Cu_2O/ZrO_2$ reference electrode behaved very well in all three tests over a total of about 8500 hours. In the first test (c96, SKI specimen #30), the corrosion potential of the "blacked" Pt electrode was stable during periods of constant chemistry (apart from some initial drift early in the test), and responded essentially instantaneously to changes in water chemistry (Figure 3). The corrosion potential of the stainless steel CT specimen drifted up throughout the test, consistent with the formation of an increasingly protective oxide. Representative corrosion potentials are given in Tables 11 and 12. There is no evidence of problems or drifts in the reference electrode – e.g., the slow drift in both the Pt and CT corrosion potentials were in opposite direction.

In the second test (c107, SKI specimen #22), the corrosion potential response was similar to the first test, although the detailed response was different because of differences in the water chemistry. During the last 1000 hours of this 3050 hour test, the test conditions were very constant, and both the Pt and CT corrosion potentials were also very stable. In the third test (c112, SKI specimen #5), the conditions were constant for the first 1250 hours, then were changed for the last 800 hours of the test. The corrosion potential of Pt was quite stable, and it responded very rapidly to the change from 500 ppb to 2000 ppb O_2. The corrosion potential of the CT specimen steadily increased during the first 1250 hours, but was very constant during the last 800 hours. The steady state corrosion potentials are given in Table 11, and the range of measured potentials in Table 12.

Studsvik Corrosion Potentials.

In the first test (SKI specimen #26), the corrosion potential of the CT specimen increased throughout the 1025 hour test (Figure 4). Early in the test, the corrosion potential measured vs. the GE CRD $Cu/Cu_2O/ZrO_2$ reference electrode was $\approx$ -150 mV_{she}, about 50 mV higher than the Studsvik external 0.01N KCl Ag/AgCl reference electrode. The potential increased to $\approx$ +20 mV_{she} vs. the $Cu/Cu_2O/ZrO_2$ reference, but to only $\approx$ -90 mV_{she} vs. the Ag/AgCl reference, a difference of 110 mV, which represents a drift of 60 mV between the two references. The Studsvik report noted that the potentials measured by the $Cu/Cu_2O/ZrO_2$

Table 11 – Long Term, "Steady State" Corrosion Potentials of Pt & Stainless Steel vs. the GE CRD Reference Electrode in 288 C Water
GE CRD data from another study also included (c101/2/8/9)

ID	O_2, ppb	H_2, ppb	Pt, mV_{she}	SS, mV_{she}	Exposure time, h
ABB	2000	0	290	95	350
ABB	200	0	260	60	200
ABB	500	0	270	90	1300
AEA Tech #1	200	0	--	80	1100
GE CRD c96	200	0	292	140	2100
GE CRD c96	2000	0	321	207	450
GE CRD c96	500	0	303	175	100
GE CRD c96	325	0	297	164	70
GE CRD c96	200	0	290	150	650
GE CRD c107	2000	0	310	220	1800
GE CRD c107	500	0	297	192	2600
GE CRD c112	500	0	305	180	1200
GE CRD c112	2000	0	310	211	800
GE CRD c101	400	0	310	140	1800
GE CRD c102	400	0	280	145	1800
GE CRD c108	8000	0	325	244	2900
GE CRD c108	0	95	-460	-480	500
GE CRD c109	8000	0	320	242	2100
GE CRD c109	0	95	-500	-500	400
Studsvik #1	200	0	---	30	1000
Studsvik #2	2000	0	---	90	800
Studsvik #2	500	0	---	20	2200
Studsvik #3	500	0	---	-20	1000
VTT #1	200	0	260	100	2000
VTT #1	400	0	265	120	170
VTT #1	600	0	275	135	350
VTT #2	2000	0	270	185	2600
VTT #2	500	0	245	155	1000
VTT #3	500	0	260	150	1700

Table 12 –Corrosion Potentials of Pt & Stainless Steel vs. Multiple Reference Electrodes in 288 C Water – Changes Shown After ≈100 hours into Test

ID	O_2 ppb	Pt, mV_{she} vs. GE CRD	Pt, mV_{she} vs. Lab's Ref.	SS, mV_{she} vs. GE CRD	SS, mV_{she} vs. Lab's Ref.	Comments
ABB #1	2000	300 → 290	215	95 → 100	20 → 25	[1] corrected φ_c close to GE
ABB #1	200	260	185	60	-15	Side-stream autoclave
ABB #1	500	270	195	75 → 90	0 → 15	ABB RE = 75mV lower
AEA #1	200	--	--	40 → 80	n/a	[2] 80 - 100 mV below GE
AEA #2	500	--	--	n/a	80 → 50	RE #1 - close to GE CRD
AEA #2	500	--	--	n/a	90 → -20	RE #2 likely leakage
GE #1	200	292	--	140	--	[3] no second reference
GE #1	2000	321	--	207	--	φ_c data consistent but high
GE #1	500	303	--	175	--	
GE #1	325	297	--	164	--	
GE #1	200	290	--	150	--	
GE #2	2000	310	--	220	--	
GE #2	500	297	--	192	--	
GE #3	500	305	--	180	--	
GE #3	2000	310	--	211	--	
Studs. #1	200	--	--	-150 → 30	-190 →-90	[4]
Studs. #2	2000	--	--	20 → 100	-40 → -30	
Studs. #2	500	--	--	20	-100	
Studs. #3	500	--	--	-20	-80 → -120	
Studs. #3	H_2	-600	-680	-530	-610	150ppb H_2- why is Pt low?
VTT #1	200	225 → 260	150 → 240	60 → 100	-20 → 70	[5]
VTT #1	400	265	255	120 → 125	105 → 110	
VTT #1	600	275	270	135 → 140	125 → 135	
VTT #2	2000	-130 → 270	–130 → 295	140 → 185	175 → 220	
VTT #2	500	245	295	155	180	
VTT #3	500	-80 → 260	-50 → 290	125 → 150	160 → 180	

n/a = reference electrode not available (not functioning)

[1] ABB internal pure water Ag/AgCl in side-stream was 75 mV lower than GE CRD's reference. However, the ABB RE was 75 mV higher on CT specimen than in the side stream autoclave, so measurements similar to GE's if corrected for both location & reference electrode.

[2] AEA - in test #2 there were two ext. 0.1N KCl Ag/AgCl reference electrodes. Measurements are similar to those made using the GE CRD reference, but are 80 - 100 mV lower than reported by GE.

[3] GE CRD - corrosion potentials are fairly consistent from test to test, and with reference electrode comparison measurements done in a separate autoclave.

[4] Studsvik - φ_c measurements on external 0.01N KCl Ag/AgCl reference electrode are lower than usual, apparently because of its different position (to accommodate the GE CRD reference).
[5] VTT - difference between VTT and GE CRD reference electrodes decreases during first test.

reference were typical of those typically measured with the Ag/AgCl electrode when it was placed in its usual location in the autoclave (occupied by the $Cu/Cu_2O/ZrO_2$ reference). This suggests that there is some sensitivity to the placement of the reference electrodes. This was confirmed in measurements undertaken in a subsequent study at Studsvik [2] using various reference electrodes that included the GE CRD reference, although the potentials they reported on stainless steel and Pt were still lower than observed at GE CRD.

A broadly similar observation was made in the second test (SKI specimen #40). The corrosion potential difference between the two references started at ≈ 60 mV and grew to ≈ 140 mV. The corrosion potential of the CT specimen was fairly stable throughout the last 2500 hours of this test at ≈ +20 mV_{she} vs. $Cu/Cu_2O/ZrO_2$ and ≈ -120 mV_{she} vs. Ag/AgCl in 500 ppb O_2. The third test (SKI specimen #6) was also performed in 500 ppb O_2, and showed a very similar response, with an initial difference between the two references of ≈ 50 mV that increased through the test to ≈ 100 mV. In the last 500 hours of the test, the corrosion potential of the CT specimen was ≈-20 mV_{she} vs. $Cu/Cu_2O/ZrO_2$ and ≈ -120 mV_{she} vs. Ag/AgCl. At the end of the test, the Studsvik report indicates that corrosion potential measurements on Pt were made in 150 ppb H_2 of -600 mV_{she} vs. $Cu/Cu_2O/ZrO_2$ and -680 mV_{she} vs. Ag/AgCl, both of which are below the theoretical value of ≈ -535 mV_{she}. The very low potential measured vs. Ag/AgCl is consistent with drift in its reference potential vs. time, e.g., from dilution of its KCl electrolyte. Since no seal leakage or cracks in the ceramic were observed on the $Cu/Cu_2O/ZrO_2$ reference (and it was shown to give thermodynamic behavior before being sent from GE CRD), it is reasonable to wonder whether the low potential (by 70 mV) represents a sensitivity to the positioning of the reference in the autoclave. Indeed, if 70 mV were added to the reported potentials, the values would be closer to those reported by some other labs.

VTT Corrosion Potentials.

During the first test (SKI specimen #24), the corrosion potential of the CT specimen slowly drifted up from ≈ 60 mV_{she} at 100 hours into the test to ≈ 100 mV_{she} from 1000 to 2000 hours into the test (Figure 5). Increases from 200 ppb O_2 to 400 and 600 ppb O_2 caused the potential to rise to about 120 and 135 mV_{she}, respectively. The potentials on Pt were higher at about 260, 265, and 275 mV_{she} in the 200, 400, and 600 ppb O_2, respectively. In all cases the potentials measured using the VTT reference electrode were lower by an amount that varied during the test. Initially, it was ≈ 100 mV lower, but this difference decreased to ≈ 5 mV by the end of the test.

In the second test (SKI specimen #42), the corrosion potentials measured vs. the VTT reference electrode were higher than the GE CRD electrode. In 2000 and 500 ppb O_2, the GE CRD electrode registered corrosion potentials of 190 and 130 mV_{she}, respectively, for the CT specimen, and about 270 and 250 mV_{she} for Pt. The VTT reference electrode gave the same potentials early in the test, but slowly drifted up by ≈ 40 mV. Only one GE CRD reference electrode and one VTT reference electrode were used for all tests. However,

perhaps the drift observed during the first test (which ended with the two electrodes being fairly similar) merely continued during the second test.

During the third test, the difference between the VTT and GE CRD reference electrodes remained constant at ≈ 40 mV. This test was performed at 500 ppb O_2, and the corrosion potential of the CT specimen ended at ≈ 150 mV_{she} vs. the GE CRD reference and ≈ 180 mV_{she} vs. the VTT reference. The corrosion potential was fairly constant during the first 700 hours, then a slow increase by ≈ 25 mV occurred between 700 and 1400 hours (perhaps due to the change in the outlet conductivity and pH), then the potential was again constant. The response of Pt was peculiar, because during the first 1300 hours of the test it was anomalously low (-100 to +50 mV_{she}), then a sudden change occurred, and the potential at the end of the test was +260 mV_{she} vs. the GE CRD reference and +300 mV_{she} vs. the VTT reference. Subsequent discussion of this issue with VTT indicated that the initial Pt values were not correct, and should not have been reported.

Summary of Corrosion Potential Measurements During SCC Testing.
Comparison of the corrosion potential data from the five laboratories is complicated by reference electrode problems, measurement of Pt potentials only in some laboratories (not AEA Technologies, and only limited data in deaerated water at Studsvik), and the absence of some measurements directly on the CT specimen at ABB. However, it is clear that there are significant differences in measured corrosion potential from both reference electrode differences and differences in lab / autoclave / electrode positioning.

Figures 6–8 compare the corrosion potential measurements made in this program, and highlight the significant differences that exist in reported corrosion potentials on stainless steel and Pt. When each laboratory's own preferred reference electrode is used, the reported corrosion potentials span 340 mV, from -120 mV_{she} to +220 mV_{she}. Even when a common reference electrode is used (Figures 6 and 7), the range is 240 mV, from -20 mV_{she} to +220 mV_{she}. The spread of the Pt measurements (Figure 6) is smaller at 245 mV_{she} to 321 mV_{she} when a common reference was used, but perhaps mostly because fewer labs reported Pt potentials.

Among the issues that surface – but were not resolved or even necessarily confirmed – were reference electrode problems (e.g., AEA, Studsvik, and VTT), unusual observations during the test (various labs), apparent sensitivity to the placement of the reference electrode (in the Studsvik and ABB measurements), etc. While it is difficult to determine which electrode provided the most thermodynamic response, most evidence suggests that the GE CRD $Cu/Cu_2O/ZrO_2$ membrane reference electrode is closest – and provided good stability and reliability. Clearly a great deal more work needs to undertaken to resolve the simple issue of corrosion potential measurements, not to mention the corrosion potential behavior of stainless steel and other structural materials.

Summary and conclusions – corrosion potential measurements

These data in Tables 11 and 12 and Figures 6–8 show very wide scatter in all of the corrosion potential measurements, despite well controlled conditions of water chemistry, temperature, material, etc. This cannot simply be ascribed to reference electrode problems, because the scatter was almost as large when all laboratories used the GE CRD reference electrode.

Important issues included reference electrode problems, unusual observations during the test (drift, sudden changes, abnormally low potentials, etc.), and apparent sensitivity to the placement of the reference electrode (in the Studsvik and ABB measurements). It was not the intent of this program to resolve these issues, and indeed it is difficult to identify which reference electrode or corrosion potential measurements were the most thermodynamically accurate. However, evidence suggests that measurements performed at GE CRD using their $Cu/Cu_2O/ZrO_2$ membrane reference electrode may be the most accurate, and were quite stable and reliable. More emphasis and cross-comparisons between laboratories is clearly needed to identify the proper techniques of corrosion potential measurements, then characterize, understand and model the corrosion potential behavior of stainless steel and other structural materials.

The VTT measurements on the stainless steel CT specimen are broadly similar to those measured at GE CRD, although their measurements on Pt are lower, perhaps because they used "bright" rather than "blacked" Pt. However, the stainless steel corrosion potentials measured at ABB (on a stainless steel coupon in a separate autoclave from the crack growth tests) and Studsvik (on the CT specimen) are significantly lower. Studsvik measurements were also consistently lower on the CT specimen in deaerated water, or on Pt in aerated or deaerated water. They noted that the their Pt readings were below the theoretical value of -540 mV_{she}, i.e., -680 mV_{she} vs. their AgCl electrodes and -600 mV_{she} vs. the GE $Cu/Cu_2O/ZrO_2$ membrane reference electrode, which represents a consistent different (a) between their measurements in 200 - 2000 ppb O_2 and VTT's and GE's, and (b) between their AgCl electrode and the GE $Cu/Cu_2O/ZrO_2$ electrode.

However, the lower corrosion potentials clearly point to concerns for the autoclave set up or measurement technique, since the water chemistry and stainless steel were nearly identical at all laboratories. Again, no definitive answers can be identified, but possible explanations include: inadequate insulation of the CT specimen from dissimilar materials (e.g., in the loading linkage or autoclave); positioning of the reference electrode too far from the stainless steel CT specimen (or coupon, for ABB), coupled with potential gradients in the solution which can cause the reference electrode to "see" the wrong potential; presence of stray currents in the autoclave, especially from contact with very dissimilar metals (e.g., Pt) or from leakage of the current used for the dc potential drop measurements; inadequate

insulation of the lead wire connected to the CT specimen, e.g., in the area of autoclave seal; inadequate insulation outside the autoclave, a low impedance path in the cabling or switching electronics, or low input impedance in the voltmeter used to make the corrosion potential measurements, etc.

It was not the objective of this study to identify the origin of the discrepancies, or conclude which corrosion potential is the correct one in 300 ppb O_2 (in 150 ppb H_2, the correct potential is defined by the reversible Pt response). The relatively high corrosion potentials on stainless steel and Pt produced by the GE CRD electrode are entirely credible, and fully consistent with long-observed response of this electrode (using either copper oxide or iron oxide internal junction). Because the electrode is a sealed (membrane) reference electrode that is impermeable to O_2 or H_2, and has no ionic junction or electrolyte to leak out, the possible mechanisms for it to be influenced by test conditions and water chemistry are very limited.

It is interesting to note that there have historically been large discrepancies in reported corrosion potentials, e.g., over the last three decades. Some of the differences relate to:

- known problems with the reference electrodes used (e.g., offsets in the half-cell reaction, or problems induced by the ion junction (e.g., asbestos wick or porous zirconia plug);
- inadequate pre-oxidation of the stainless steel electrodes;
- poor control of water chemistry – both high impurity levels (which can shift pH and increase the corrosion rate of the stainless steel) and poorly controlled dissolved gas concentrations (including errors in gas equilibration, or large consumption of dissolved oxygen because of the very low autoclave refresh rates used).

Additionally, the surface preparation and perhaps even subtleties of composition of the stainless steel (which should not play a significant role in these tests using the same heat of material) may influence the oxide that forms and the corrosion rate of the metal. The presence of dissolved hydrogen, even at moderate to high oxygen levels, is also important, and represents a difference between many laboratory measurements and in-reactor conditions, where some H_2 is always present. Clearly more extensive efforts to resolve discrepancies between reference electrodes and to characterize the real corrosion potential of BWR structural materials need to be undertaken before any international / industry consensus will be achieved.

Stress corrosion crack growth rate data: issues and comparisons

Introduction

The primary objective of the Round Robin was to compare stress corrosion crack growth rate response among five laboratories. 23 CT specimens (50 mm), fabricated and pre-cracked by a separate vendor, were tested by the five laboratories, producing 157 crack growth rates (127 were non-zero growth rates). Of these, 92 data were obtained at constant load (69 were non-zero growth rates), and 65 were run under "gentle" cyclic loading conditions (58 had a non-zero growth rate), as summarized in Table 13. Some challenges were encountered in tabulating the crack growth data and test conditions, because there were differences in reporting from lab-to-lab and much of the crack growth data and associated measurements in this report had to be extracted from graphs in the individual reports [3-7]. These factors coupled with the desire to be consistent in the reporting and comparison of the data may have led to some differences in specific crack growth rate and corrosion potential values between this report and the individual reports written by each laboratory. Somewhat less emphasis was given in this analysis to "no growth" observations, and the significance and interpretation of "no growth" is complicated by factors such as whether one includes long periods of no growth if they are followed by subsequent growth under the same test conditions, whether growth is considered to have occurred if the total crack increment during that period is less than the crack length resolution, etc.

Table 13 – Number and Type of Crack Growth Data Obtained in the Round Robin

Laboratory	Total Data	Growth Rate > 0	Constant Load Data	Growth Rate > 0	Gentle Cyclic Load Data	Growth Rate > 0
ABB Atom	67	49	37	24	30	25
AEA Tech	10	7	9	7	1	0
GE CRD	49	45	26	23	23	22
Studsvik	8	8	6	6	2	2
VTT Labs	23	18	14	9	9	9
Total	157	127	92	69	65	58

A variety of differences and discrepancies existed from lab-to-lab. Examples include: (1) measured corrosion potentials under nominally identical conditions, (2) stress intensity values (most tests were to have been performed at 30 MPa$\sqrt{m}$, although ABB intentionally studied a range of stress intensities, and other variations also existed), and (3) outlet conductivity. To account for these differences, various techniques were employed in the analyses and comparisons of the data. In some graphs, the data are shown "raw" or "uncorrected". In many cases, data are grouped, so that specific ranges of stress intensity, dissolved oxygen, or conductivity can be compared.

In some plots a *"corrected corrosion potential"* was used. Because the test conditions and materials were very similar and well controlled – and experience has shown that the corrosion potential shouldn't vary by more than 20 - 30 mV under these conditions – it was deemed appropriate to use a consistent set of corrosion potential values to make some of the comparisons of the data. A typical corrosion potential (based on extensive measurements experience at GE CRD) was chosen for each of three dissolved oxygen "groupings" of 2000 ppb ± 50 ppb (+180 mV_{she}), 500 ± 100 ppb (+150 mV_{she}), and 200 ± 100 ppb (+120 mV_{she}) – however these values should not be viewed as the "correct" potentials, because it was not the objective of the Round Robin (nor any other comparative experimental study to this author's knowledge) to determine what the "correct" corrosion potential is under any given circumstances. To prevent the crack growth data from simply falling on top of each other, a random scatter of up to 20 mV amplitude was individually added to the data.

Similarly, in some cases, a *"corrected crack growth rate"* was calculated so that all data could be compared – this involved normalizing all data to 30 MPa$\sqrt{m}$ using a power law relationship between growth rate and stress intensity, $V_{corr} = V_{orig}\,(K/30)^{2.4}$. This power law relationship is characteristic of most models and correlations. While there is clearly justification for varying the "2.4" exponent based on water chemistry, the change would not have had much effect in the data, and therefore adds unnecessary complications, if not suspicions. In various plots and at various points in the discussion, the data are also compared with several important SCC "response references", including the SKI disposition lines [8], the NRC disposition line [9], the BWRVIP correlation [10], and the PLEDGE prediction model [11-13].

Review of crack growth rate data

Appendix B and Figures 9 - 11 show the observed (uncorrected) data grouped by laboratory for constant load and "gentle" cyclic loading conditions. "Gentle cyclic loading" describes loading conditions that induce relatively little enhancement in crack growth, typically by using a moderately high load ratio R = 0.7, very low frequencies (≤ 0.001 Hz), and often long hold times between load cycles. Different laboratories employed different "gentle" loading cycles, and these are compared later. Figures 9 and 10 clearly show that all laboratories observed a range of crack growth rates – even under nominally identical test conditions – although the data in these figures cover a range of stress intensity (especially within the ABB data, which ranges from 27 to 51 MPa$\sqrt{m}$) and water chemistries (e.g., 200 to 2000 ppb O_2). The effects of these variables are separated in later graphs.

Stress corrosion cracking is a complex phenomena requiring expertise in multiple disciplines. It is increasingly understood that experimental "subtleties" can have a dominant role in the observed data. Thus, expert judgment is essential in evaluating SCC data. Nonetheless, even fairly simple screening strategies can show that not all crack growth data should be treated equal. One such simple strategy for ranking or "weighting" the data is to

use as a "figure of merit" the product of *"the crack growth increment (mm)"* times *"the test time in that increment (hours)"*. Comparisons on this basis are shown in Figures 12 - 15 for both the constant load and "gentle" cyclic loading data, for all data grouped together, and for data grouped by lab. This "figure of merit" is somewhat biased in favor of test segments that exhibit high crack growth rates, but this is not inappropriate given that there are numerous reasons why retarded crack growth rates occur, but fewer reasons why rates are artificially accelerated (provided test conditions are well controlled). Of course, it does a good job of de-emphasizing short term data (e.g., over a < 50 hour period), which might be prone to anomalies, particularly if growth rates are reported based on the *fastest* rate over a short time period. It should be pointed out that this report only identifies the *test time* for an entire test segment – it does not list (or use) only the time when the crack is growing. This would have some effect on the ranking, but not a large one – and no discernible effect on the overall findings and conclusions. Note also that the growth rates in Figures 12 - 15 are neither corrected (for the range in stress intensity), nor grouped (or corrected) for differences in water chemistry. Nonetheless, this simple ranking shows the 1 - 3 x 10^{-7} mm/s rates are much more credible than the 1 - 3 x 10^{-8} mm/s rates indicated by other data sets [10]. More complex and "judgment driven" analysis and selection of the data will be presented later.

Stress Intensity Factor (K) Effects.

Stress intensity factor was an intentional variable only in the ABB tests, where there data were obtained at stress intensities of 51, 46, 39 - 42, and 27 - 31 MPa$\sqrt{m}$. However, because of the increase in K with crack length (tests were designated as constant *load*, not constant K), the difficulty in obtaining stress corrosion cracking (resulting in an intentional increase in K), and post-test corrections (e.g., where the fatigue pre-crack was different than the nominal a/W = 0.45 in the specimens received by each laboratory), the data from the other laboratories often deviated substantially from the intended 30 MPa$\sqrt{m}$. The specific ranges of K_{max} (including "gentle" cyclic data) are AEA Techn. = 30.8 - 42.1 MPa$\sqrt{m}$; GE CRD = 29.9 - 31.6 MPa$\sqrt{m}$; Studsvik = 29.1 - 35 MPa$\sqrt{m}$; and VTT = 29.1 - 30 MPa$\sqrt{m}$.

The effect of stress intensity on crack growth rate is shown in Figures 16 - 19 for constant and "gentle" cyclic loading. Figures 16 and 18 show the original data along with growth rate corrections based on the $V_{corr} = V_{orig} (K/30)^{2.4}$ formulation presented earlier. While this approach does a reasonable job at normalizing the data, several things are apparent:

- the proportion of "no-growth" or "very low growth rate" data are significantly greater at ≈30 MPa$\sqrt{m}$ than at >38 MPa$\sqrt{m}$. This may only reflect the expected trend – i.e., that as K is decreased to 25, 20, 15 ... MPa$\sqrt{m}$, achieving and sustaining crack growth becomes more difficult – but likely also reflects the effect of increased plasticity in the specimen (see below).
- the growth rates (even as-corrected) at high K (especially ≥ 45 MPa$\sqrt{m}$) may be somewhat higher than at 30 MPa$\sqrt{m}$. This could be associated with the extent of plasticity in the 304 stainless steel CT specimens, which likely does not meet linear elastic fracture mechanics size / plasticity criteria above 40 - 45 MPa$\sqrt{m}$

(depending on the high temperature yield and ultimate tensile strength, remaining ligament, etc.).

- however, even when the K / size criteria are exceeded to some degree (i.e., at higher K values), this does not immediately produce greatly exaggerated crack growth rates.
- the data (considering only the uncorrected growth rate data, since the correction is designed to remove the effect of K) show an effect of K which is consistent with a power law response of about $K^{2.4}$ (for these materials and water chemistry conditions). However, the quantity and quality of the data are not sufficient to make a definitive statement in this regard, at least not when considered alone.
- superficial support for the concept of a K_{Iscc} can be gleaned from Figures 16 - 18, but it must in fact be viewed as an unsupportable concept, as there is overwhelming evidence that crack growth can occur in sensitized type 304 stainless steel down to K values below 8 MPa$\sqrt{m}$ [14].

Water Chemistry Effects.

Since the test conditions were highly similar at all laboratories – and the CT specimens nominally identical – the dissolved oxygen and ionic solution chemistry (sulfate and conductivity) were used for comparing data in preference to the *measured* corrosion potentials, which varied markedly from lab-to-lab (Figures 6 - 8, 11). Figures 20 and 21 compare the constant load and "gentle" cyclic load data in three groups of dissolved oxygen concentration, with the effect of the variations in stress intensity corrected using the $V_{corr} = V_{orig} (K/30)^{2.4}$ relationship. Note that all of the 2000 ppb and $\leq$ 400 ppb O_2 data are "pure water", while much of the 500 ppb O_2 data include 25 ppb sulfate as H_2SO_4. The distribution of growth rates is lower at the lower O_2 concentrations, and there is an increased fraction of "no growth" data – however, the effect is not huge, as expected given the limited change in corrosion potential between 200 and 2000 ppb O_2.

Figure 22 breaks down the constant load data into finer gradations of dissolved oxygen, and separates the 25 ppb sulfate data. The figure also shows the outlet conductivity – the data are first grouped by dissolved species (O_2 and sulfate), then presented in order of decreasing conductivity. This figure, which uses "corrected growth rates" for stress intensity variations, shows that the scatter in the data are not primarily due to (or explainable by) nominal testing controls and measurements like dissolved oxygen and conductivity – rather, more "subtle" testing issues like specimen machining, pre-cracking practice, artificial crack retardation along parts or all of the crack front, etc. dominate what should be similar-growth-rate data.

While these data indicate that there is an effect of dissolved O_2, attempting to quantify an effect that might cause a 3 - 5X change in growth rate when the data at each O_2 level varies by 1000 - 10,000X is almost guaranteed to produce a misleading result. However, there were two separate experiments, one by ABB and one by GE CRD, in which the effect of dissolved O_2 was evaluated during a period of continuous crack growth, which is a vastly

more reliable method. Figure 23 plots these two data sets, both obtained in pure water (no sulfate added) at 2000, 500, and 200 ppb O_2. The GE CRD tests were performed at ≈30 MPa√m and at an outlet conductivity of <0.070 μS/cm. The ABB tests were performed at ≈39 MPa√m (but the growth rate data in Figure 23 are back corrected to 30 MPa√m) and at an outlet conductivity of 0.35 μS/cm at 2000 ppb O_2 and 0.15 μS/cm at 500 and 200 ppb O_2. As in the prior graphs, Figure 23 uses an *assigned* corrosion potential rather than the *measured* values, as the latter vary greatly from lab-to-lab for nominally identical conditions. As is evident in literature data, the crack growth rate dependence is quite steep, and is in good agreement with the predictions of PLEDGE.

The effect of chromate on SCC has been widely discussed, with some laboratories reporting relatively little or no effect and others reporting a moderate effect, particularly above ≈20 ppb. While it was not the intention of the Round Robin to address this issue directly, both VTT and GE CRD increased the chromate levels to determine if its presence would improve the likelihood of achieving and sustaining SCC. This was done by bypassing the demineralizer in the closed loop autoclave water system, which permits the chromate level to rise (other impurities may also be present, but at *much* lower concentrations than chromate). While the control of a given chromate (or conductivity) level was relatively crude, it was clear in the results of both laboratories (see Figures 6b and 8 in [7] and Figure 10 in [5]) that 30 - 45 ppb chromate did increase the crack growth rates.

Sustained Crack Growth.

With the advent of high resolution crack following techniques like reversing dc potential drop, there is little need to continue test segments for prolonged time periods – especially when moderately high growth rates are involved. However, this has led some to wonder whether SCC is sustained at a given rate over long time periods, especially when "no growth" and "retarded growth rate" observations are both fairly numerous and excluded from some analyses. Figures 24 and 25 show the data grouped by the total time increment employed in a given test segment; in some cases crack growth did not occur (or did not occur uniformly) throughout this time period. These figures show no consistent trend in growth rates as a function of time-increment-in-test-segment, although the constant load data does show some tendency toward a lower proportion of "no growth" observations in the longer test time intervals – this is consistent with the characteristics of the individual crack length vs. time plots, some of which show an initial period of no growth followed by a stable, well-behaved growth rate.

While Figure 24 only shows the total time in a given test segment, it is also important to note that there were a number of instances of sustained, well-behaved crack growth that continued for over 500 hours, and some over 1000 hours – almost all of these exhibited quite constant rates. In several instances tendencies to accelerate or slow vs. time were observed, although approximately in equal numbers, which lends more credence to the majority observation that stress corrosion crack growth rates can sustain over long periods of time.

"Gentle" Cyclic Loading Effects.

There is no question that the use of "gentle" cyclic loading is invaluable in helping to ensure a complete transition to intergranular cracking from the transgranular fatigue pre-crack. It also helps enhance the likelihood of growth as well as sustain stable, well-behaved crack growth – if chosen properly, it is effective without significantly enhancing the observed crack growth rates. The "gentle" cyclic loading conditions used in the Round Robin were chosen for these characteristics. Figures 26 - 28 compare two or three different "gentle" cyclic conditions that were used, with each figure addressing different water chemistry conditions. These figures show that "gentle" cyclic loading greatly enhances the likelihood of achieving the "correct" crack growth rate, although it does not provide an automatic guarantee of this, particularly if sensible pre-cracking and intergranular transitioning response has not been observed. The proportion of "no growth" and "low growth" data are smaller than in the constant load data set, although the constant load data set is itself a major beneficiary of the "gentle" cyclic loading, which was often a critical precursor stage to achieving crack growth at constant load.

The specific type of "gentle" cyclic loading is not as critical, although these data suggest that the R = 0.7, 0.001 Hz (perhaps with a 9,000 second hold time) may be close to optimal, defined as the ability to initiate and sustain the "correct" crack growth rate while inducing minimum upward bias in the observed rates. While not undertaken in the Round Robin, literature data clearly show that, more often than not, higher load ratio (R) values (e.g., R > 0.8, and especially R > 0.9) do not produce the desired benefit, apparently because of crack closure from oxides in the crack. The deeper cycle associated with R = 0.7 is apparently sufficient to overcome this effect in many instances, although it *alone* is not a guarantee that the desired effect will always be achieved.

A related observation was made by various laboratories in the Round Robin – namely, that cyclic loading, even at R = 0.5 or 0.7 and high frequency (e.g., 1 or 0.1 Hz) is also no guarantee that crack growth will occur. On the surface, this is a very surprising observation, although in fact it has been widely observed – but not so widely documented. Examples include:

- several of the ABB tests, where many hours of cyclic loading at R = 0.7 at 1, 0.1 and 0.01 Hz were performed. In many cases substantial crack growth occurred. However, in specimens 44 and 28, relatively little growth occurred – not surprisingly, these were tests performed at the lower K_{max} level of ≈ 27 MPa$\sqrt{m}$, so that the ΔK level is much lower than, e.g., tests performed at a K_{max} of 45 MPa$\sqrt{m}$, as in specimens 27 and 33 (see Appendix C of the ABB Final Report [4]).
- more pronounced and well documented problems were reported by AEA Technology (see Table 3 of the AEA Final Report [5]). On their second test (specimen 35) they reported difficulties associated with achieving sensible fatigue crack growth rates extending for over 500 hours, despite increasing K_{max}

from 33.7 to 42.6 MPa$\sqrt{m}$ and using 0.1 Hz and load ratios of 0.3 (mostly) and 0.7. Their Table 12 compares the observed rates (often zero) to the expected inert fatigue rate, which typically shows a three order of magnitude discrepancy, even at ΔK values of $\approx$ 30 MPa$\sqrt{m}$. It can be no surprise that the subsequent behavior at constant load was also poor. There is no evidence that this is associated with improper handling or experimental procedures at any of the laboratories (it is most likely associated with various problems identified in the machining and original fatigue pre-cracking done before the specimens were sent to each laboratory, as discussed elsewhere). However, it does reinforce the *requirement* that crack growth testing not be blindly conducted following a simple-minded recipe – careful monitoring of cracking behavior is essential to ensure that the response is sensible and reproducible at each stage.

- on the initial fatigue pre-cracking done at VTT on their third CT specimen, crack growth was obtained at R = 0.3 and 0.5 at 1 Hz, but not subsequently at R = 0.7 at 1 Hz, despite remaining at this loading conditions for 165 hours (see Table 12, page 37 and Figure 18 on page 42 of the VTT Final Report [7]). A subsequent return to R = 0.5 at 287 hours (all at same K_{max} of 27 MPa$\sqrt{m}$) also produced no growth (actually recorded as 1.1×10^{-8} mm/s, but this is effectively zero given the time duration and crack length resolution), despite the fact it had earlier produced rapid fatigue crack growth at 3.1×10^{-5} mm/s. Raising K_{max} to 30 MPa$\sqrt{m}$ at R = 0.5 at 314 hours did finally restore crack growth (to 3.4×10^{-5} mm/s), and growth was sustained as the K_{max} was reduced to 29 MPa$\sqrt{m}$. However, on shifting to a K_{max} = 27 MPa$\sqrt{m}$ and an R = 0.7 at 338 hours, the observed growth rate was substantially retarded (5.4×10^{-7} mm/s vs. 1.7×10^{-5} mm/s at R = 0.5). Perhaps not surprisingly, dropping to 0.01 Hz produced effectively no crack growth (reported as 3.0×10^{-9} mm/s), although raising K_{max} from 27 to 28 MPa$\sqrt{m}$ did produce some growth (although again somewhat retarded) of about 7.5×10^{-8} mm/s. A subsequent change to constant load at 526 hours produced essentially no crack growth. A final "gentle" cyclic loading phase at R = 0.7 and 0.001 Hz started at 1128 hours produced more reasonable rates, but still somewhat lower than average. Clearly, obtaining well-behaved crack growth under near-constant load conditions (and even other aggressive cyclic loading conditions) requires that good response be obtained at every step of the process.

Machining and Fatigue Pre-Cracking Issues.

As is clear from the discussion above, sensible crack growth rate behavior depends strongly on establishing well-behaved response during fatigue pre-cracking, and making a well-controlled transition from the transgranular pre-crack to an intergranular stress corrosion crack. While difficulties in achieving the expected crack growth behavior are common, the difficulties experienced by all laboratories in the Round Robin were very unusual. The most likely cause of these problems was identified as the machining and fatigue pre-cracking that was performed before the specimens were shipped to each laboratory. The initial shipment

of specimens revealed an unusual machining appearance, with metal plastically deformed into the notch region by > 1 mm at the side grooves, as if they were formed after the specimen had been machined by broaching (a linear machining process) from the back to the front of the specimen. These specimens were not tested, and changes were made to subsequent specimens. However, examination of the fracture surfaces after the first test revealed a very unusual fatigue pre-crack appearance (see Figure 11 in the GE CRD Final Report [5] – similar fractographs appear in all reports) in which crack growth occurred only in the central 75% of the specimen during the latter stages of fatigue pre-cracking, with cracking "pinned" at one location near the edges of the specimens.

This is a highly unusual appearance, and all laboratories observed crack growth (if any) only in the central area. The uneven fatigue pre-crack front also led to mis-estimation of the starting crack length (which was determined by examining crack extension in the side grooves), and causes some problems for the reversing dc potential drop technique, which is quite sensitive to uneven crack fronts. This is not an inconsequential issue, because uniform crack advance along the entire crack front is considered an important, if not essential, ingredient in obtaining good test results. Growth along isolated areas – or even the majority –of the crack front will be under-registered by all potential drop measurement techniques; conversely, if there is a thin, uncracked ligament that begins cracking, it will be registered as a very rapid crack growth rate. Worst of all, there is no way to know how non-uniform a crack front was throughout a test – the only evidence appears during fractographic examination. Even if occasional evidence of uneven crack fronts is observed in some specimens, there is a reasonable basis for suspicion about what may have existed in the middle of other test specimen, so that the issue must be considered of broader concern in the data.

Crack front unevenness is the major cause of post-test corrections of crack length. Unfortunately, unless the unevenness remains constant throughout the test – which is exceedingly unlikely – the correction factor will not be constant for the data obtained throughout the test, but will start small (assuming the cracking front started uniform) and increase. Thus, correction factors of 2.7X (e.g., from Table 2, page 8 of the ABB Final Report [3]) might best be applied by correcting the early test data by 1.2X, and the later data by 5X. Using a constant correction factor produces artificially high growth rates for early test data, and artificially low rate for data obtained late in a test. The problem becomes more extreme as the correction factor increases, and some literature data have correction factors above 10X. Unfortunately, there is no way to know how to accurately distribute the correction factor throughout any test.

Selection and interpretation of crack growth rate data

Figure 11 shows the entire collection of constant and "gentle" cyclic loading crack growth rate data vs. the reported corrosion potential. Given that the test conditions were quite similar for all of these data – yet the reported data are quite divergent – it is not reasonable

to treat all of the reported corrosion potential or crack growth data as equally reliable or "correct". Of course, there are some variations in stress intensity and water chemistry that must be accounted for, although the data can either be "grouped" or "corrected" (normalized) to account for these effects (the measurement differences and errors from lab-to-lab are small for both stress intensity and solution conductivity).

There is no ideal solution to the problem of the wide differences in reported corrosion potential, because neither this program nor any other has been designed to *identify* and *correct* differences in corrosion potential measurements, so that an agreed-upon "correct" value of corrosion potential can be identified for any given water chemistry condition. The strategy used in this report is to *assume* that the measurements performed at GE CRD are approximately correct, then *assign* corrosion potentials to all crack growth data based on their dissolved oxygen level. This was done by setting a baseline corrosion potential for each of the water chemistry ranges (e.g., 180, 150 and 120 mV_{she} for 2000, 500, and 200 ppb O_2, respectively), then applying a random +20 mV variation to prevent data from being plotted on top of each other. This procedure changes the appearance of Figure 11 to that shown in Figure 29 – a much tighter distribution in corrosion potential.

However, this still leaves the bigger problem of the unexpected and unacceptable range – which span three orders of magnitude in Figure 29 – in reported crack growth rates. This wide distribution can be seen more clearly in Figures 30 and 31 for constant and "gentle" cyclic load, respectively. Figures 32a and 33a show this same information on a log normal - probability basis, where the non-normal behavior is readily seen from non-linearities (perfectly normal data would all fall on a straight line). Because the data are widely dispersed, and "no growth" data are included, the standard deviation of the overall data sets is very large, and a simple measure of the typical scatter in medium sized data sets – $\pm$ 2 standard deviations – is very high.

Recognizing that there are no simple recipes for identifying the "right" or "correct" data from such a scattered collection, several approaches will be discussed. The first (not necessarily the best) involves removing "no growth" data, then selecting the data nearest the mean of the remaining data that is "most statistically normal". The selected data is shown by the arrows in Figures 32a and 33a, and re-plots of the selected data are shown in Figure 32b and 33b. This produces a mean growth rate that is about an order of magnitude higher than the mean of the overall data set, and reduces the $\pm$ 2 standard deviation "scatter" by about three to four orders of magnitude! This collection of selected data is also shown in Figure 34, which shows the relatively small effect of the correction for stress intensity (in these selected data), as well as the good agreement between the constant load data and the "gentle" cyclic load data (the horizontal arrows show the averages, which differ only by 1.56X (1.68×10^{-7} mm/s vs. 2.62×10^{-7} mm/s).

The constant load data is replotted in Figures 35 and 36 to show the effect of both normalization to 30 MPa$\sqrt{m}$ and differences in water chemistry. Figure 35b simply shows a

more restricted range of the data, i.e., by removing the "tails" of the data in Figure 35a. The difference between the data in 2000 ppb O_2 pure water and in 500 ppb O_2 plus 25 ppb sulfate is relatively small, although the data in 200 ppb O_2 pure water exhibits a mean growth rate that is about 1.71X lower. Figure 35 also identifies the data obtained over the longest time intervals, up to 1132 h.

Another approach for identifying the highest quality data can be based on selecting the data using the product of *"the crack growth increment (mm)"* times *"the test time in that increment (hours)"*. Figures 37 and 38 show plots of the data selected on the basis of an arbitrary threshold of 10 in the weighting factor. Figure 37 shows the data both as-reported and normalized to 30 MPa$\sqrt{m}$; the data in Figure 38 are not normalized.

Ultimately, the identification of the best data requires expert judgment ideally based on years of experience in stress corrosion crack growth testing, evaluation and modeling. The range of complex stress corrosion responses are large, and often dominate even moderately well controlled, well behaved data such as has been generated in this program. This subset of the Round Robin data are shown in Figure 39, and have been normalized to 30 MPa$\sqrt{m}$ and plotted on the basis of "corrected" (*assigned*) corrosion potential. The mean of this data is not greatly different from the mean of the data selected by the various other "screening" techniques.

Crack Growth Rate Data, Testing, and Implications.

The objective of the Round Robin program was to determine how closely five highly qualified laboratories could reproduce each other's corrosion potential and crack growth rate data. While some scatter in results was recognized as inevitable, in fact large differences in both measured corrosion potentials and crack growth rates were observed in this program. Measurement of any physical process leads to scatter, although the range of the observations (e.g., about 400 mV in potential and four orders of magnitude in growth rate) vastly exceeds the scatter associated with either physical process. While it was not the objective of this program to track down the origins of the scatter, it is likely the result of:

- the desire of the program to utilize long time periods under fixed conditions, even when the crack growth behavior was abnormally low (especially zero). In some cases, this patience was rewarded with an eventual transition to well-behaved crack growth, but more often no growth, or highly retarded growth rates were observed – and these constituted a significant fraction of the overall observations.
- the significant problems with specimen machining and fatigue pre-cracking (as noted in the fractographic evaluation), the greatly retarded fatigue crack growth rates (e.g., at $R \leq 0.5$, ≥ 0.1 Hz), and in the difficulty in achieving a straight fatigue crack front all had a synergistically negative effect.
- the significant non-uniformity in the final SCC crack front resulted from preferential IGSCC growth in some areas, and inhibited (or zero) crack growth in some regions of the crack front had a significant role, especially in the accuracy and interpretation of potential drop crack length data. Potential drop is very sensitive to uneven crack

fronts, and the evolution of unevenness during a test makes it impossible to back correct data with any confidence.

The Round Robin results confirm that high quality stress corrosion cracking test data not only require "nominally" well-controlled conditions (good water chemistry, stable temperature, good corrosion potential measurements, etc.) but depend strongly on the intervention and good judgment of the experimentalist. Whether the experience in this program of *one* or *all* laboratories is considered, it is clear that, in the vast majority of instances, stress corrosion crack growth did not readily occur by merely following "high quality" procedures and establishing "well-controlled" test conditions, even under conditions that are moderately aggressive (high corrosion potential) and ultimately produce high growth rates (e.g., $\geq 10^{-7}$ mm/s). At least as importantly, some sustained crack growth rates, which gave the appearance of being reasonable and linear, were more than a factor of 5 - 10X lower than many other growth rates that were obtained (earlier and later) under precisely the same test conditions by the same laboratory (a significant factor here may be that growth occurred only along parts of the crack front, giving the appearance (by potential drop) of a slower growth rate). Clearly, meaningful data are not obtained by simple "dunk and check" testing approaches.

Consensus Values and Application of Growth Rate Data.

Figure 39 (and many other plots, including the individual crack length vs. time plots from each laboratory) show that well controlled tests in 288 °C water containing 200 - 2000 ppb O_2 produce crack growth rates of 1 - 3 x 10^{-7} mm/s. This is consistent with other GE CRD data and modeling at high corrosion potential (Figure 40) [5,11-13,15-16]. However, these rates are substantially higher than those estimated by a correlation [10] (2.86 x 10^{-8} and 8.24 x 10^{-8} mm/s at 0.06 and 0.1 μS/cm, respectively, for 30 MPa$\sqrt{m}$ and 0.15 V_{she}), which is supposed to represent an *upper bound* (95 percentile) of the crack growth rate response of stainless steel. It is, however, based on a limited set of readily available data from only three sources, although it encompasses 122 data. The scatter in these data clearly dilutes all trends in SCC response, as the correlation, e.g., with corrosion potential (with all other effects normalized in the correlation model) is quite weak (R^2 <0.1) – in addition to the dependence on crack growth being shallow (see also Figure 23). The origin of the weak correlation, shallow dependence, and poor agreement with other sets of well-controlled data is a myriad of experimental and interpretational complexities and flaws, so that the mean of such data is the *mean of the flaws, not the mean of the true SCC response.* The assumption that such a collection of data adequately characterizes the *real* stress corrosion cracking response is clearly wrong, and attempts to merely expand such a data set are guaranteed to be unsuccessful because of the powerful diluting force of the existing data coupled with the limited resources and facilities to produce new data. Substantial improvements in testing procedures, diligence in initiating and sustaining stress corrosion cracking, and careful interpretation of existing data are essential, and these data must not be diluted with data of inadequate quality.

Statistical analyses of various data sets clearly show what has also been demonstrated in this program in the more limited regime of high corrosion potential [15]. If one statistically analyzes a large collection of "nominally" well-controlled crack growth data (well known labs, relatively good water chemistry, etc.) for stainless steel or Alloy 182 weld metal, one obtains distributions similar to that shown in Figure 41. This figure shows that, even for a relatively limited set of test conditions, the standard deviation of the log-normal distribution is ≈0.7956, which corresponds to 6.25X (= $10^{0.7956}$) in crack growth rate. The range (mostly scatter) in data sets of this size is generally about ± 2 standard deviations which, in this instance, represents a range of ≈ 1526X. Data correlation can reduce the range to some extent, but (as with the stainless steel data) only based on weak correlations, unusable corrections (e.g., with "heat", which does not translate into any ability to predict – e.g., via composition – the behavior of other heats; indeed, this correlation may actually result from machining or pre-cracking practice), etc.

However, large scatter is not an inherent characteristic of the physical SCC process, because data obtained for single laboratories show *much less* scatter (i.e., lower standard deviation). For example, well controlled crack growth tests on austenitic materials in high temperature water from our laboratory (which employed a fairly aggressive periodic unloading sequence) show a standard deviation of only ≈ 0.15 (1.41X in growth rate). A comparable ± 2 standard deviation measure represents a range of ≈ 3.95X (Figure 42). A similar analysis [15] of well controlled crack growth tests on austenitic materials in high temperature water from another laboratory shows a standard deviation of only ≈ 0.115 (1.30X in growth rate). A comparable ± 2 standard deviations represents a range in the data of ≈ 2.86X.

The large scatter in data could perhaps be tolerated if it accurately represented the fundamental, physical characteristics of stress corrosion. However, this is not the case, because the large scatter in SCC data primarily represents the effects of inadequate definition of testing conditions, poor or missing measurements of important test parameters (e.g., of corrosion potential), and flaws in the measurements and procedures used to evaluate crack growth rate (e.g., uneven crack fronts; pinned crack front from poor machining or pre-cracking; lack of a complete transition from transgranular fatigue crack front to an intergranular SCC front; inadequate "encouragement" of crack advance via brief or continuous use of "gentle" unloading; etc.)

This Round Robin was not immune from these problems, primarily because of problems with the machining, precracking, and subsequent uneven crack front. Such unevenness, including complete pinning of cracking in some areas of the fracture surface, create substantial variability in the crack growth rate. Nonetheless, much of the data obtained in this program are in good agreement with other high corrosion potential data (e.g., Figure 40). Viewed statistically, and when poorly behaved data are included, the Round Robin data still show moderate amount of scatter, although less so than in other fairly large data sets.

The distribution tends to possess roughly a bimodal characteristic, with a higher slope (corresponding to less scatter) at the higher crack growth rates (e.g., Figure 32).

Various selection or screening approaches have been examined in this report, and all lead to a similar conclusion regarding the "correct" mean stress corrosion crack growth rate. The mean crack growth rate is nearly 2×10^{-7} mm/s, a value which obviously depends on the corrosion potential (Figure 23). The difficulty in achieving crack growth in most of these tests is no indication that crack growth is difficult to sustain, or should be expected to occur only intermittently in practice. A significant collection of data, notably from ABB and GE CRD, show that crack growth was sustained for fairly long periods of time and over a significant range in crack depth and crack increment. This is not surprising, since plant components are essentially never fatigue pre-cracked or subject to many of the peculiarities of many laboratory tests that can produce absence or retardation of intergranular crack growth.

The crack growth rate and corrosion potential measurements in this Round Robin program have led to a great deal of clarity and insight, but a variety of cautions should be exercised with regard to the application of these data to BWRs. First, in most areas of the BWR, the high corrosion potentials used in these tests are not directly relevant. In all areas of a BWR, both oxidants and reductants are present (from radiolysis of water), although the balance is rarely stoichiometric (because gases like O_2 and H_2 partition to the steam phase, while H_2O_2 – which is formed in abundance in the core – remains behind in the liquid). Nonetheless, the presence of H_2 has an important influence on corrosion potential. Further, the 500 to 2000 ppb O_2 used in most of the testing in this program is higher than in the BWR, and gives an especially high corrosion potential in the absence of H_2. The dependence of crack growth rate on corrosion potential is quite steep, as shown in Figure 23. Even in areas where such high potentials exist – in the core – it is inappropriate to simply apply a growth rate measured under a specific set of conditions (e.g., 30 MPa$\sqrt{m}$, heavily sensitized 304 stainless steel, etc.) to a particular plant component such as core shroud (where, e.g., heavy sensitization has never been observed, and stress intensities above $\approx$15 MPa$\sqrt{m}$ exist, if ever, only for very small periods in time (or fraction of through-wall thickness).

Lessons learned & recommendations for testing guidelines

While it was not the purpose of this Round Robin program to develop guidelines to improve stress corrosion testing, the need for improvements is clear and many issues were brought to light in this program. In relation to stress corrosion cracking the overall topic of "data quality" is a complex one, and one best divided into several categories related to:

- ***Experimental Quality*** – the optimal scientific and technical design of the experiments and measurements, including: crack length monitoring, corrosion

potential, inlet and outlet chemistry, maintaining stable conditions of K/loading, flow, etc.

- ***Behavioral Quality*** – does the observed data represent real SCC, active crack response? Other issues include stalled crack growth on part or all of the crack front, and the response of dc potential drop.
- ***Interpretational Quality*** – can reported parameters be accurately interpreted and compared, e.g., for sensitization (minimum Cr profile) and conductivity (specific ionic chemistry)?
- ***Quality Assurance*** – documentation of procedures, calibrations, data acquisition...

Of these topics, the first three are of paramount interest, and will be discussed further.

Experimental Quality.

There are a large number of experimental parameters and factors that must be considered and controlled in stress corrosion cracking. These do not necessarily translate into expensive test systems, but do require well designed systems and care in all phases of specimen preparation, handling, and testing. A guideline summarizing many of the issues is given in Appendix A, but some of the most common problems are itemized below.

1. *Simpler issues associated with problems in controlling or reporting:*
   - *water purity* – especially at system outlet, which is a must-know item, and should be controllable to levels relevant to modern BWR operation (i.e., outlet <0.08 μS/cm for pure water testing). If impurities are added, their specific concentration should be controlled and known. Dissolved gas concentrations should be characterized for both inlet and outlet, as consumption of gases can account for significant losses.
   - *material characteristics like sensitization, cold work, microstructure...*– the effects of chromium depletion (sensitization) and cold work on stress corrosion cracking are widely acknowledged. These and other critical characteristics of the material must be accurately described.
   - *specimen machining and pre-cracking* – cold work and residual stresses from poorly machined specimens can have a large effect on subsequent behavior, and processes that induce damage must be avoided. Anomalies in pre-test or post-test (fractography) appearance should be carefully noted and corrected. Similarly, pre-cracking must achieve as straight a crack front as possible, and end below but preferably within <20% of the maximum stress intensity factor to be used in subsequent stress corrosion testing.
   - *transition from transgranular fatigue to intergranular SCC along entire front* – while attempts to accomplish this are rarely factored into SCC testing, it cannot be assumed that a quick or complete transition will occur during SCC testing. The consequences to SCC results can be very large, because in some areas of the crack front the transition from a pre-crack that ends in the middle of a grain to an intergranular stress corrosion crack can be difficult, and contribute substantially to uneven crack fronts at the beginning and even at the end of test. Since this is

totally an anomaly of laboratory testing (plant components are not fatigue pre-cracked), every effort must be made to ensure that this factor plays no role in the results. Several of the final phases of pre-cracking should be done in-situ to ensure the transition to an intergranular crack front and to a crack tip stress field condition (e.g., plastic zone size / configuration) that is as representative as possible of what forms under SCC conditions.

- *stability in load, temperature, water chemistry...* – obviously any significant variation in test conditions is important, and the unknown variations are the most problematical because no awareness of their effect can exist. Noise and total unloading during power blips can affect servo-hydraulic loading systems, and internal pressure fluctuations from high pressure pump and pressure regulation problems, especially the absence of a pulse dampener, can have significant effects. Temperature fluctuations should generally be < 1 °C, although at this level they likely affect the resolution in crack length monitoring more than the SCC process itself.

2. *More complex issues associated with:*
   - *corrosion potential measurement* – after many decades of corrosion potential measurements in hot water, there is still international ambiguity regarding how reproducible corrosion potentials should be, not to mention what the correct corrosion potential is under given conditions. In this program, the range in observed potentials under conditions where the potential should be very well behaved (identical material and water chemistry) is very large, even when all laboratories used the same reference electrode. The origins of these differences were not proven, but are undoubtedly related to:
     a) interaction with the dc potential drop crack monitoring system, which was shown in one lab to produce a ± 1.1 V shift – large enough to cause effects for a significant period of time after the potential drop current was no longer applied.
     b) other leakages of current or galvanic interactions that can produce potential fields within the autoclave, especially between the reference electrode at CT specimen.
     c) placement of the reference electrode relative to the working electrode.
     d) electrical isolation of the stainless steel specimen from loading linkage and autoclave system.
     e) impedance of the wiring and the instrumentation for measuring corrosion potential.

   The water chemistry conditions evaluated in this program produce well-behaved corrosion potentials – nonetheless, many problems existed. The corrosion potential behavior in other water chemistry regimes (e.g., 1 to 20 ppb oxygen) is much more complex and subject to real variability, and therefore much more reliant on the best possible corrosion potential measurements.

- *dc potential drop requirements* – the *requirements* of dc potential drop are often not recognized. In addition to the highest stability in current and temperature, necessary to achieve the highest possible crack length resolution, it is essential that a straight front be maintained during testing. This requirement is a result of the highly non-linear sensitivity of potential drop (also true of compliance) to the last ligament of uncracked metal, which is associated with the current flux lines in a CT specimen, which distribute to the region near the loading pin holes then converge / concentrate near the crack tip. This issue should not be confused with whether cracks in components are more or less straight than in the laboratory – it is simply that the laboratory measurement tool, potential drop, mandates that a relatively straight crack front be maintained.
  Particularly problematical are post-test corrections related to crack front unevenness (this should be the only origin of correction factors, since the potential drop method itself should always be accurate to within several percent – perhaps 20% at the extreme). Many examples exist of correction factors that range up to (and beyond) 10X (1000% correction), and back-attributing this correction uniformly throughout the entire test leads to serious errors (except in the nearly impossible and unprovable case where the degree of unevenness remains constant during the test, in which case no correction factor should be needed). If one considers a simple case where part of the crack front is pinned at the fatigue pre-crack, then the initial error in the potential drop reading is very small (i.e., 1.1X rather than the 10X nominal correction); near the middle of the test the error represents about the average error (10X), and near the end of the test, the error becomes increasingly large (e.g., >100X).
  Because there is no way to know how the crack front unevenness evolved during the test, there is no way to back-correct data. Worse still, if unevenness is noted only in some tests, it is impossible to be confident that it did not exist at the intermediate periods of other tests – here the concern is that, while no post-test correction is needed, retarded growth rates could have been registered by potential drop at some point in the test (as unevenness develops), then as the regions of retarded cracking begin to respond to their ever-increasing stress field, rapid "unzipping" can occur, and this will be registered as much more rapid crack growth rate. These isolated periods of retarded and accelerated crack growth, which are not necessarily short-lived, introduce very serious ambiguities into the interpretation of the entire "real-time" measurement of crack length. Since the problem occurs as any unevenness develops, it is hard to place a fixed criteria on what is an acceptable level of crack front unevenness, although obviously the absolute minimum is preferred. Since the biggest concerns revolve around unevenness that can change with time, it is particularly problematical to have local unevenness (e.g., on a few mm scale along the crack front), or evidence that unevenness on a larger scale (e.g., a curved fatigue pre-crack front) changed significantly during the test. Thus, it might be possible to have some level of confidence in a shallow fatigue pre-crack curvature (e.g., < 0.1 B, or <0.1-inch in

a 1T CT specimen) if there were no evidence that the subsequent stress corrosion crack produce a significant net change in the curvature. It would still have to be recognized that crack advance at the deepest areas of curvature would be under-registered by potential drop to some extent.

Behavioral Quality.

There is clear evidence that, even when all experimental parameters are well controlled, a reproducible stress corrosion cracking response is not always achieved. While the origins of this behavioral problem are not proven, it is likely associated with the tendency for some stress corrosion cracks to retard or arrest. Because dc potential drop is highly sensitive to any portion of the crack front that stops growing (assuming that an initially straight crack front exists), a wide distribution in *apparent* crack growth rate measurements is possible associated with the nature of the unevenness and the fraction of the crack front that retards or arrests, then later may begin to grow rapidly ("unzip").

If "artificial" reasons for this behavior are ignored (machining problems, fatigue pre-cracking anomalies, large changes in stress intensity factor that may produce plastic blunting, etc.), there are two primary factors that may induce this retardation (or local arrest). First, metallurgical inhomogeneities (e.g., grain boundaries where carbide precipitation and Cr depletion does not occur; very large, unfavorably oriented grains which may force transgranular cracking to occur locally; melting defects, etc. Second, it is likely that stress corrosion cracking is inherently probabilistic. If the importance of crack tip strain rate and passive films in stress corrosion cracking is acknowledged, then one origin of this characteristic may be the inter-dependence of a continuing crack tip strain rate on crack advance itself, which produces a redistribution of the stress and strain fields around the crack tip. If this synergy is disrupted for any reason, then both processes are disrupted, at least on a local scale. Since the disruption is most likely at low crack growth rates, it is possible to conceptualize a probability of sustaining crack advance that is proportional to (the log of) the crack growth rate – even at moderately high growth rates the probability (especially on a local scale) may be $<< 1.0$. Support for this concept comes from the well-known tendency for aggressive water chemistries to induce a high fraction of the specimens tested to show similar (high growth rate) behavior.

The repercussion of this concept is that, in addition to all of the "purely" experimental quality controls that must be enforced, there is a further need to carefully evaluate the stress corrosion response for consistency and reproducibility. Approaches include duplication of experimental results, comparison with results obtained under broadly similar conditions, and verification that the observed behavior is consistent with that observed when a smooth transition is made from increasingly "gentle" cyclic loading (e.g., $R = 0.7$, ≤ 0.001 Hz with hold periods at K_{max}) to constant loading. Differences of >3 - 5X in stress corrosion crack growth rate at constant load should be viewed with suspicion, since there is as yet no evidence that well controlled tests should deviate by more than this amount. While these behavioral factors may have implications for plant components (i.e., retardation and arrest

may also occur), it is premature to claim direct credit for these factors because of the large population of possible cracking sites in most circumstances. Also, the time frame involved in operating plants is vastly greater that laboratory tests, and there many operating perturbations that may re-activate cracks just as "gentle" cycling does in laboratory tests.

Interpretational Quality.

In addition to the reasons for observations of anomalously low and high stress corrosion crack growth rates discussed below, there are a variety of *confusion factors* that can severely complicate the interpretation of stress corrosion cracking response.

- mis-representation of test conditions, e.g.:
  - ⇒ water purity, e.g., from release of impurities from system, lack of reporting of outlet conductivity, failure to identify types and levels of specific anionic additions...
  - ⇒ mis-measurement of corrosion potential
  - ⇒ loading "noise" from the machine or fluctuations in the internal autoclave pressure
  - ⇒ imprecise description of sensitization (i.e., absence of the Cr profile – especially the minimum Cr level), cold work, etc.

Determining Correct SCC Growth Rates.

From the Round Robin and other experience, it is possible to suggest techniques to help determine the correct stress corrosion crack growth rate.

- Avoid problems with test controls and stability, e.g., corrosion potential measurements, inlet and outlet water quality, load and temperature fluctuations, etc.
- Ensure a complete transition from the transgranular fatigue pre-crack to an intergranular stress corrosion crack, which can only be accomplished using an in-situ pre-cracking / transitioning phase. During this phase, the K_{max} should be shifted to the stress intensity factor to be used for stress corrosion testing, the load ratio R shifted to R = 0.7, and the frequency slowed and/or hold time at K_{max} increased. These shifts prevent plastic blunting on initial loading, and help develop a plastic zone configuration representative of that which forms during stress corrosion testing.
- Prevent uneven cracks and dc potential drop errors by using the best possible machining and pre-cracking practice, and using periodic unloading during some phases of testing to help keep the crack front as straight as possible.
- Duplicate experimental results and compare with results obtained under broadly similar test conditions. For identical test conditions, a difference of >3 - 5X is indicative of problems.
- Verify that the constant stress intensity factor data are consistent with that obtained using a smooth transition from increasingly "gentle" cyclic loading, e.g., R = 0.7 and a shift from 0.001 Hz to a ≥ 9,000 second hold time at K_{max}.

It is further possible to suggest some reasons for observations of *anomalously low* stress corrosion crack growth rates:

- dc potential drop influences the apparent crack growth rate because it tracks the approximate minimum crack depth along a crack front. Thus, if cracking in any portion of the crack front is retarded or arrested, it will have an abnormally large effect of the observed behavior.
- incomplete transition from the transgranular fatigue pre-crack to an intergranular stress corrosion crack, which may pin portions of the crack front (see prior item)
- SCC crack retardation or arrest along part of front resulting from:
  - ⇒ test perturbations in load, temperature, chemistry...
  - ⇒ metallurgical inhomogeneities than pin part of the crack
  - ⇒ residual stress / damage from fabrication, machining, or fatigue pre-cracking
  - ⇒ inherent probability of sustaining SCC, whose origin is the inter-dependence of crack tip strain rate and crack growth rate at constant load

Reasons for observations of *anomalously high* stress corrosion crack growth rates include:

- dc potential drop influences apparent crack growth rate because it tracks the approximate minimum in crack depth. When a (narrow) uncracked ligament begins to "unzip", potential drop will register this a rapid advance of the entire crack
- pre-existing cracks (not SCC), e.g., hot cracking in Alloy 182
- mis-use of (i.e., any use of) post-test corrections for dc potential drop errors in final crack length. There is no basis for knowing how to back-correct the data throughout the test
- the use of stress intensity factors "significantly" in excess of LEFM validity

While simplistic estimates of the characteristics of the international data cannot be used quantitatively, in general the "too low" growth factors are perhaps ≈3 – 5X more numerous than the "too high" factors. Thus, in general, more credibility must be given to the upper, but not necessarily the highest, data in a highly scattered data set.

Conclusions

1. Consistent, high crack growth rates, e.g., 1 - 3 x 10^{-7} mm/s were obtained in high purity water in 500 - 2000 ppb O_2. Growth rates decreased with dissolved O_2, with about a 5 - 10X decrease on changing from 2000 to 200 ppb O_2 in pure water. Several laboratories observed a consistent effect on crack growth rate as the chromate level was changed from <20 ppb to >50 ppb by partially bypassing the demineralizer.

2. The observed crack growth rates were fully consistent with other data performed using the same types of experimental controls and care that were used in the Round Robin. It

was also consistent with predictions based on the PLEDGE crack growth model, as well as the SKI and NRC disposition lines, but were considerably higher than those predicted by the BWRVIP correlation. However, the more aggressive water chemistry conditions used in the Round Robin are not directly relevant to "normal water chemistry" in all areas of the BWR, because of a combination of (a) high K levels, (b) high O_2 levels, (c) the absence of reducants (e.g., H_2), and (d) the presence of levels of sulfate (25 ppb) in many tests.

3. All laboratories achieved very good test controls and monitoring, e.g., for water purity, load, temperature, dissolved O_2, etc. Differences in laboratory capability existed in the areas of crack length resolution, control outlet water purity, performance of their own preferred reference electrode, etc. Even when a common reference electrode was used, there was a large difference in measured corrosion potentials, the origins of which can only be guessed. Clearly more work is needed to resolve these differences so that reproducible, high quality measurements of corrosion potential and crack growth rate data can be made.

4. Obtaining crack growth under constant load conditions (or even under "gentle" cyclic loading conditions in some instances) proved quite difficult, much more so than is normal based on the experience of all laboratories. This is most likely associated with problems during machining and pre-cracking of the as-received specimens. This also almost certainly contributed significantly to the scatter in the crack growth rate data under the well-defined, well-controlled used in the Round Robin, although the problems were overcome in many instances by additional fatigue pre-cracking and the use of "gentle" cyclic loading.

5. Several elements important to obtaining high quality crack growth data are evident from the Round Robin. The best data came after well behaved cracking under (corrosion) fatigue conditions were achieved. It is also important to obtain intergranular stress corrosion cracking along the entire crack front. This requires that the fatigue pre-crack front be relatively uniform, and that a complete transition from the transgranular precrack to an intergranular stress corrosion cracking occur. The latter is best accomplished under water chemistry conditions that give moderate to high stress corrosion crack growth rates using a series of transitional cyclic loading conditions involving, e.g., R = 0.7 and decreasing frequency and/or increasing hold times.

6. Because of (a) difficulties with pinning of the crack front, (b) incomplete transition from transgranular to intergranular cracking, and (c) the tendency for the crack front to become uneven under constant loading conditions, the use of a "gentle" cyclic loading condition is highly valuable. Cyclic loading at R = 0.7 and 0.001 or 0.0001 Hz (with or without a 1,000 to 10,000 s hold time at the maximum load) proved adequately "gentle" such that crack growth rates were not consequentially increased (i.e., biased by <50%) in the 2000 ppb O_2, high purity water regime.

"Gentle" cyclic loading plays a crucial role in helping: (a) crack growth to commence (both the transgranular to intergranular transition, and intergranular "re-initiation"); (b) to maintain stable crack advance over time; and (c) to maintain a straight crack front that is important both to accuracy and interpretability of dc potential drop crack monitoring and to a uniform and interpretable stress intensity distribution at the crack front. It should be considered a crucial element in stress corrosion testing, because the effect on testing and data interpretation are severely complicated if not completely compromised by these problems. The use of $R > 0.75$ should be avoided, because of its lack of consistent effectiveness. While $R = 0.7$, 0.001 or 0.0001 Hz should be adequately gentle for most test conditions and materials, the effect (or assumed lack of effect) of cycling should be verified for the specific test conditions.

7. Stable crack growth over long time periods (several for >1000 hours, quite a few for >500 hours) and crack depth increments were obtained at constant load in many tests. While there were problems in achieving (somewhat fewer problems in maintaining) stress corrosion crack growth rates, it is not reasonable to expect that crack retardation or arrest will predominate in practice – at least not under moderate to high crack growth rate conditions (e.g., $>10^{-8}$ mm/s). The best understanding of the crack arrest phenomena is that at constant load the probability of sustaining cracking is proportional to the crack growth rate; thus, at growth rates below $\approx 10^{-8}$ mm/s (e.g., for hydrogen water chemistry or noble metal coatings), the likelihood of crack arrest is much higher.

8. The effects of dissolved O_2 (e.g., 2000 vs. 500 vs. 200 ppb) were not nearly as apparent in the overall mean response of the complete data set as in well-controlled experiments in which O_2 was systematically changed during a single test. "Overall mean" responses are too prone to diluting the effects of individual variables to be nearly as reliable as controlled tests, although clearly more than a few controlled tests are needed to establish a trend.

9. Thus, "high quality" stress corrosion crack growth is not produced by merely following "high quality" procedures and establishing "well-controlled" test conditions, even under conditions that are moderately aggressive. This applies equally to the interpretation of data, since some sustained crack growth rates, which gave the appearance of being reasonable and linear, were more than a factor of 5 - 10X below the mean of the high quality data. Clearly, good SCC data are not obtained by simple "dunk and check" testing approaches.

References

1. P.M. Scott, "Recommended Test Procedure for Studies on Crack Growth in Simulated LWR Water Environments", Proc. Third Intl. Atomic Energy Agency Specialists Mtg on Subcritical Crack Growth, Moscow, USSR, May 1990, NRC NUREG/CP-0112 (ANL-90/22), Vol. 1, p.117-128.

2. K. Pein and A. Molander, "Jämförelse av refernselektroder för BWR-miljöer", Studsvik Report to K. Gott (SKI), March 1998.

3. M. Stigenberg, "SKI Round Robin: IGSCC Crack Propagation Rate Measurements in BWR Environments", ABB Final Report to K. Gott, SKI, PBB 97-212 Rev. 1, Nov. 20, 1997.

4. P. Hurst, I.L. Bramwell, and D. Dodson, "IGSCC Crack Propagation Rate Measurements in BWR Environments", AEA Technology Final Report to K. Gott (SKI), AEAT-2702, Jan. 1998.

5. P.L. Andresen, P.W. Emigh, and Y.J. Kim, "IGSCC Crack Propagation Rate Measurements in BWR Environments", GE Corporate R&D Final Report to K. Gott (SKI), Feb. 27, 1998.

6. P. Lidar, "Crack Growth Rate Measurements of Type 304 Stainless Steel in Simulated BWR Environments", Studsvik Material Final Report to K. Gott (SKI), M-97/103, Nov. 1997.

7. U. Ehrnstén and P. Aaltonen, "IGSCC Crack Propagation Rate Measurements in BWR Environment", VTT Manufacturing Tech. Final Report to K. Gott (SKI), VALC464, March 23, 1998.

8. "Statens kärnkraftinspektions föreskrifter om mekaniska anordningar i kärntekniska anläggningar", SKIFS 1994:1, ISSN 1400-1187, SKI, Stockhom, Sept. 26, 1994.

9. W.S. Hazelton and W.H. Koo, "Technical Report on Material Selection and Processing Guidelines for BWR Coolant Pressure Boundary Piping", NUREG 0313 Rev. 2, US NRC, Jan. 1988.

10. "Evaluation of Crack Growth in BWR Stainless Steel RPV Internals", BWR Vessel and Internal Project, BWRVIP-14 Report, EPRI TR-105873, March 1996.

11. F.P. Ford, D.F. Taylor, P.L. Andresen and R.G. Ballinger, "Corrosion Assisted Cracking of Stainless Steel and Low Alloy Steels in LWR Environments", Report NP5064S, EPRI, Palo Alto, Feb. 1987.

12. F.P. Ford and P.L. Andresen, "Corrosion in Nuclear Systems: Environmentally Assisted Cracking in Light Water Reactors", in "Corrosion Mechanisms", Ed. P. Marcus and J. Ouder, Marcel Dekker, p.501-546, 1994.

13. P.L. Andresen and F.P. Ford, "Life Prediction by Mechanistic Modelling and System Monitoring of Environmental Cracking of Fe and Ni Alloys in Aqueous Systems", Materials Sci. and Eng., A103, p.167-183, 1988.

14. S. Suzuki and T. Shoji, "Characteristics of the SCC Surface Crack Propagation in the Low K Region in Oxygenated High Temperature Water", Proc. Eighth Int. Symp. on Environmental Degradation of Materials in Nuclear Power Systems - Water Reactors, ANS, p.685-694, 1997.

15. P.L. Andresen, "Effects of Testing Characteristics on Observed SCC Behavior in BWRs", Paper #98137, Corrosion/98, NACE, 1998.

16. P.L. Andresen, Unpublished results, GE CRD, Schenectady, NY, January 1998.

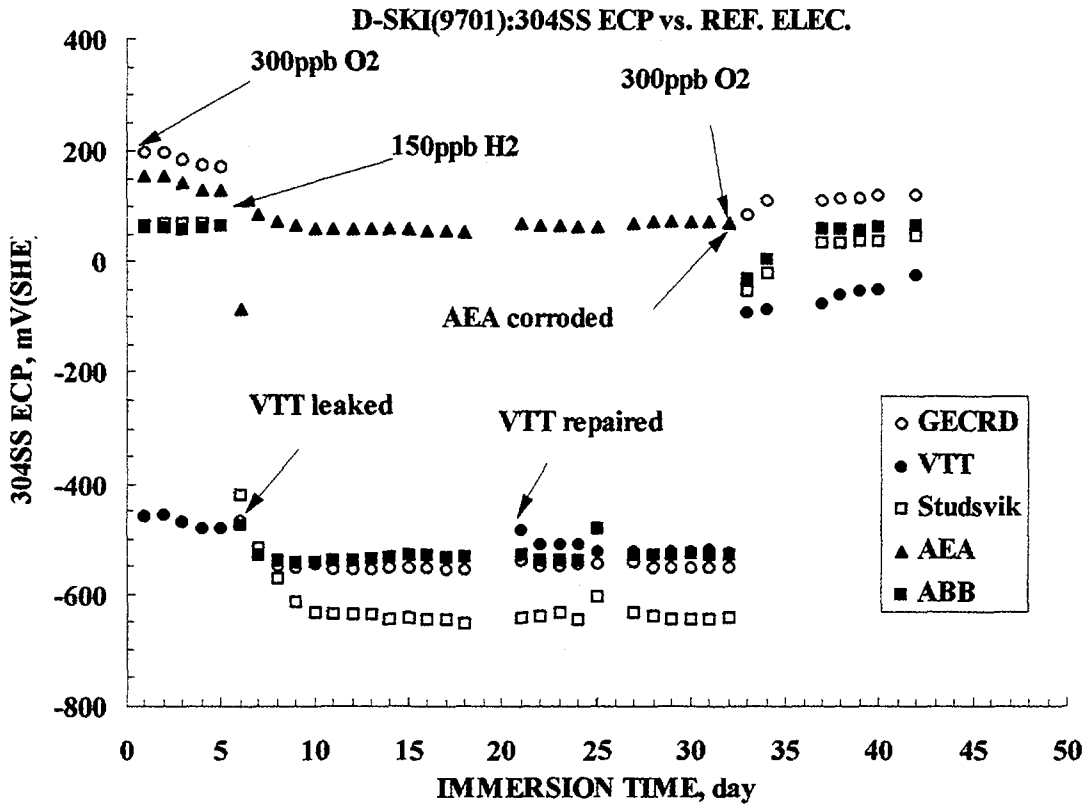

Figure 1. Corrosion potential behavior of type 304 stainless steel measured against the reference electrodes supplied by each of the five laboratories involved in this program. Tests were performed at GE CRD in 288°C pure water under various water chemistry conditions.

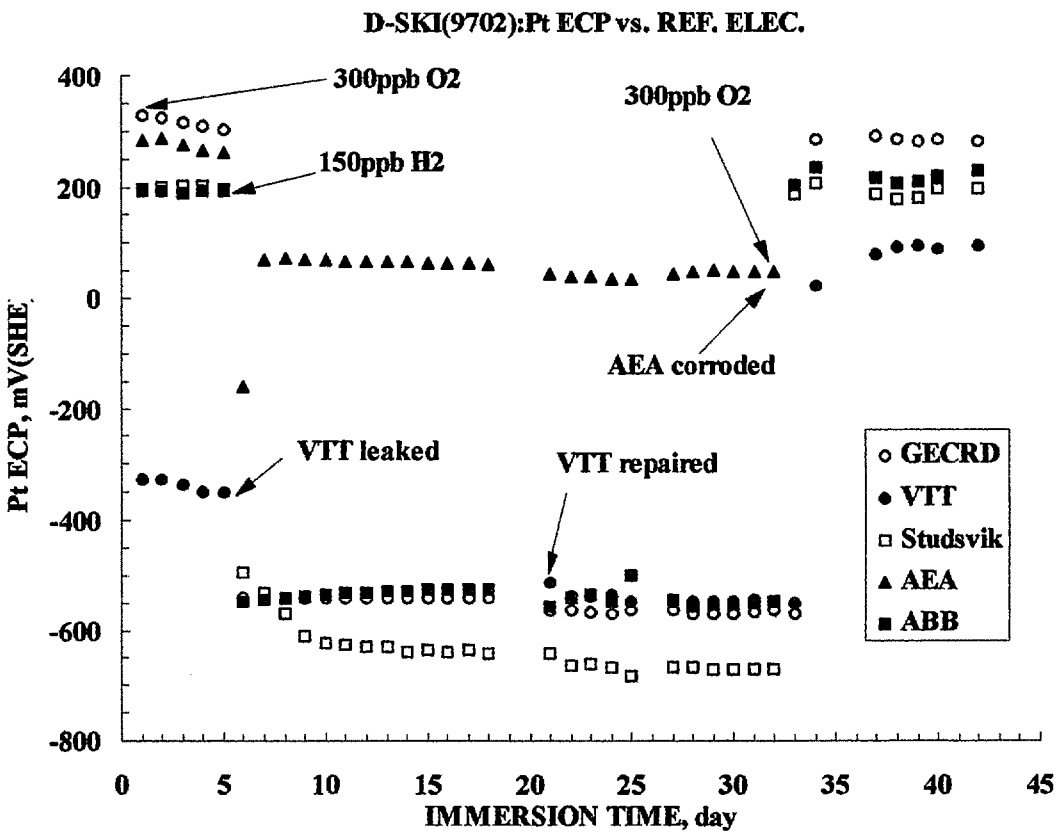

Figure 2. Corrosion potential behavior of Pt measured against the reference electrodes supplied by each of the five laboratories involved in this program. Tests were performed at GE CRD in 288°C pure water under various water chemistry conditions.

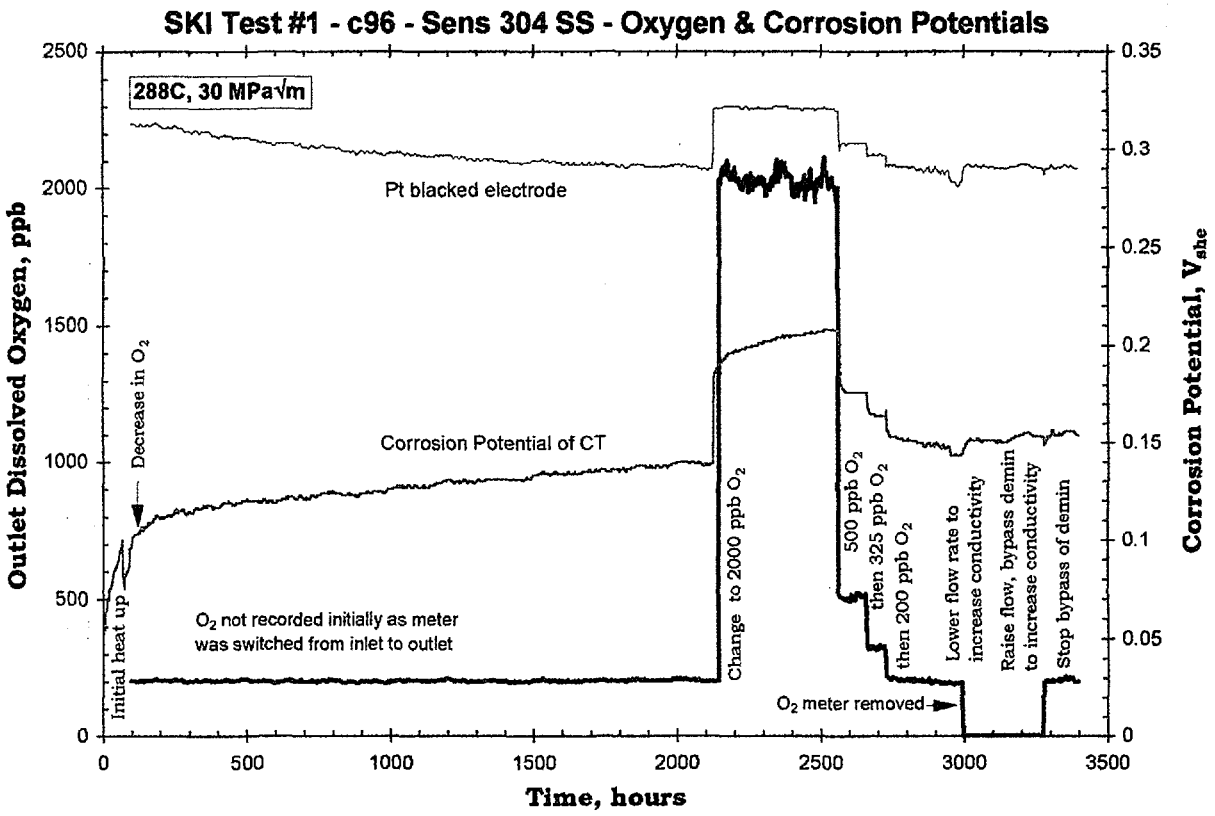

Figure 3. Overview of water chemistry and test conditions for the first test (c96) at GE CRD in 288 C water containing 200 to 2000 ppb O_2. Outlet dissolved O_2 and corrosion potentials of the CT specimen and Pt coupon are shown.

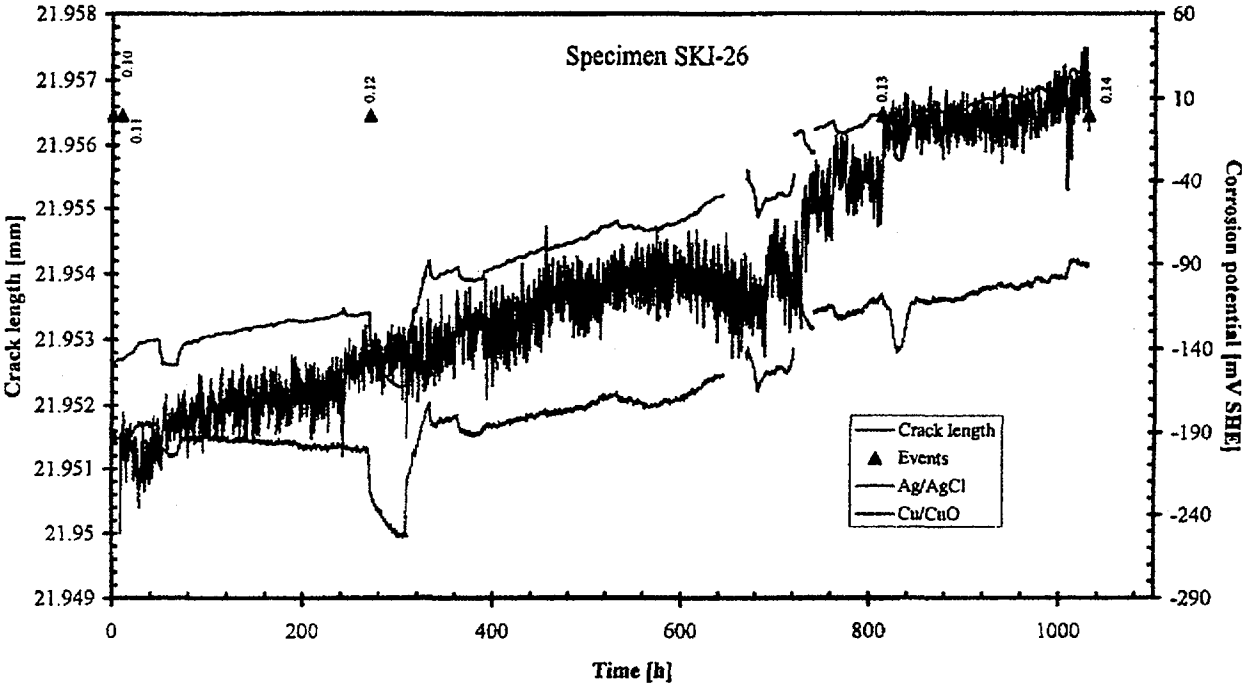

Figure 4. Crack length and corrosion potential vs. time from the first test at Studsvik (Figure B.1.6 in their Final Report [6]). Corrosion potentials are reported vs. their preferred external Ag/AgCl reference electrode and the "common" reference electrode supplied to all laboratories by GE CRD.

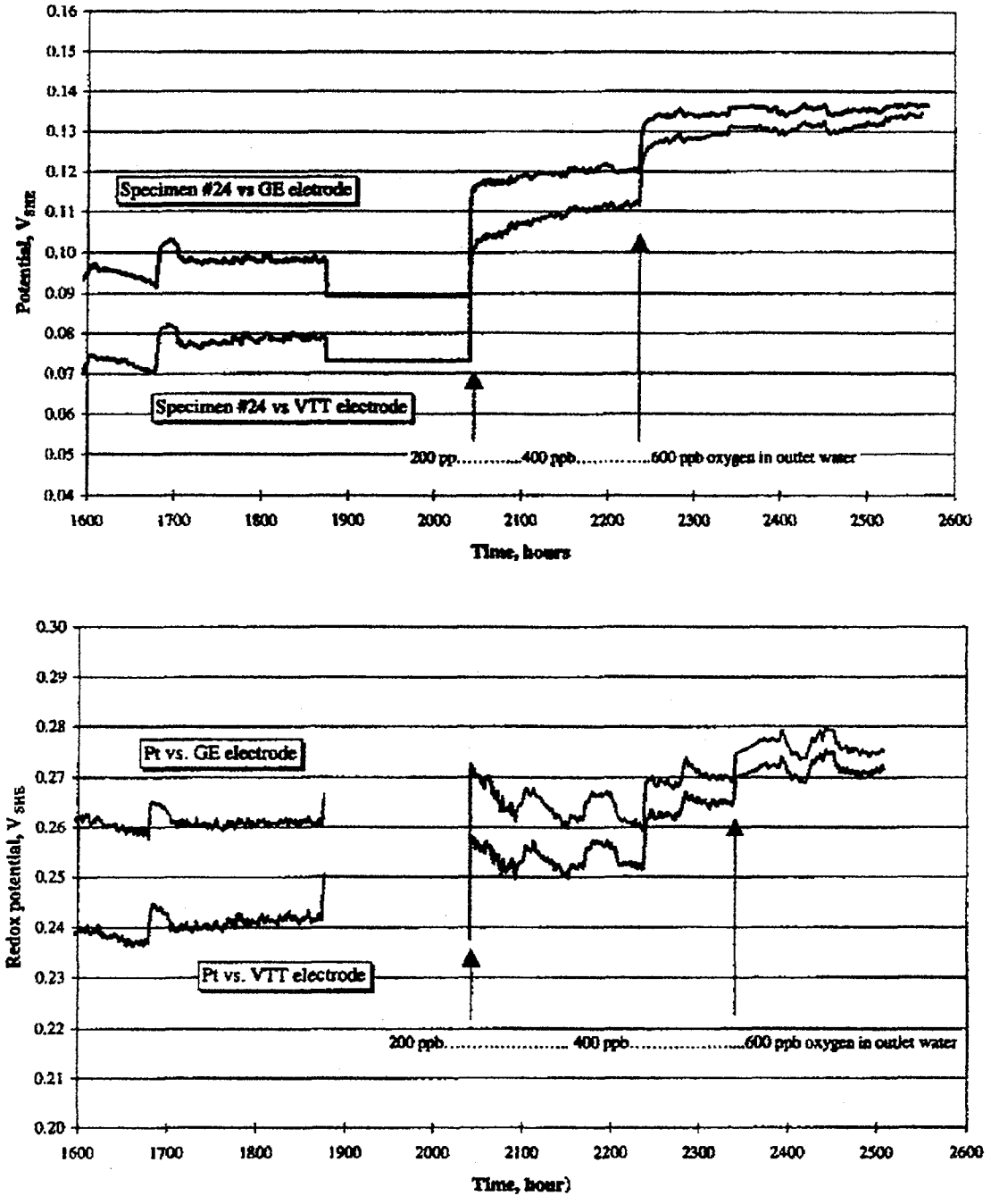

Figure 5. Crack length and specimen and Pt corrosion potentials vs. time from the first test at VTT Labs (Figure 6 d and e in their Final Report [7]). Corrosion potentials are reported vs. their own preferred reference electrode and the "common" reference electrode supplied to all laboratories by GE CRD.

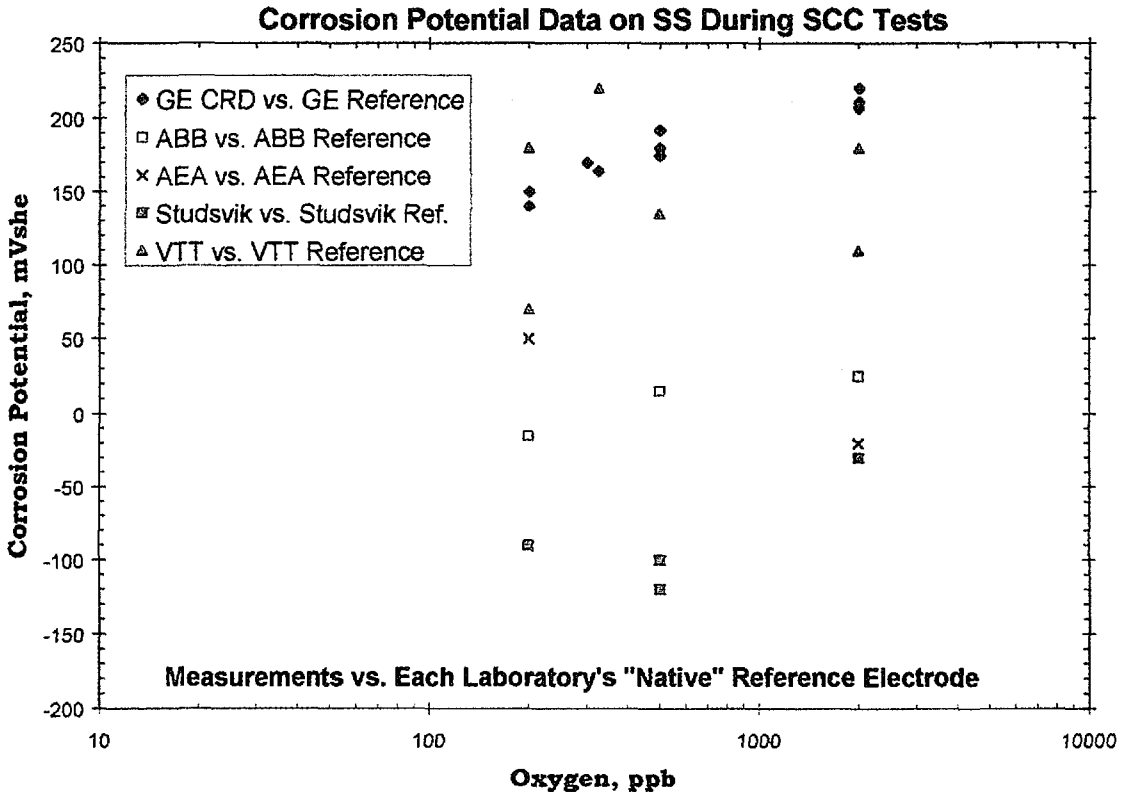

Figure 6. Comparison of the corrosion potential measurements on type 304 stainless steel CT specimens made by the different laboratories as measured using the reference electrode preferred by each laboratory.

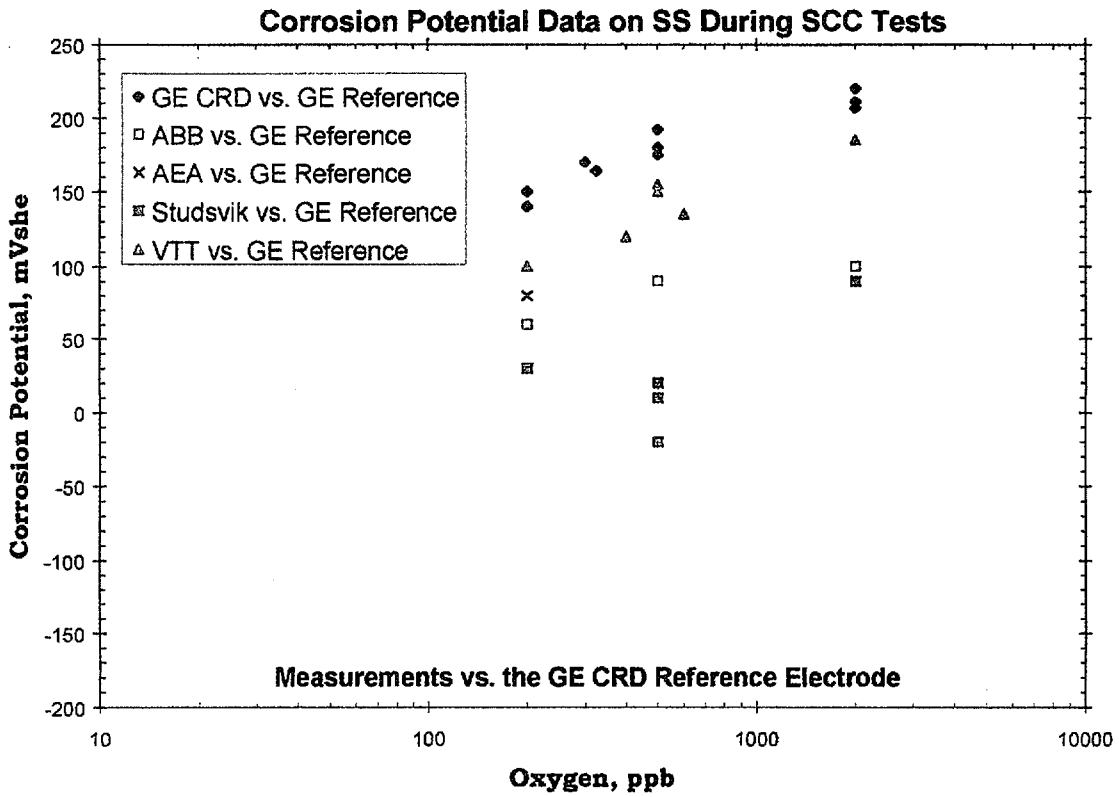

Figure 7. Comparison of the corrosion potential measurements on type 304 stainless steel CT specimens made by the different laboratories as measured using the "common" reference electrode supplied by GE CRD to each laboratory.

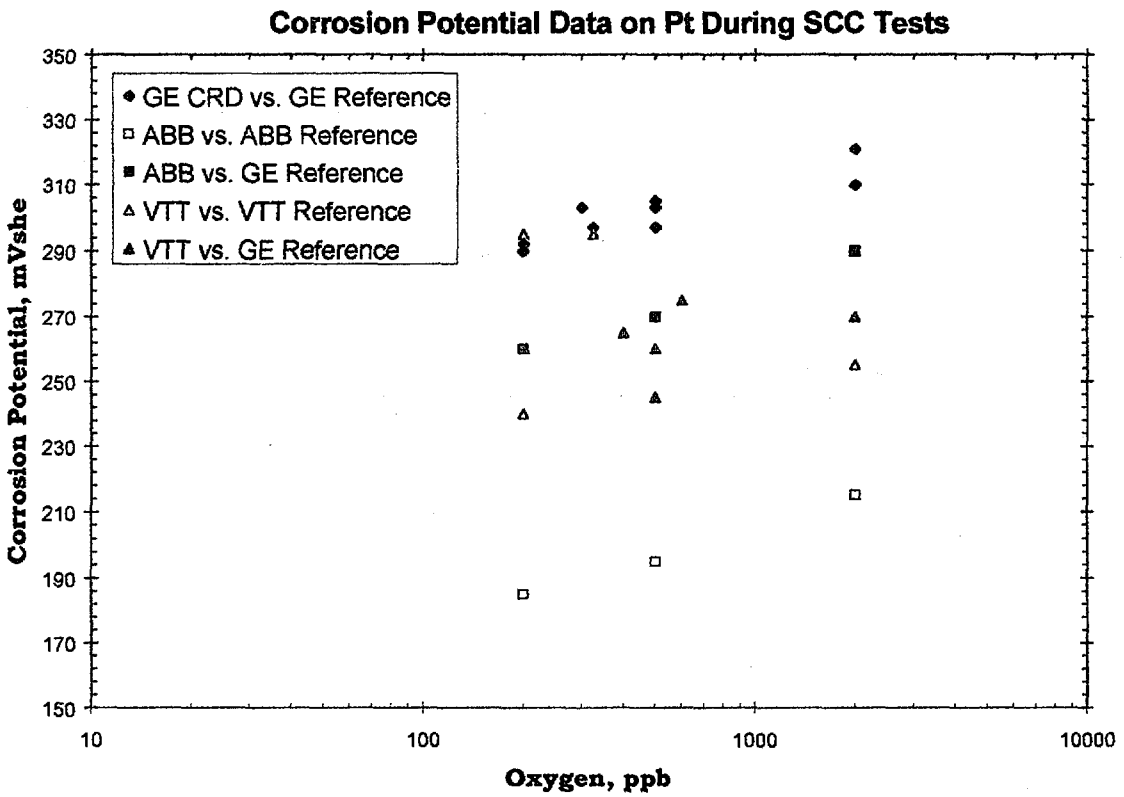

Figure 8. Comparison of the corrosion potential measurements on Pt made by the different laboratories. Values are shown for the reference electrode preferred by each laboratory and for the "common" reference electrode supplied by GE CRD to each laboratory.

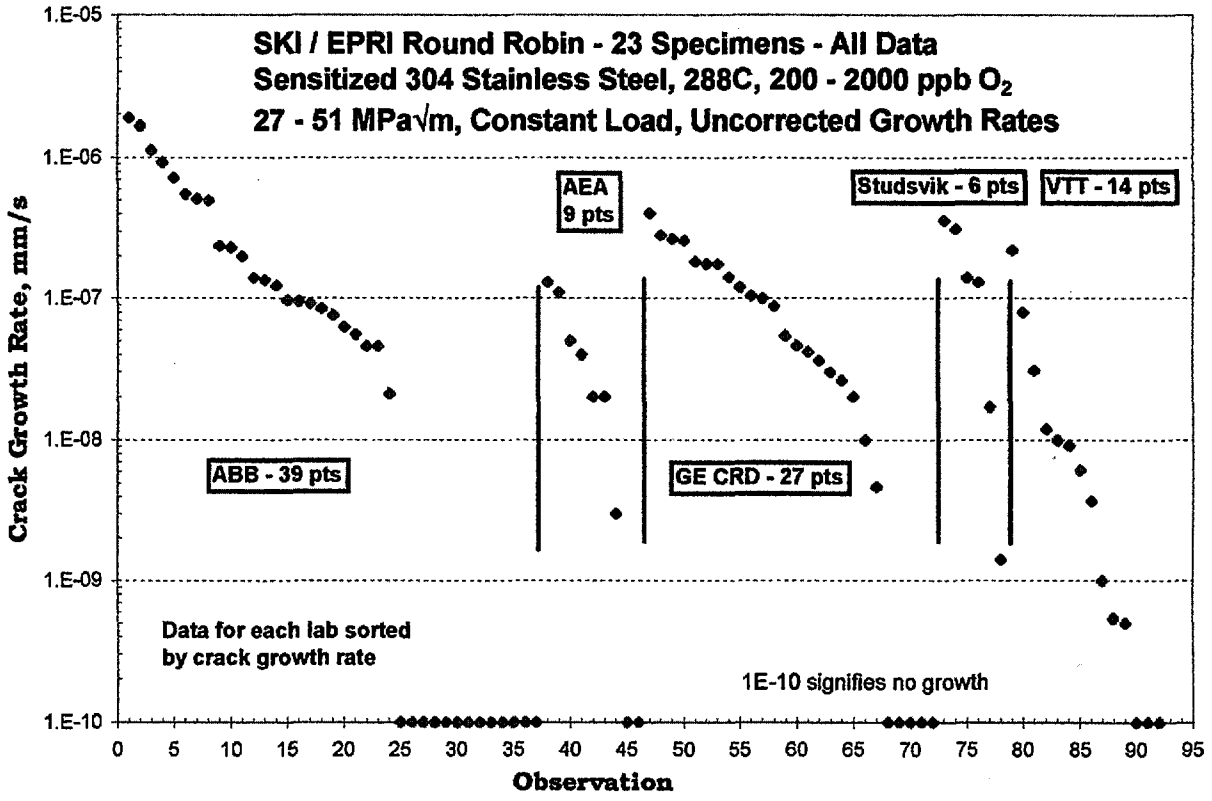

Figure 9. The observed (unscreened and uncorrected) crack growth rate data grouped by laboratory for constant load conditions. A range of water chemistry (e.g., 200 - 2000 ppb O_2) and stress intensity (27 - 51 MPa$\sqrt{m}$) conditions are present in the data, although neither effect produces large (e.g., >10X) effects on growth rate.

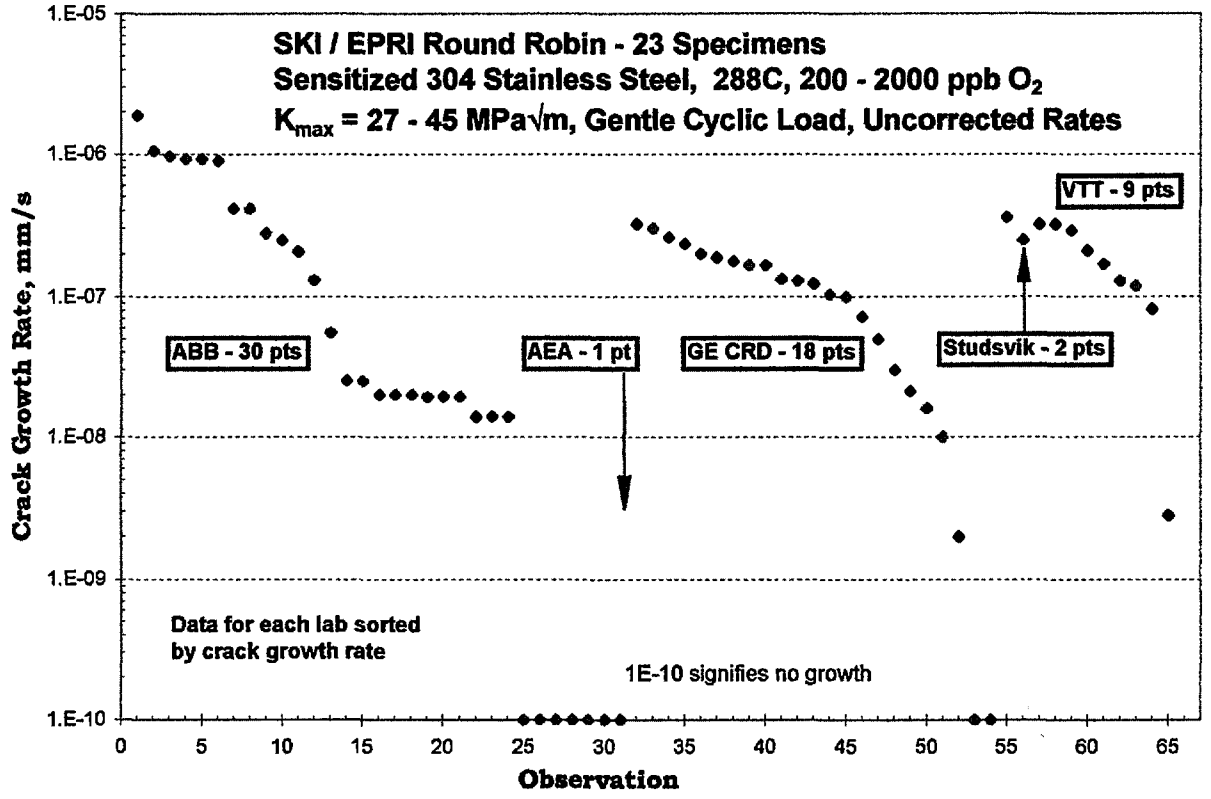

Figure 10. The observed (unscreened and uncorrected) crack growth rate data grouped by laboratory for "gentle" cyclic loading conditions. "Gentle cyclic loading" describes conditions that induce relative little enhancement in crack growth, typically by using a high load ratio (e.g., R = 0.7), low frequencies (e.g., ≤ 0.001 Hz), and often long hold times between load cycles (e.g., 9,000 s). A range of water chemistry (e.g., 200 - 2000 ppb O_2) and stress intensity (27 - 45 MPa√m) conditions are present in the data, although neither effect produces large (e.g., >10X) effects on growth rate.

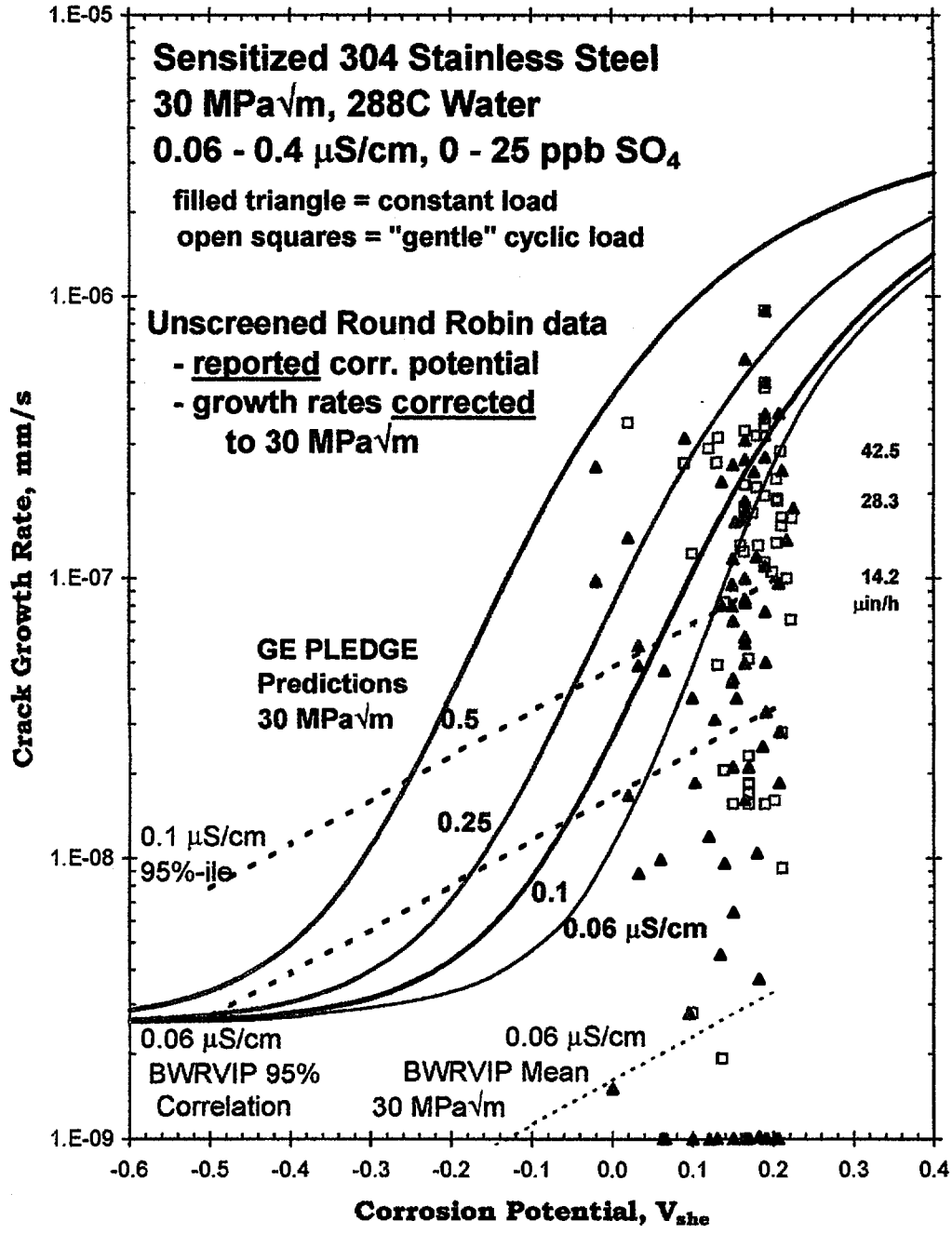

Figure 11. The observed (unscreened) crack growth rate data for constant load and "gentle" cyclic loading conditions. "Gentle cyclic loading" describes conditions that induce relative little enhancement in crack growth, typically by using a high load ratio (e.g., R = 0.7), low frequencies (e.g., ≤ 0.001 Hz), and often long hold times between load cycles (e.g., 9,000 s). A range of water chemistry (e.g., 200 - 2000 ppb O_2) and stress intensity (27 - 45 MPa√m) conditions are present in the data, although neither effect produces large (e.g., >10X) effects.

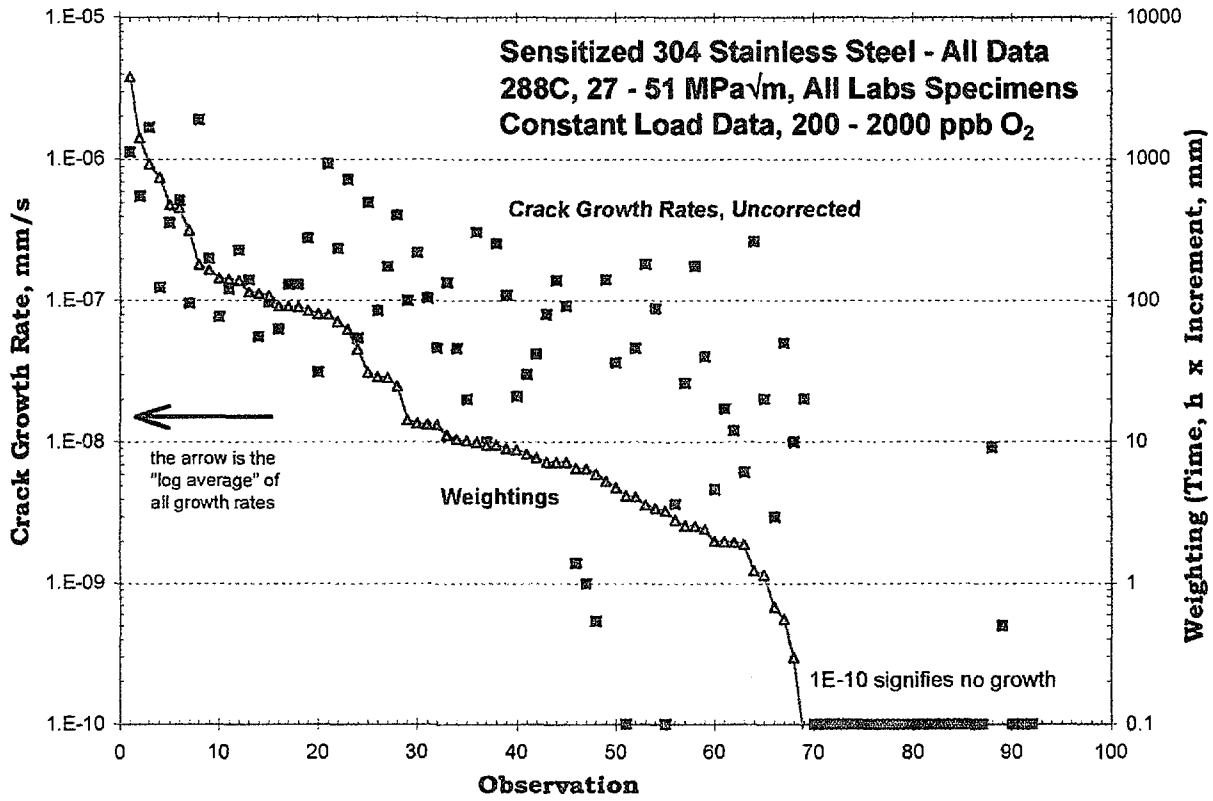

Figure 12. Constant load crack growth rate data sorted by a weighting factor that is the product of *"the crack growth increment (mm)"* times *"the test time in that increment (hours)"*. The data are uncorrected for differences in stress intensity and water chemistry, although neither effect produces large (e.g., >10X) effects. While simplistic, this simple ranking shows that more credibility should be given to the 1 - 3 x 10^{-7} mm/s rate (that will be shown the actual characteristic of the data) than the 1 - 3 x 10^{-8} mm/s rate (that represents the logarithmic mean of all of the data, obtained by computing the mean of the log of the data).

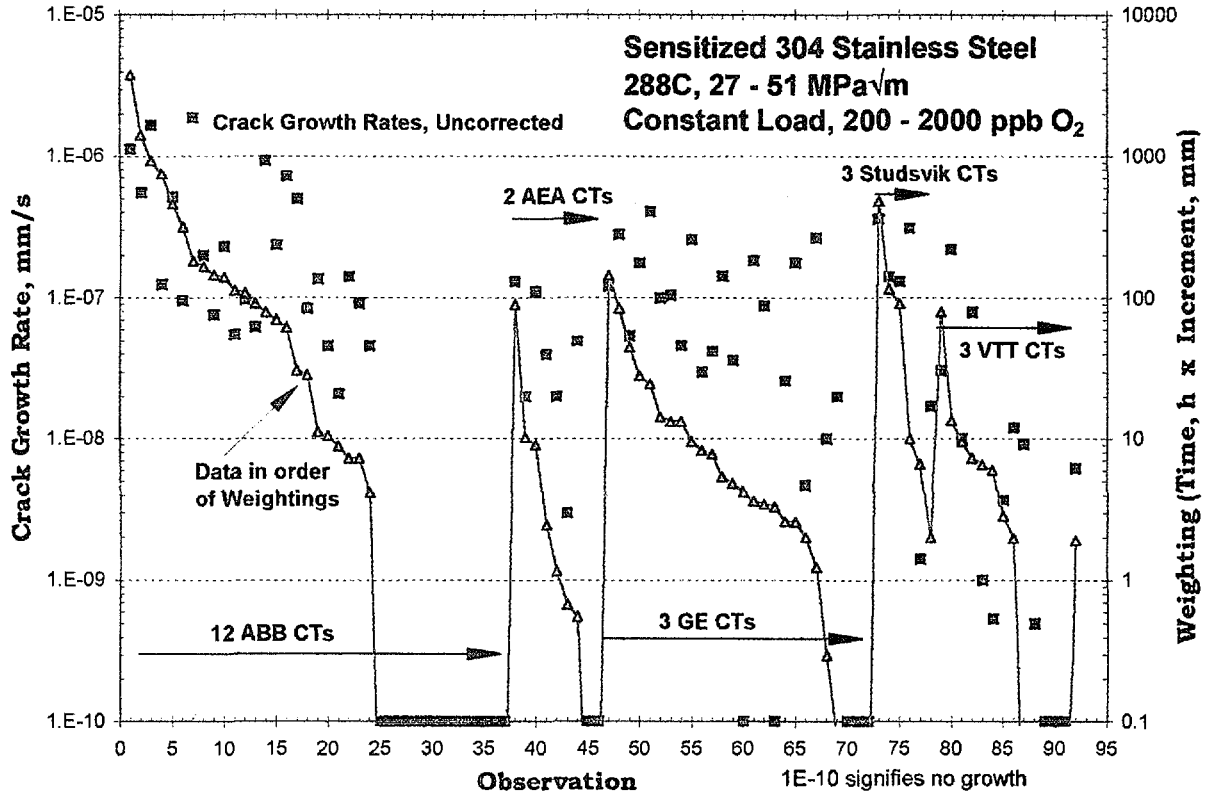

Figure 13. Constant load crack growth rate data presented by laboratory and sorted by a weighting factor that is the product of *"the crack growth increment (mm)"* times *"the test time in that increment (hours)"*. The data are uncorrected for differences in stress intensity and water chemistry, although neither effect produces large (e.g., >10X) effects.

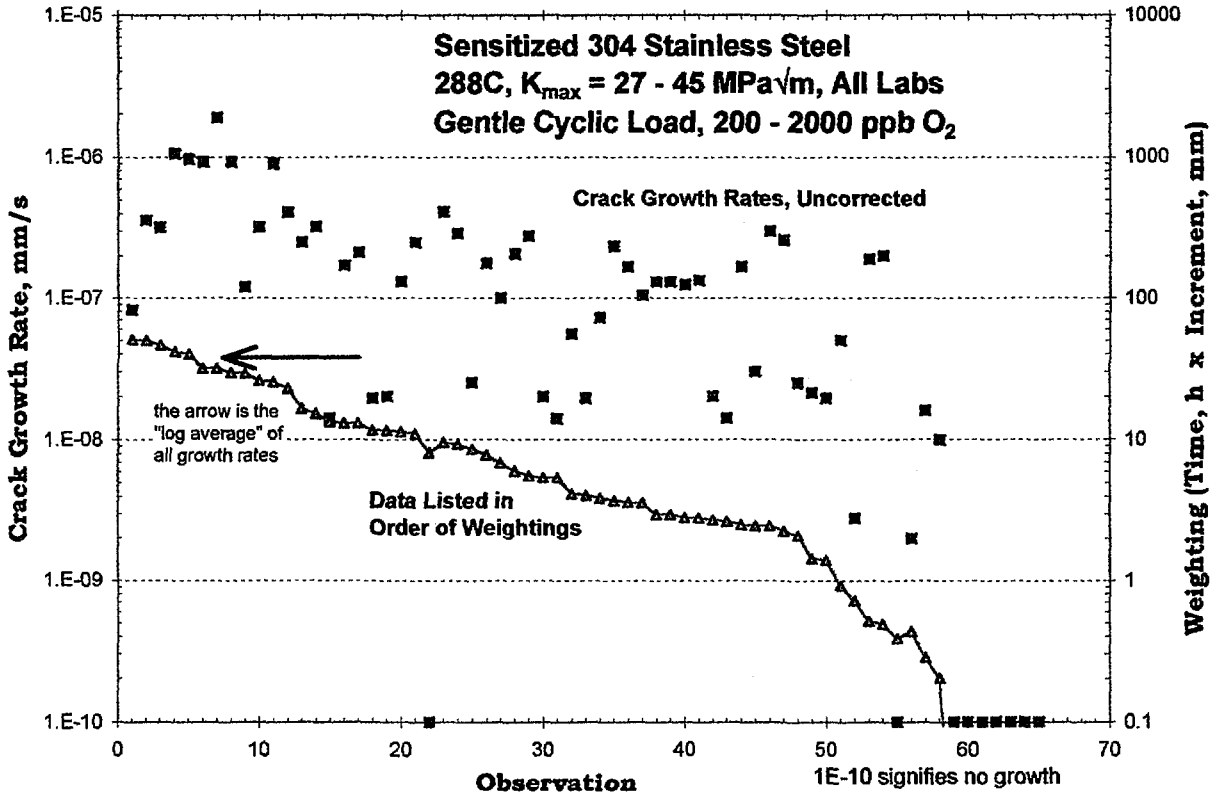

Figure 14. Crack growth rate data obtained under "gentle" cyclic loading conditions and sorted by a weighting factor that is the product of "*the crack growth increment (mm)*" times *"the test time in that increment (hours)"*. The data are uncorrected for differences in stress intensity and water chemistry, although neither effect produces large (e.g., >10X) effects.

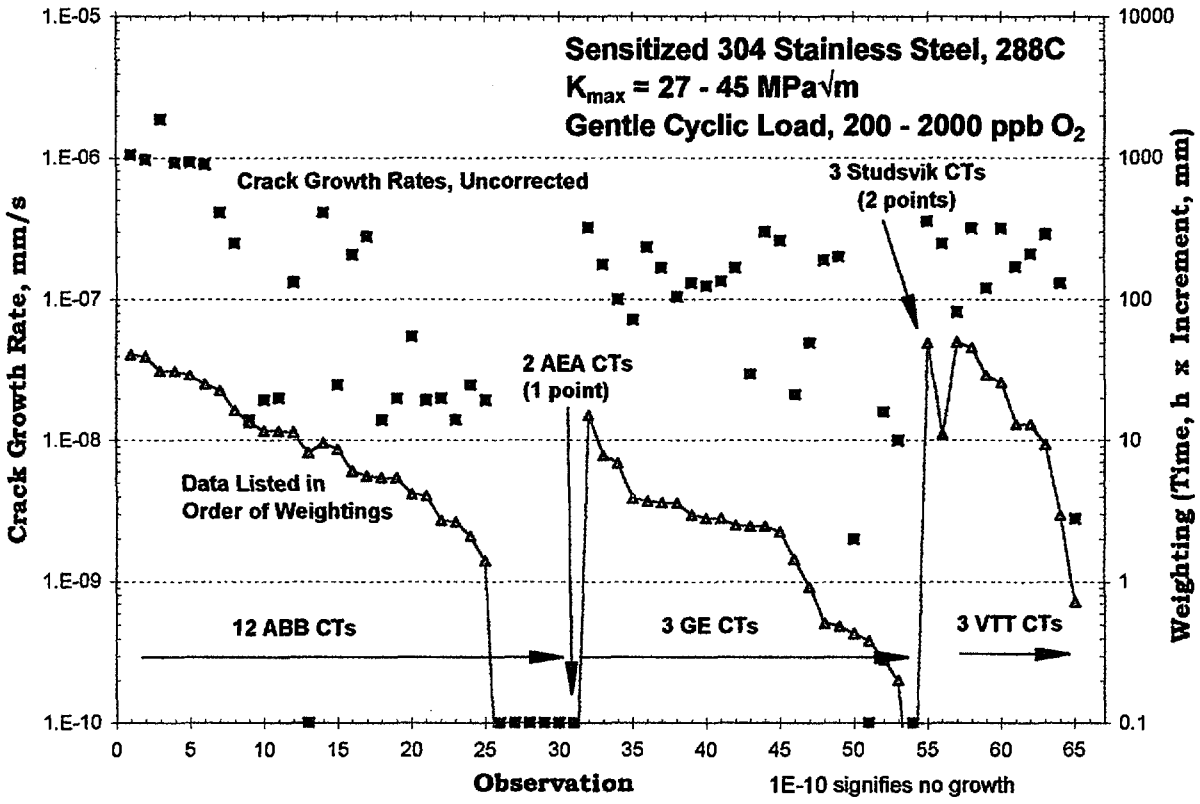

Figure 15. Crack growth rate data under "gentle" cyclic loading conditions presented by laboratory and sorted by a weighting factor that is the product of *"the crack growth increment (mm)"* times *"the test time in that increment (hours)"*. The data are uncorrected for differences in stress intensity and water chemistry, although neither effect produces large (e.g., >10X) effects.

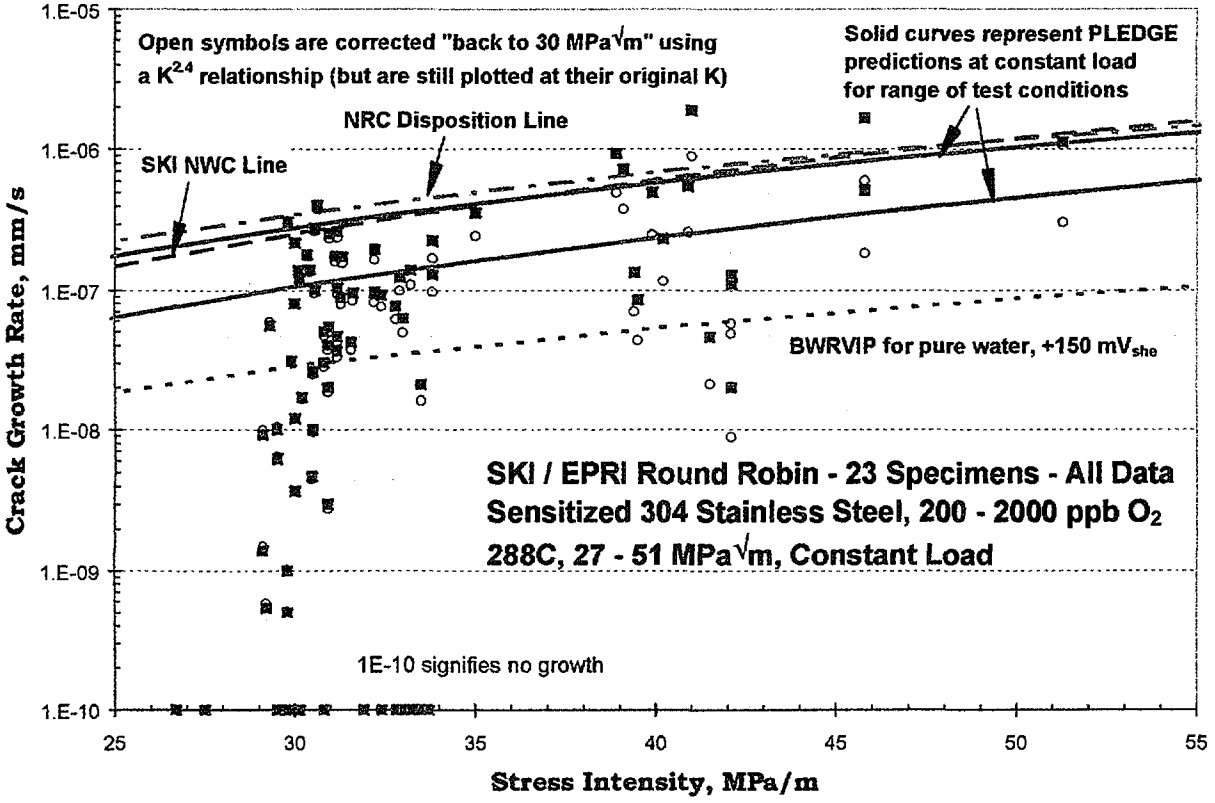

Figure 16. The effect of stress intensity on crack growth rate under constant load conditions. The filled symbols show the reported crack growth rates, while the open symbols represent growth rates corrected (normalized) to 30 MPa√m using a $V_{corr} = V_{orig} (K/30)^{2.4}$ formulation. The curves represents PLEDGE predictions for the approximate range of test conditions used.

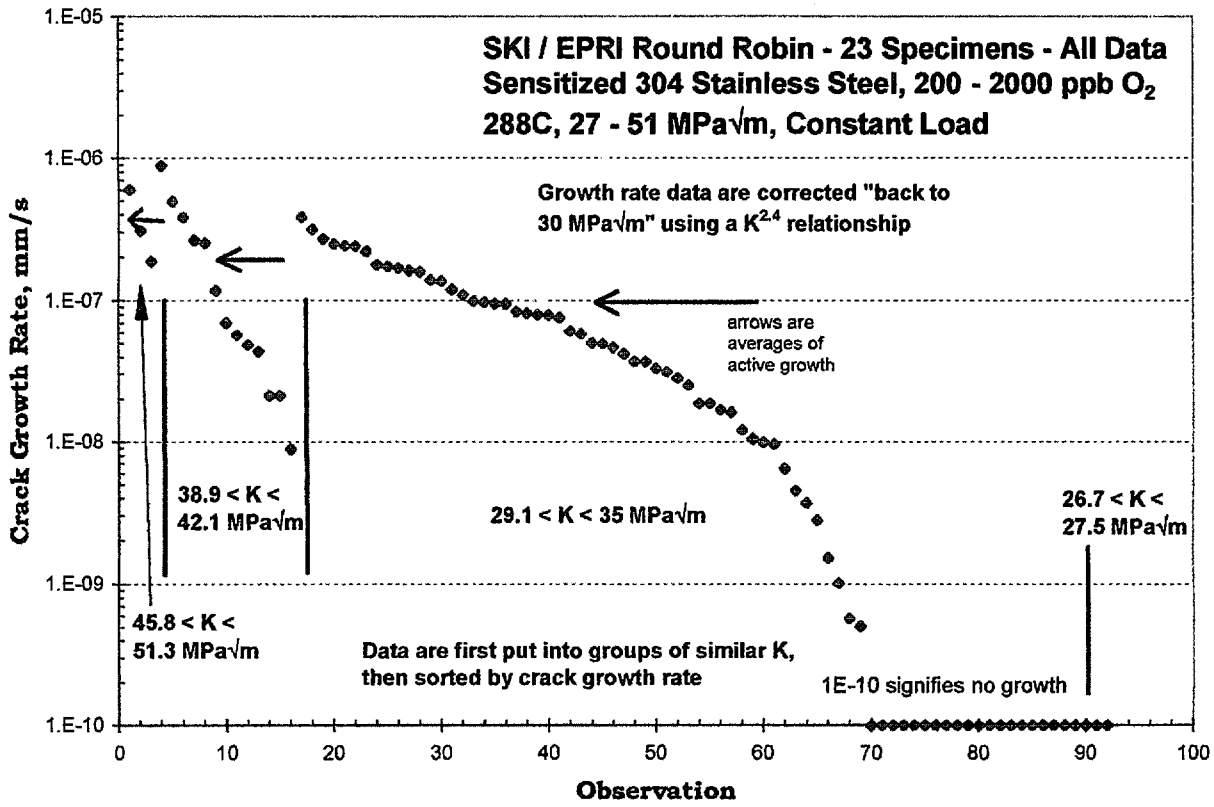

Figure 17. The effect of stress intensity on crack growth rate under constant load conditions, shown by grouping. The growth rates are corrected (normalized) to 30 MPa√m using a $V_{corr} = V_{orig} (K/30)^{2.4}$ formulation. The arrows show the linear average of the active crack growth rates.

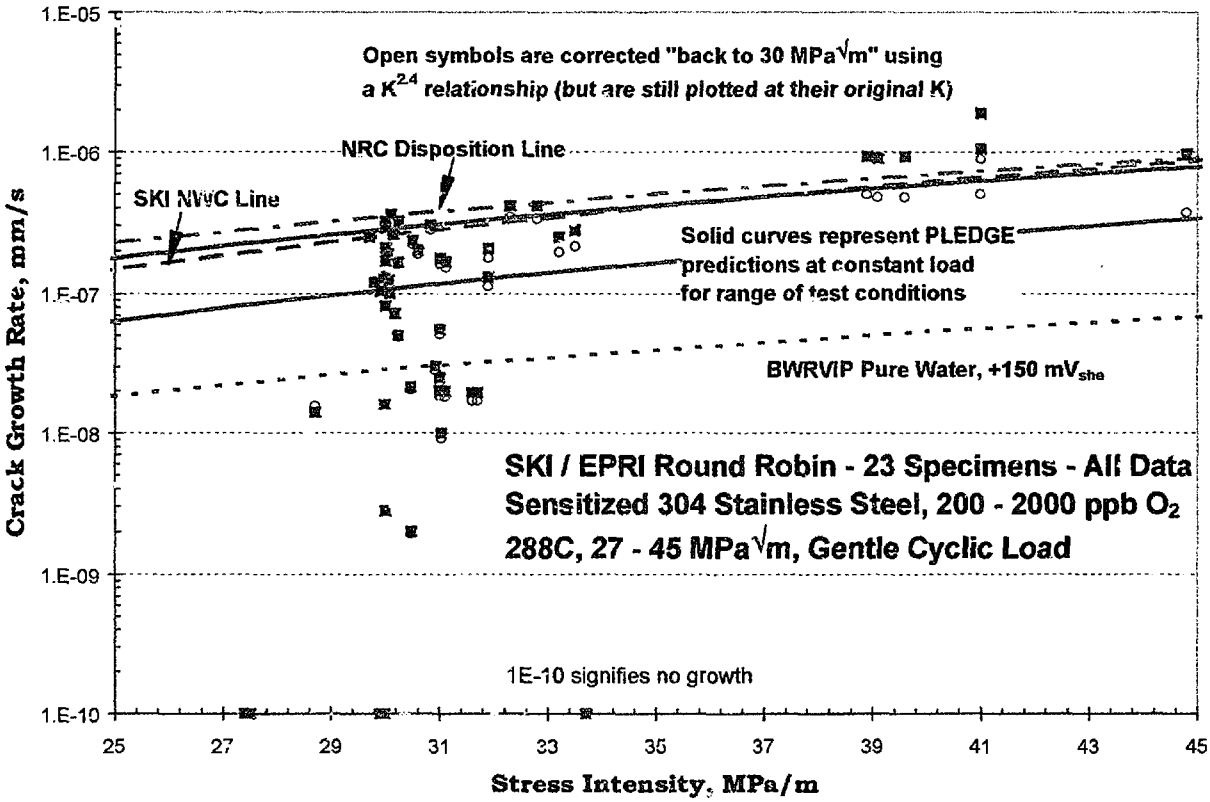

Figure 18. The effect of stress intensity on crack growth rate under "gentle" cyclic loading conditions. The filled symbols show the reported crack growth rates, while the open symbols represent growth rates corrected (normalized) to 30 MPa√m using a $V_{corr} = V_{orig} (K/30)^{2.4}$ formulation. The curves represents PLEDGE predictions at constant load for the approximate range of test conditions used.

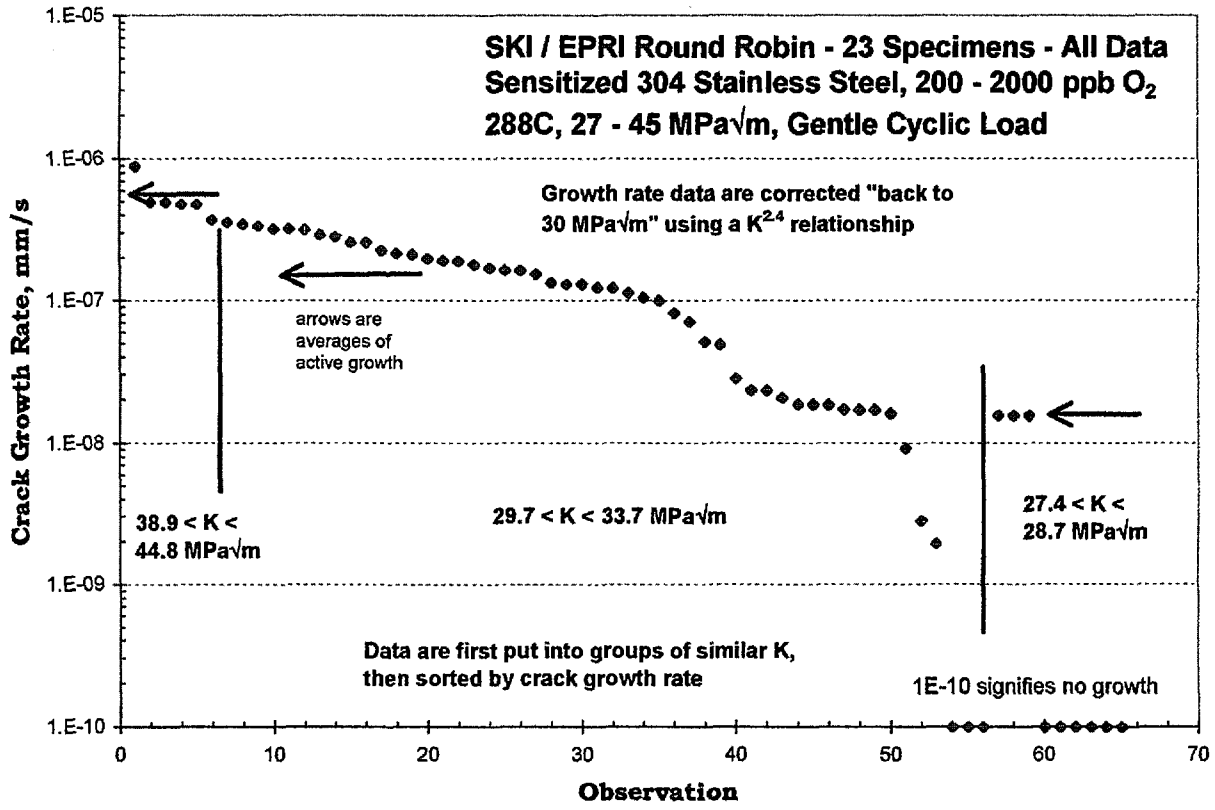

Figure 19. The effect of stress intensity on crack growth rate under "gentle" cyclic loading conditions, shown by grouping. The growth rates are corrected (normalized) to 30 MPa√m using a $V_{corr} = V_{orig} (K/30)^{2.4}$ formulation. The arrows show the linear average of the active crack growth rates.

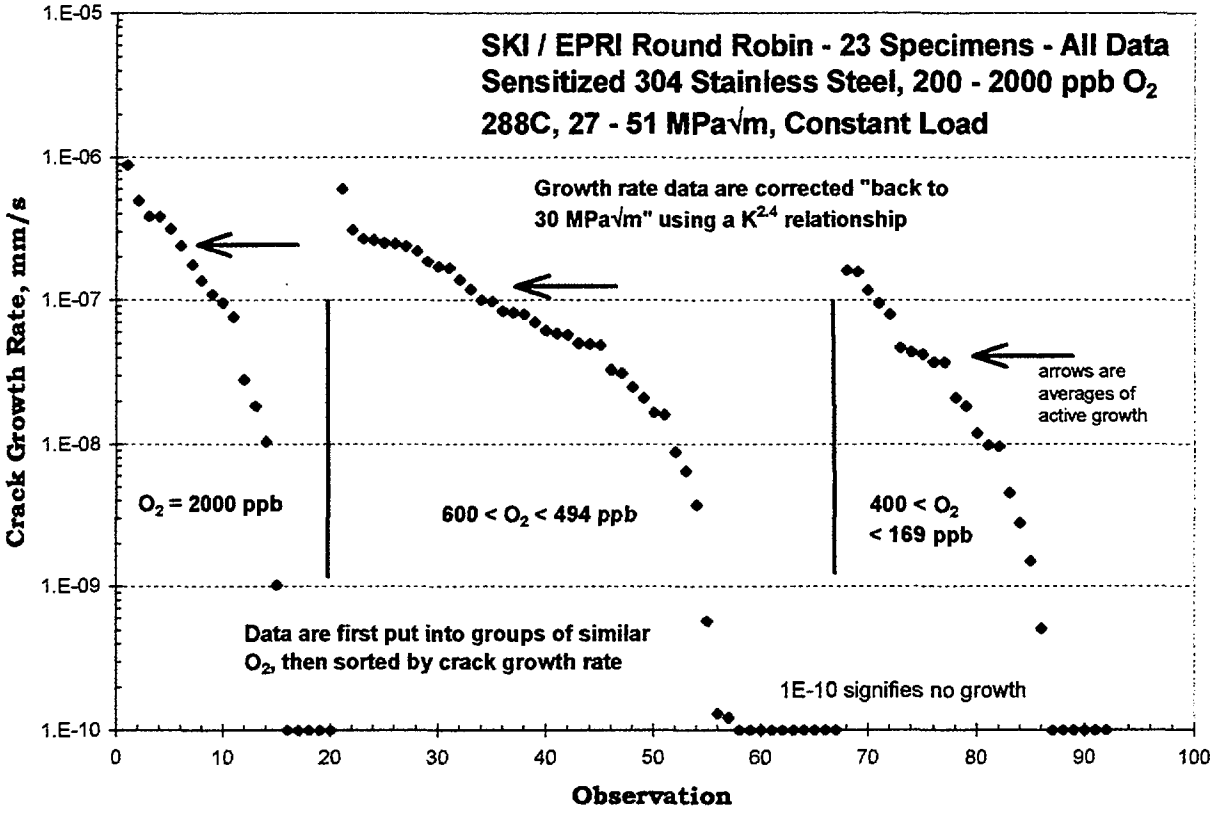

Figure 20. The effect of water chemistry on crack growth rate under constant load conditions, shown by grouping the data by dissolved oxygen. The data at 2000 ppb and 200 ppb O_2 are pure water, while most of the data at 500 ppb O_2 incorporate 25 ppb sulfate addition. The growth rates are corrected (normalized) to 30 MPa$\sqrt{m}$ using a $V_{corr} = V_{orig}$ $(K/30)^{2.4}$ formulation. The arrows show the linear average of the active crack growth rates.

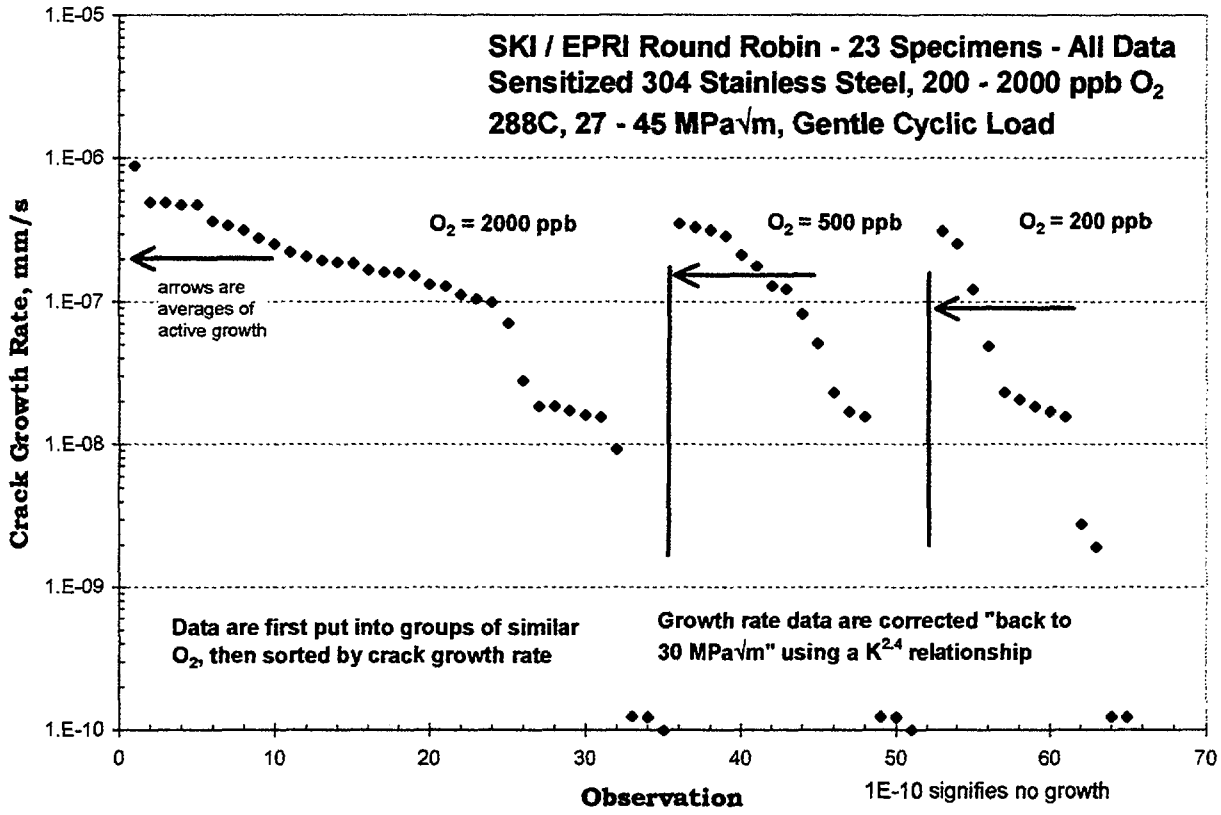

Figure 21. The effect of water chemistry on crack growth rate under "gentle" cyclic loading conditions, shown by grouping the data by dissolved oxygen. The data at 2000 ppb and 200 ppb O_2 are pure water, while most of the data at 500 ppb O_2 incorporate 25 ppb sulfate addition. The growth rates are corrected (normalized) to 30 MPa$\sqrt{m}$ using a $V_{corr} = V_{orig} (K/30)^{2.4}$ formulation. The arrows show the linear average of the active crack growth rates.

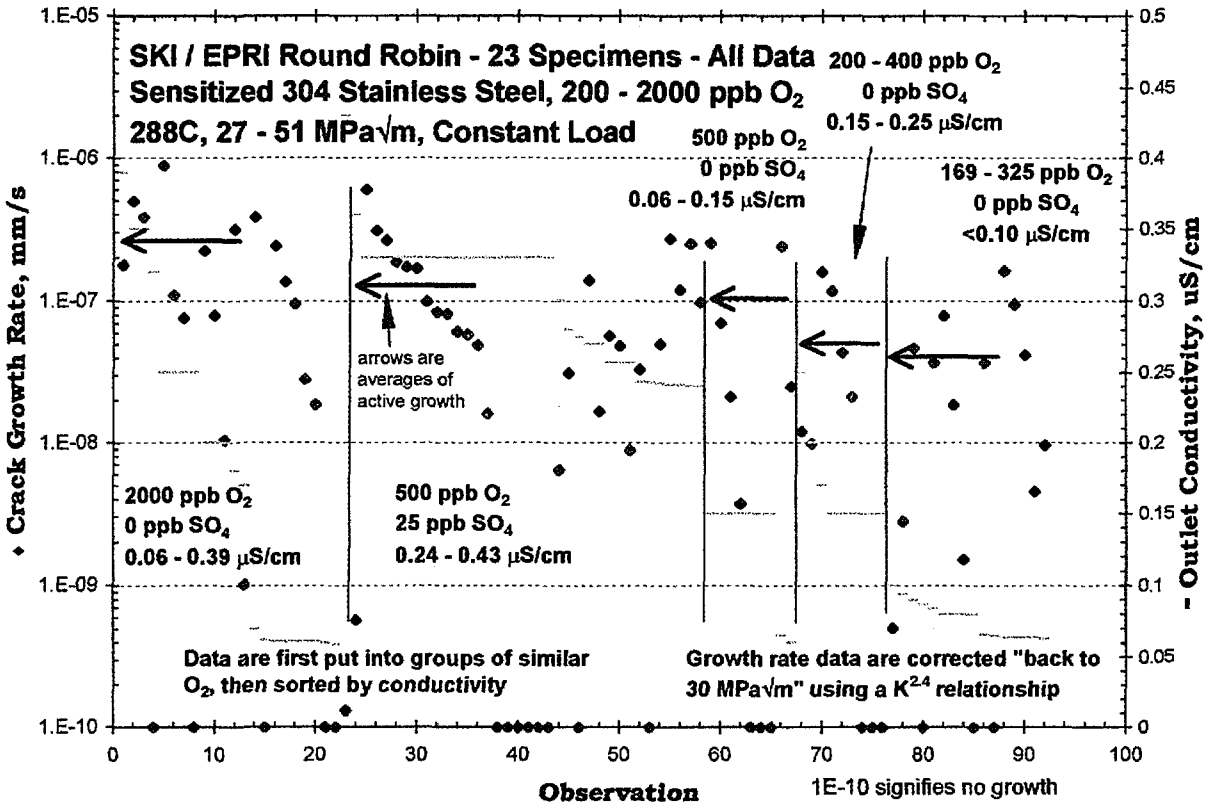

Figure 22. The effect of water chemistry on crack growth rate under constant load conditions, shown by grouping the data by dissolved oxygen, then sorted by conductivity. The data at 2000 ppb and 200 ppb O_2 are pure water, and the data at 500 ppb O_2 are separated into data obtained in pure water and in 25 ppb sulfate. The growth rates are corrected (normalized) to 30 MPa√m using a $V_{corr} = V_{orig} (K/30)^{2.4}$ formulation. The arrows show the linear average of the active crack growth rates.

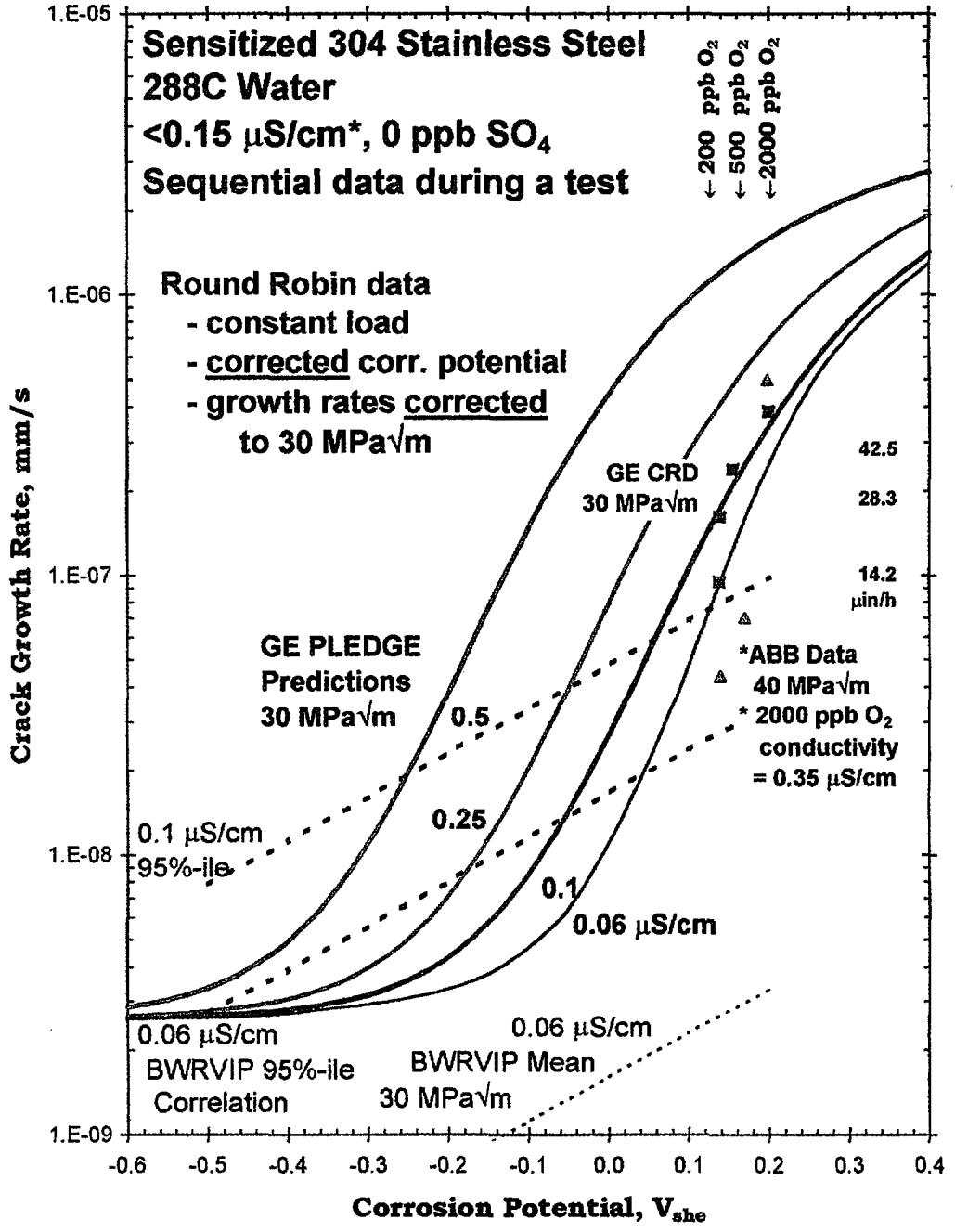

Figure 23. The effect of dissolved oxygen on crack growth rate under constant load conditions in pure water, shown using two specific specimens where changes in dissolved oxygen were made in a sequence of controlled changes.

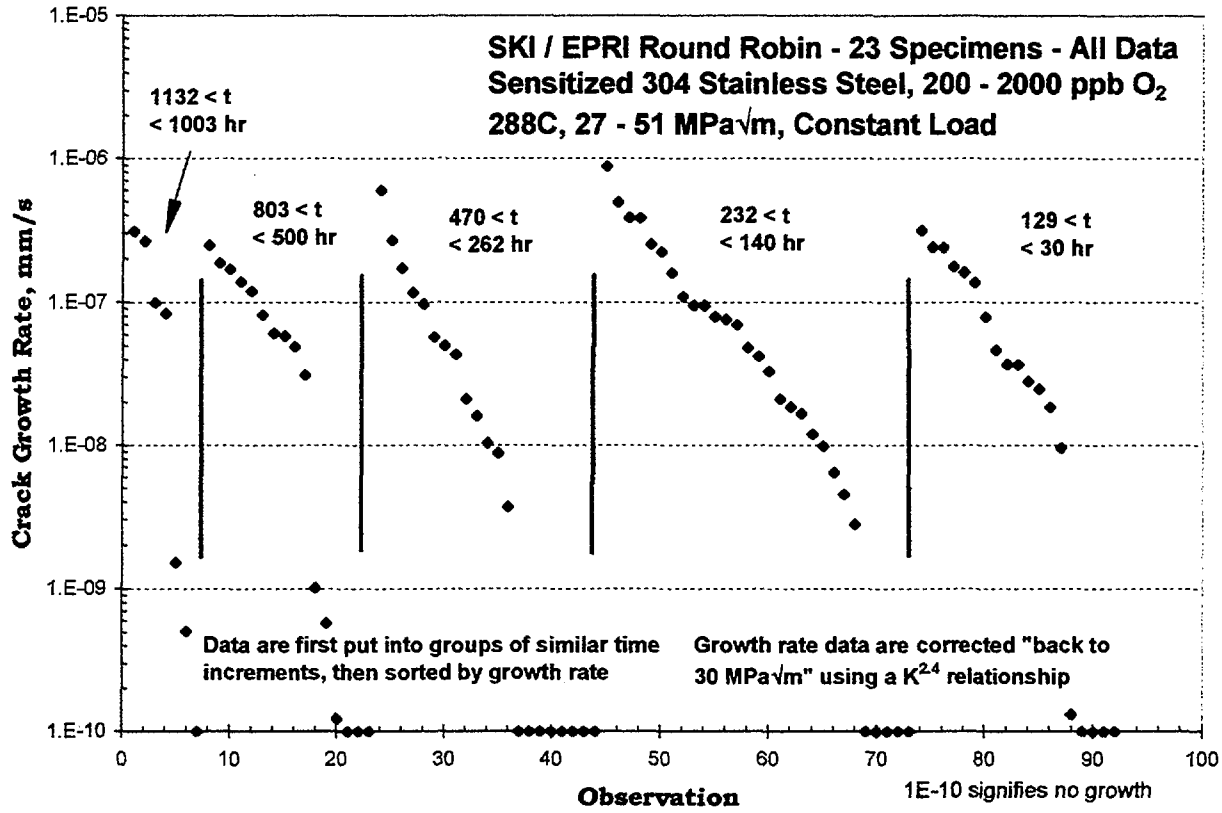

Figure 24. Crack growth rate under constant load conditions as a function of duration of test segment. A range of growth rates is observed for each of the time durations, indicating that the time in a test segment is not the primary factor in determining the "correct" growth rate.

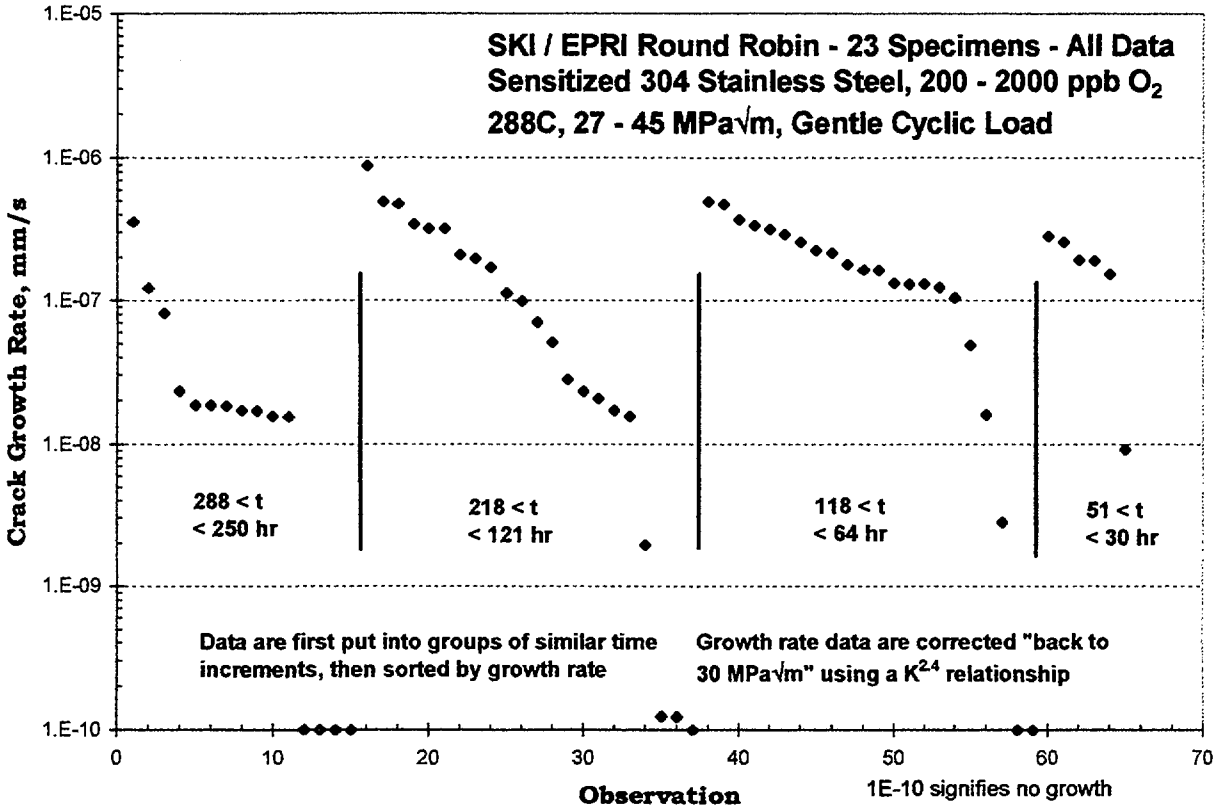

Figure 25. Crack growth rate under "gentle" cyclic loading conditions as a function of duration of test segment. A range of growth rates is observed for each of the time durations, indicating that the time in a test segment is not the primary factor in determining the "correct" growth rate.

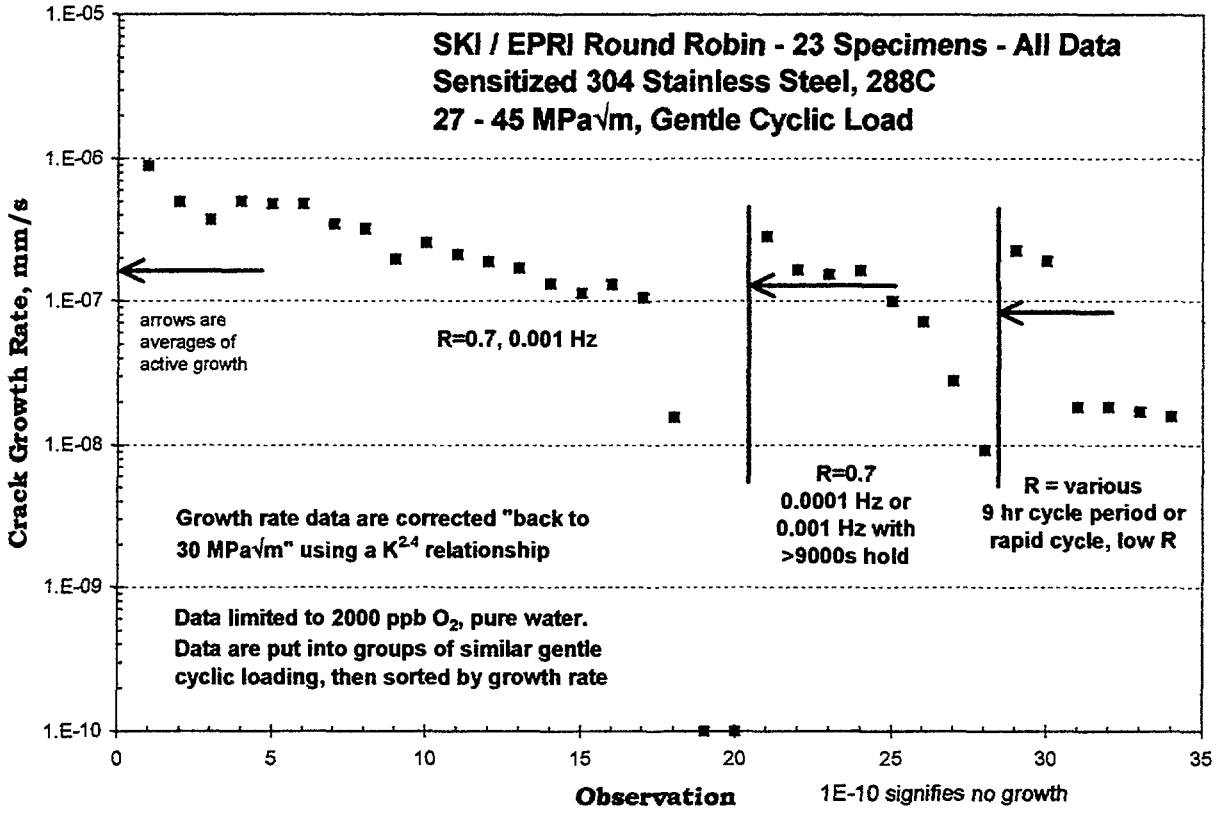

Figure 26. Comparison of three different "gentle" cyclic conditions that were used by various laboratories and/or at various times. These data are limited to 2000 ppb O_2, pure water conditions, and show some advantage for the R = 0.7, 0.001 Hz loading condition in terms of consistency of crack growth rates. The proportion of "no growth" and "low growth" data are smaller than in the constant load data set, although the constant load data set is itself a major beneficiary of the "gentle" cyclic loading, which was often a critical precursor stage to achieving crack growth at constant load.

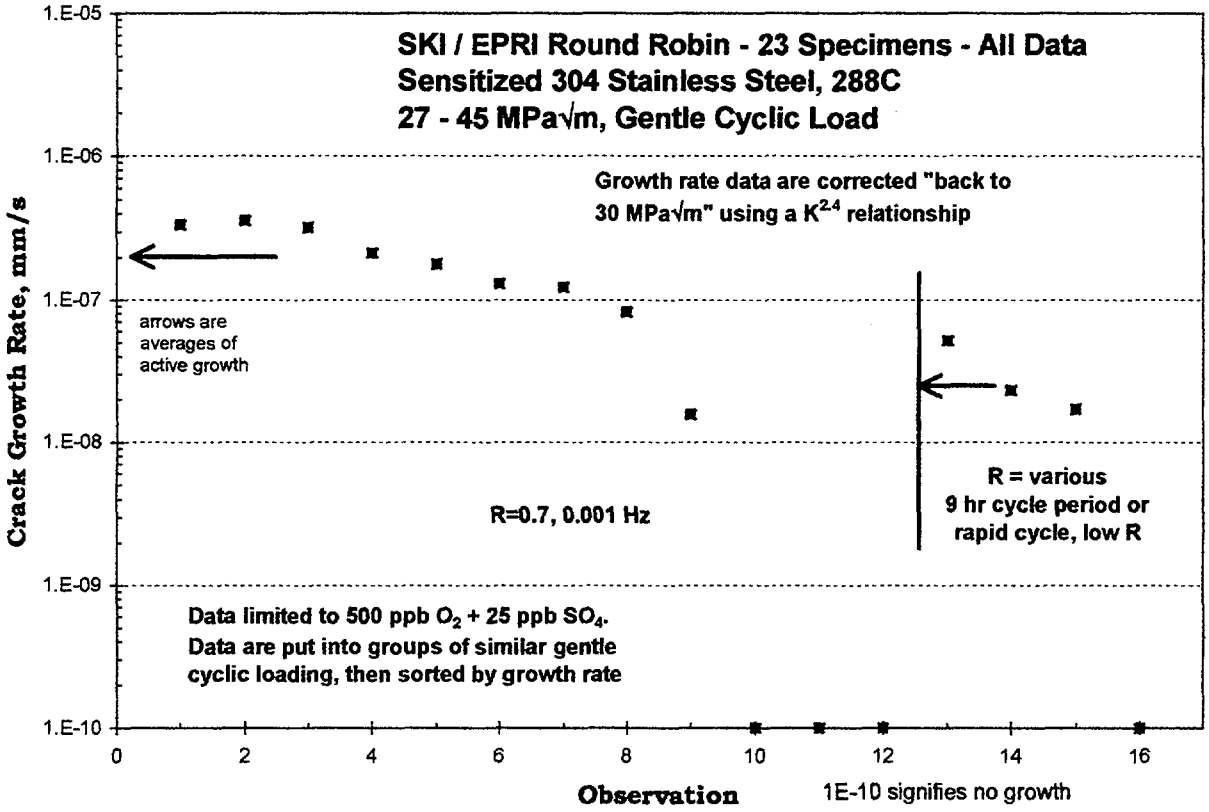

Figure 27. Comparison of different "gentle" cyclic conditions that were used by various laboratories and/or at various times. These data are limited to 500 ppb O_2 plus 25 ppb sulfate conditions, and show some advantage for the R = 0.7, 0.001 Hz loading condition in terms of consistency of crack growth rates.

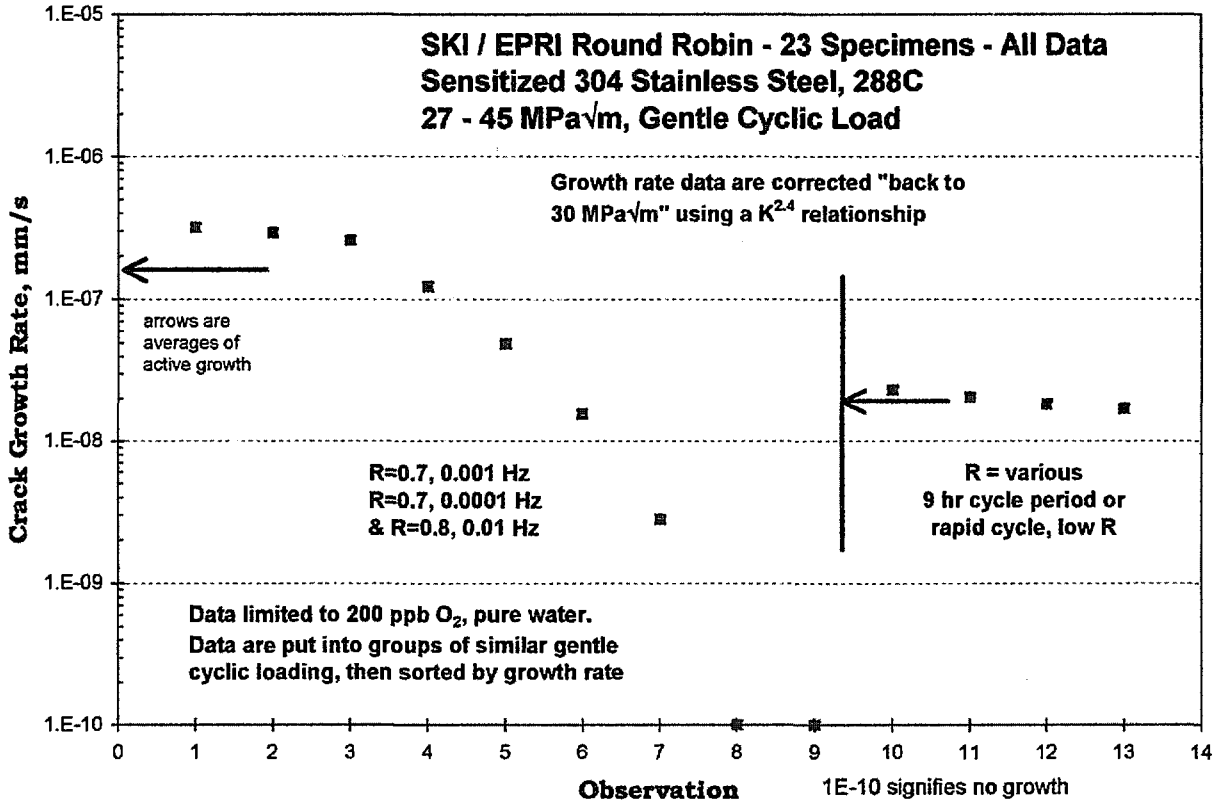

Figure 28. Comparison of different "gentle" cyclic conditions that were used by various laboratories and/or at various times. These data are limited to 200 ppb O_2, pure water conditions, and show some advantage for the R = 0.7, 0.001 Hz loading condition in terms of consistency of crack growth rates, particularly when it is noted that the "correct" rate based on the overall data set is 1 - 3 x 10^{-7} mm/s.

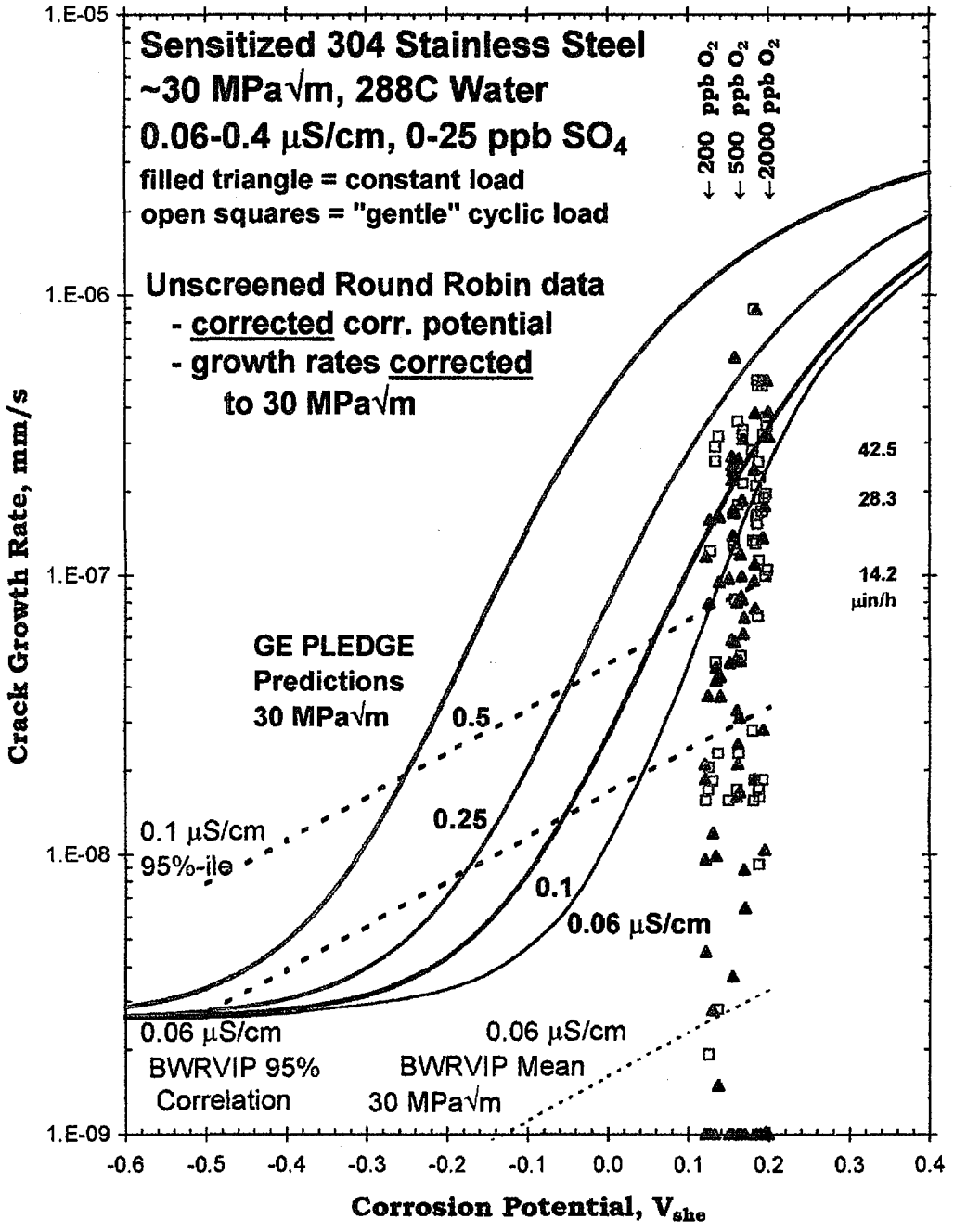

Figure 29. The full range of observed crack growth rate data for constant load and "gentle" cyclic loading conditions. Unlike Figure 11, the data are plotted by assigning a consistent corrosion potential to data under specific water chemistry conditions (some randomness is introduced to prevent data from falling on top of each other).

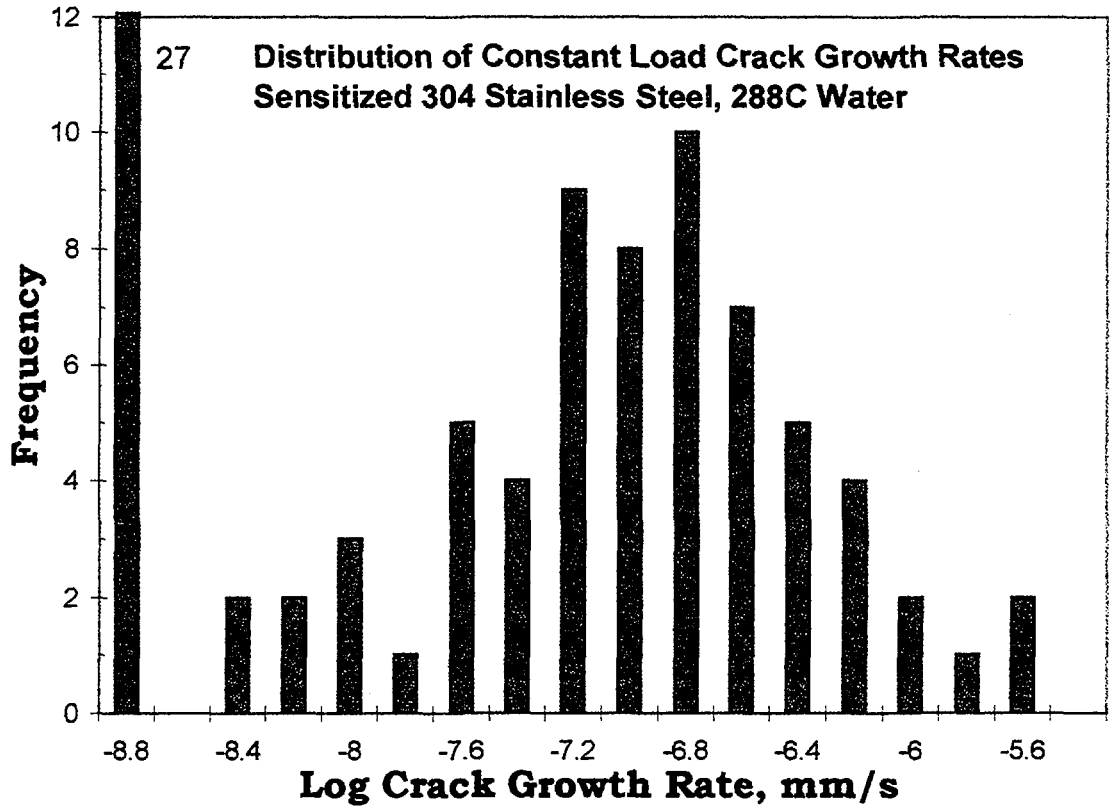

Figure 30. Frequency histogram of crack growth rates for the constant load data.

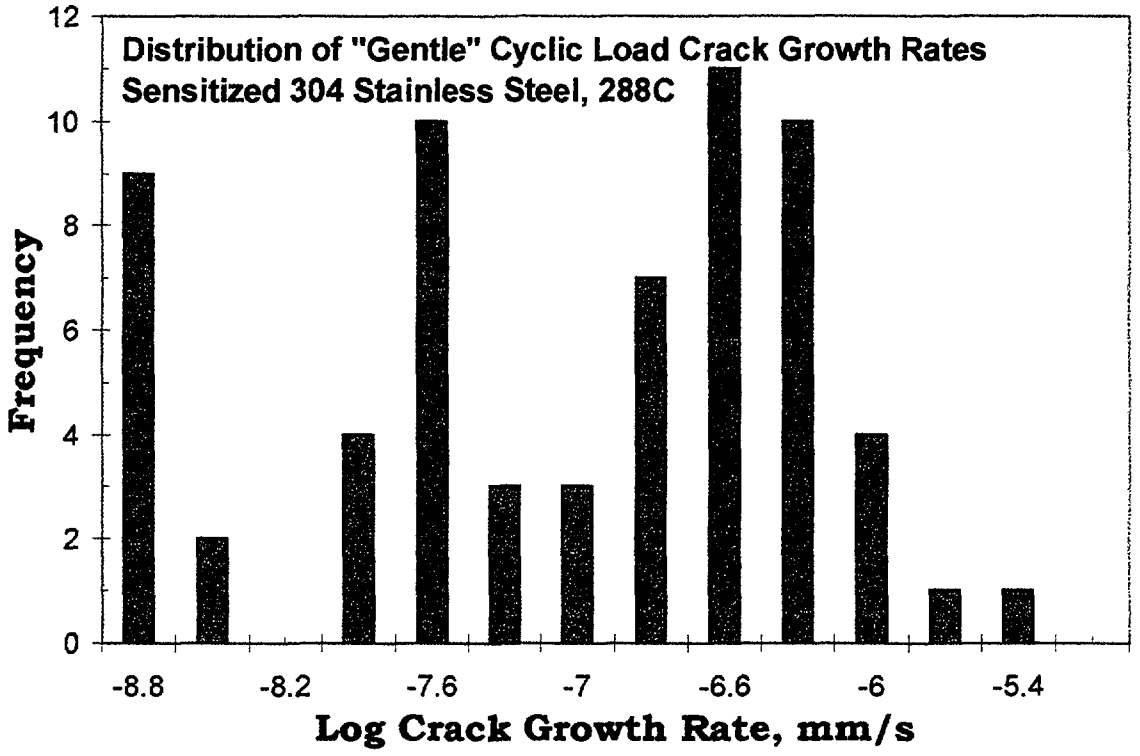

Figure 31. Frequency histogram of crack growth rates for the "gentle" cyclic loading data.

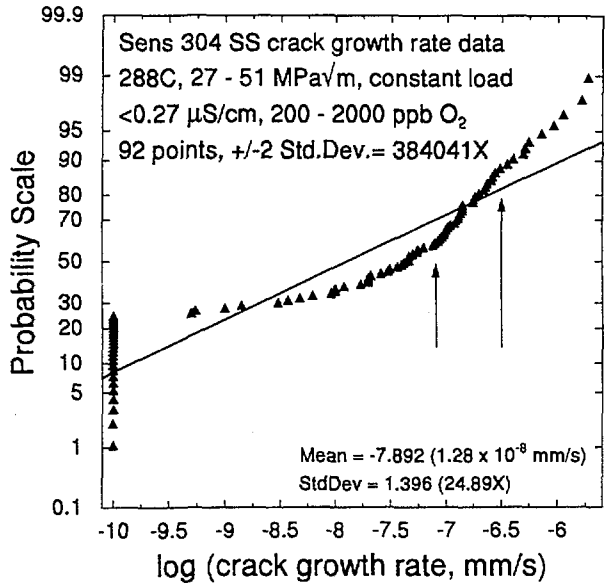

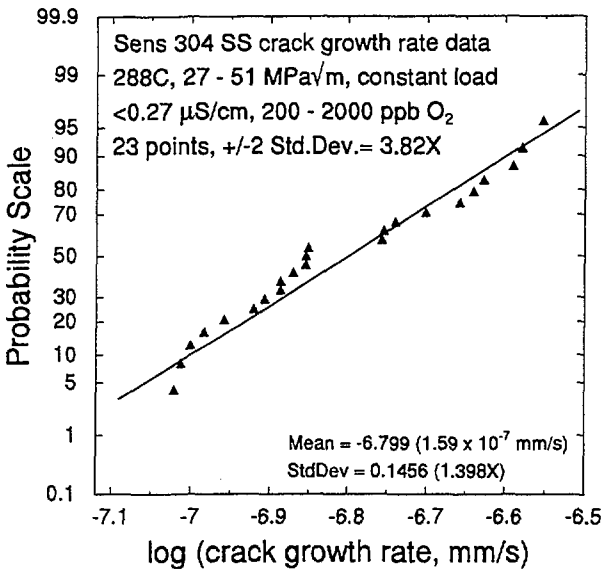

Figure 32. (a) Probability vs. log of the constant load crack growth rate showing that the overall set does not follow a normal distribution (indicated by linear response on this plot). The arrows show the densest linear segment of data that is evaluated in (b). The data in (b) are high normal, and show a vastly reduced range (as measured by the ± 2 standard deviation value) of 3.82X vs. 384,041 in (a).

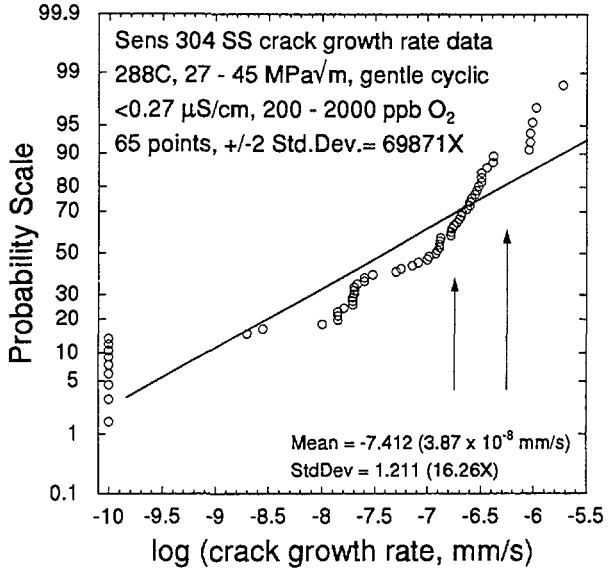

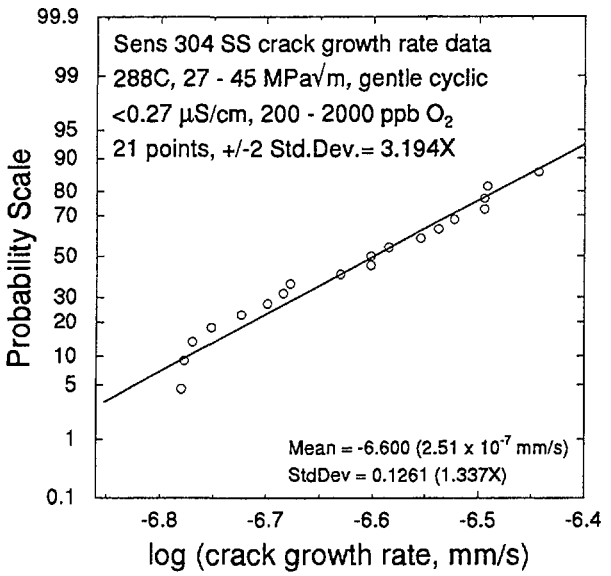

Figure 33. (a) Probability vs. log of the crack growth rate data under "gentle" cyclic load conditions showing that the overall set does not follow a normal distribution (indicated by linear response on this plot). The arrows show the densest linear segment of data that is evaluated in (b). The data in (b) are high normal, and show a vastly reduced range (as measured by the ± 2 standard deviation value) of 3.19X vs. 69,871 in (a).

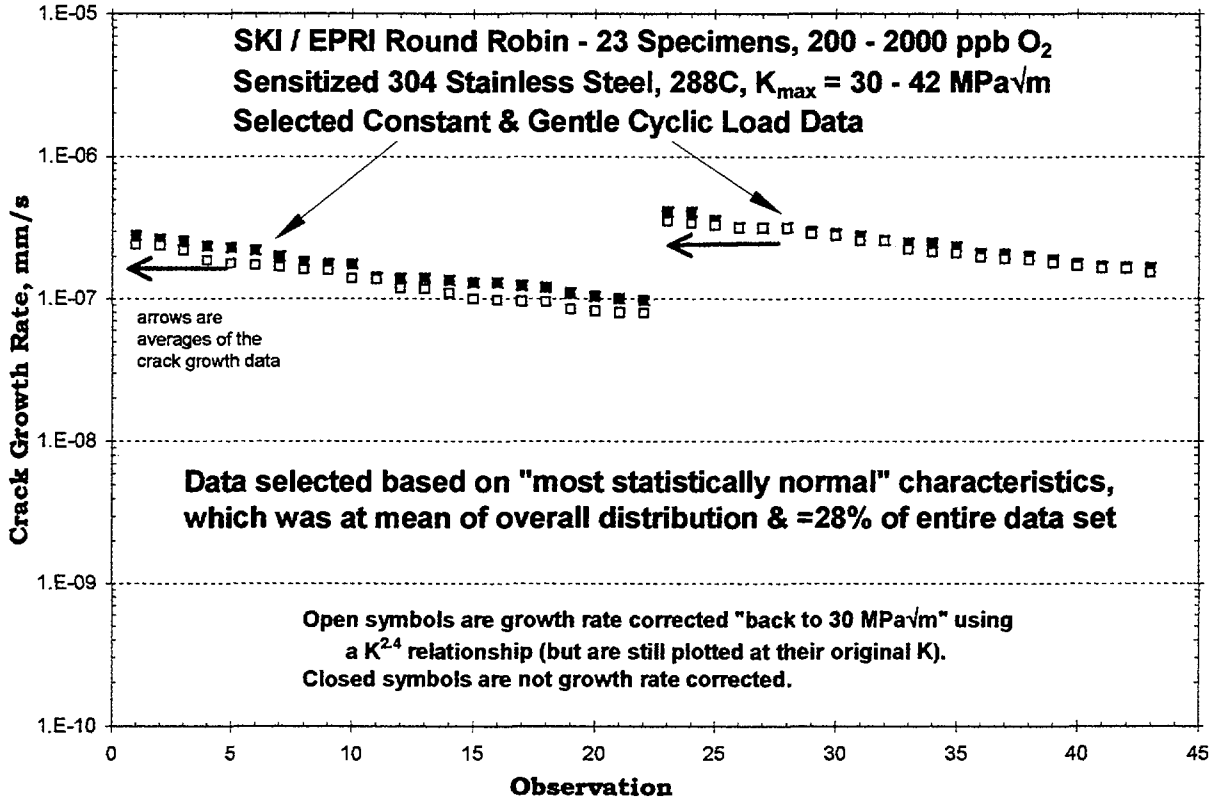

Figure 34. Constant and "gentle" cyclic loading data from the overall set which best follows a normal distribution (see Figures 32 and 33). The open symbols represent data that has been corrected "back to 30 MPa√m". The arrows show the averages of the crack growth data.

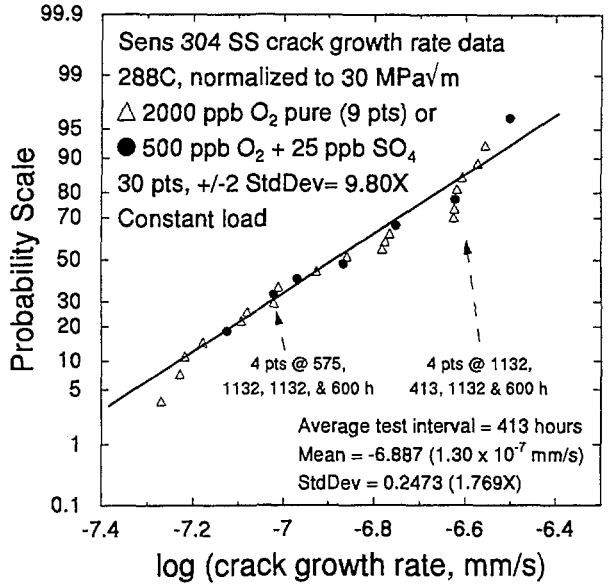

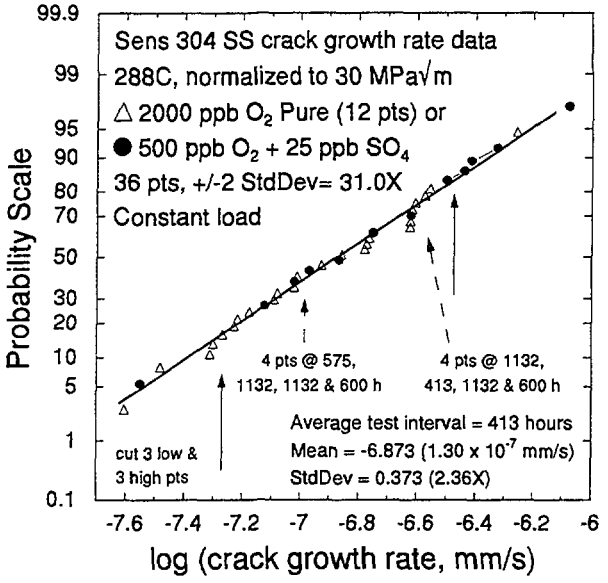

Figure 35. (a) Probability vs. log of selected constant and "gentle cyclic" crack growth rate data in pure water containing 2000 ppb O_2 and in inpure water containing 500 ppb O_2 and 25 ppb sulfate showing that the selected group of data follows a normal distribution

(indicated by linear response on this plot). "Tails" of the data can be removed to improve the standard deviation of the data (figure (b) shows the data between the arrows in figure (a)), but has no effect on the mean of the data. Several data with the longest time increments are identified.

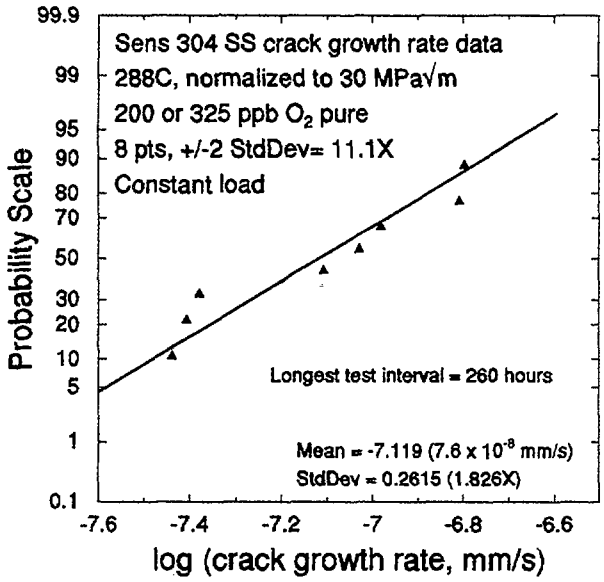

Figure 36. Probability vs. log of selected constant crack growth rate data in pure water containing 200 ppb O_2 showing that the selected group of data follows a normal distribution (indicated by linear response on this plot).

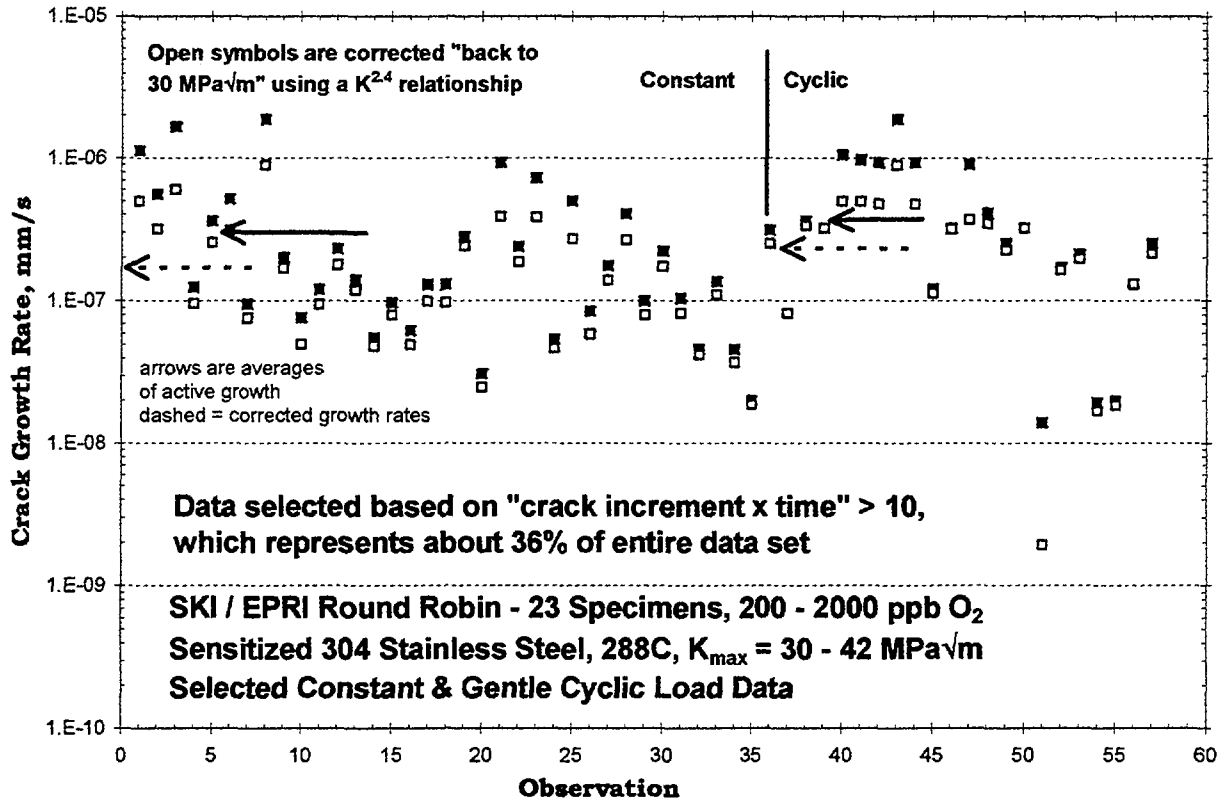

Figure 37. Collection of constant load and "gentle" cyclic loading crack growth data selected and sorted on the basis of a weighting factor > 10. This represents about 36% of the total data. The weighting factor is the product of *"the crack growth increment (mm)"* times *"the test time in that increment (hours)"*. Both the original and corrected (for differences in stress intensity) data are shown.

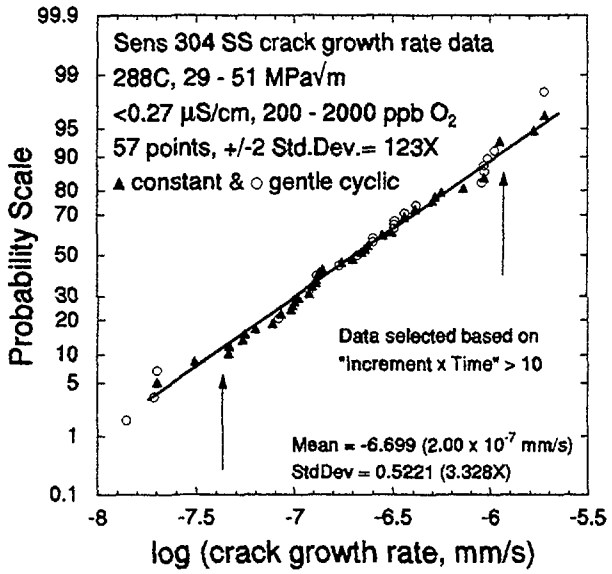

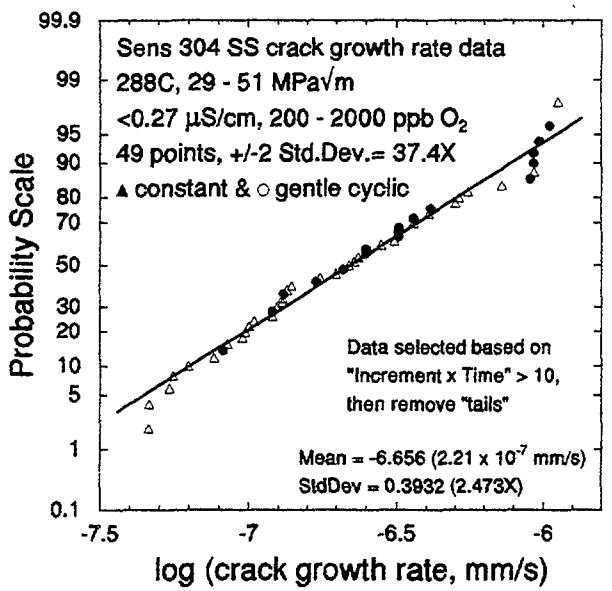

Figure 38. Probability vs. log of selected constant crack growth rate data showing that the selected group of data follows a normal distribution (indicated by linear response on this plot).

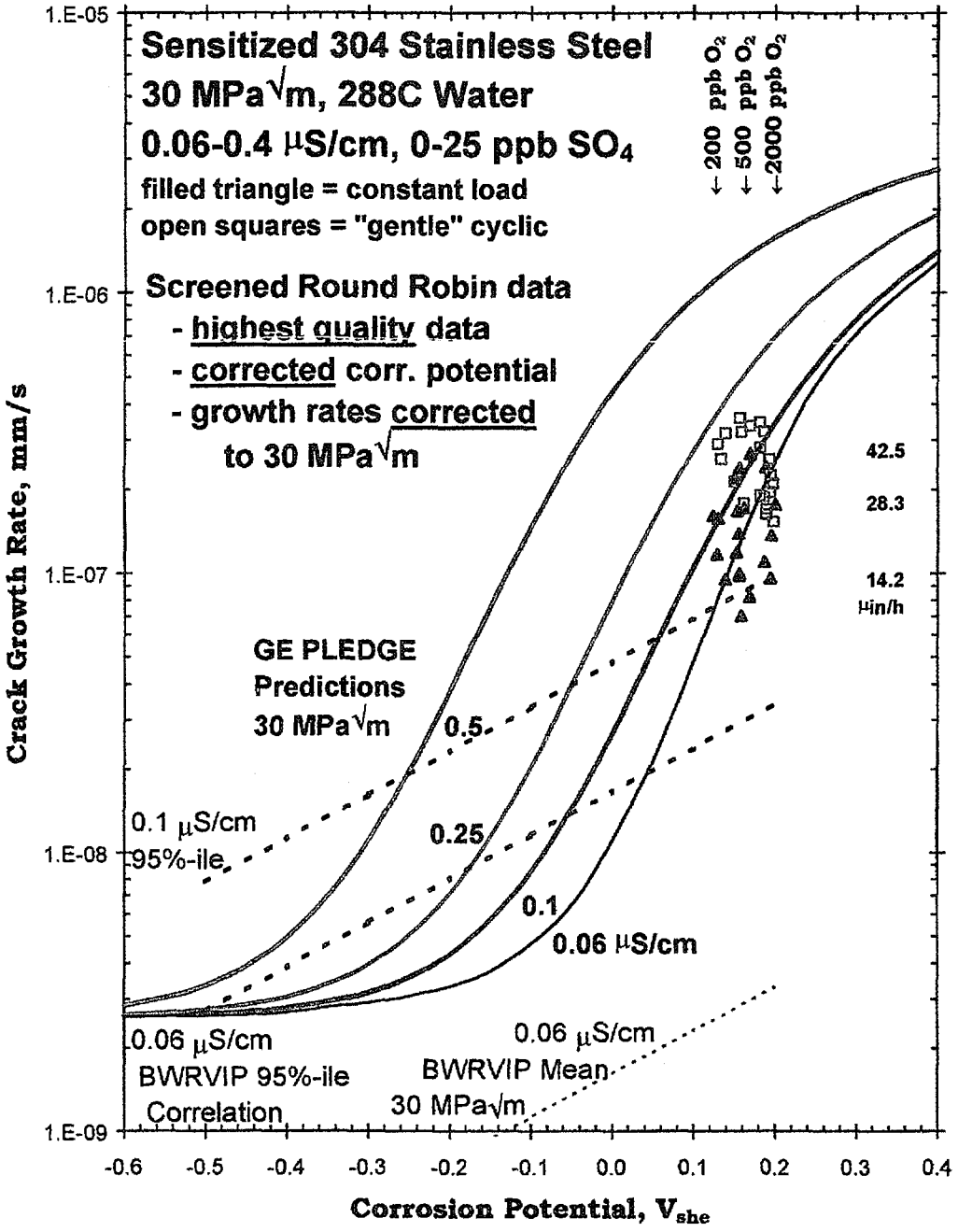

Figure 39. High quality subset of the Round Robin crack growth rate data based on the judgment of the author. The range and complexity of stress corrosion responses are large, and often dominate even moderately well controlled, well behaved data such as has been generated in this program. There are no simple or fixed screening or qualifying criteria which can be rigidly applied of identifying "high quality data"; such definitions can ultimately only be properly done based on years of experience in stress corrosion crack growth testing, data evaluation, and modeling. The mean of this data is not greatly different

from the mean of the data selected by the various other "screening" techniques, although this is not always the case.

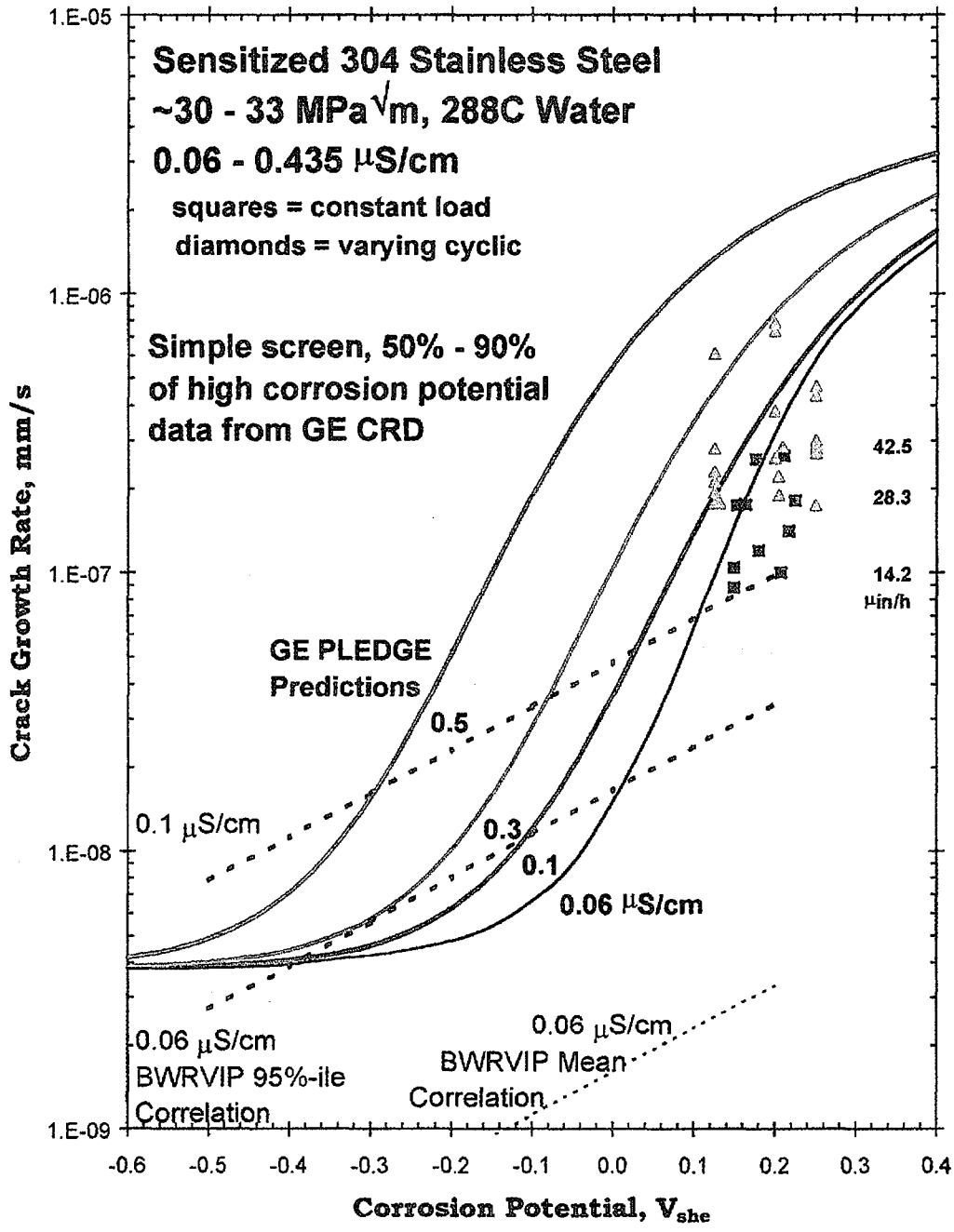

Figure 40. Collection of crack growth rate data obtained at high corrosion potential at GE CRD at ≈ 30 - 33 MPa√m on sensitized type 304 stainless steel. The data were obtained in pure water and with sulfate levels ranging up to ≈50 ppb.

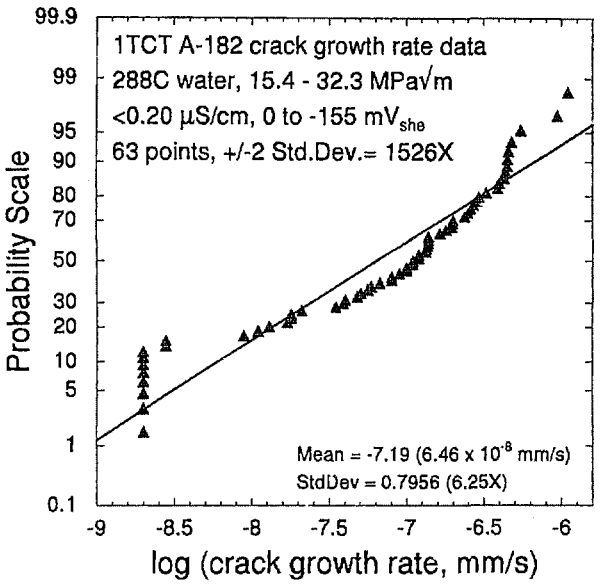

Figure 41. Probability vs. log constant crack growth rate data for Alloy 182 weld metal restricted to <0.2 µS/cm, a range of 155 mV, and about a factor of 2 in stress intensity. Despite these restrictions, there is almost three orders of magnitude range (mostly scatter) in the data, and the data clearly don't follow a well behaved normal distribution (indicated by linear response on this plot).

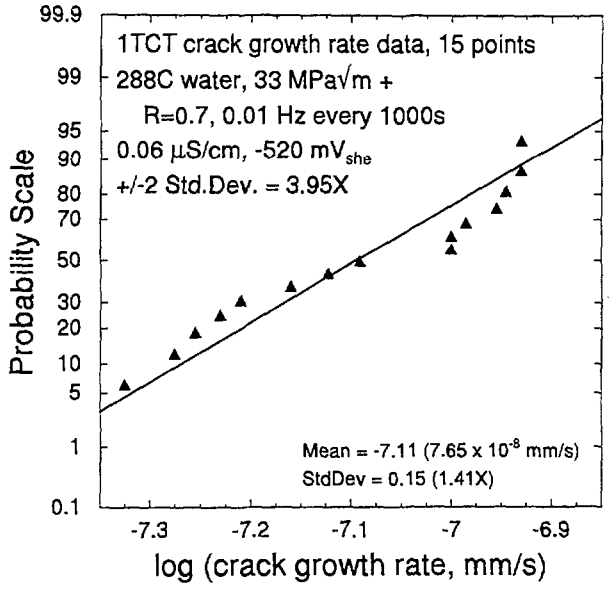

Figure 42. Probability vs. log constant crack growth rate data from GECRD under well controlled conditions. This large scatter in the previous figure is clearly not an inherent characteristic of the physical SCC process, but of weaknesses and flaws in the experimental techniques and measurements.

Appendix A - Experimental Quality Guidelines for SCC Testing

Peter L. Andresen – January 15, 1998

"There are a few ways to obtain high quality data, but innumerable ways to obtain marginal data"

Stress corrosion crack growth rate data in hot water is sensitive to a large variety of parameters. To obtain reproducible, high quality data, there are numerous controls and test procedures that are necessary. Underlying these experimental approaches is the belief that the scatter in physical process of environmental cracking under fully controlled material, environment, and stress conditions should be small. In general, it is flawed measurements and imperfect techniques that are responsible for most of the observed scatter in the data, although clearly uncontrolled (including unrecognized) variables also contribute. In our experience, well controlled environmental cracking test measurements do not *inherently* possess a scatter of >100 - 1000X, but perhaps a factor of 2 - 5X*. However, evaluations of broader collections of international data do show quite large scatter (even from one laboratory), e.g., of >100 - 1000X, indicative of inadequate (but not always obvious) test controls or procedures. One repercussion is that the scatter and mean of the broader collection of data may merely represent the deviation and mean of the *flaws* and *weaknesses* in the measurements, not of the physical SCC process.

This guideline is designed to provide suggestions for how scatter can be minimized, and reproducibility and agreement (e.g., from lab-to-lab, or test-to-test) maximized. In simple terms, this requires that all possible factors be isolated and controlled to avoid having them lumped together under the broad umbrella of "scatter", which is usually viewed as inherent and uncontrollable. This guideline is focused on crack growth rate testing, but is broadly applicable to many types of electrochemical and stress corrosion cracking tests in hot water.

The primary issues in establishing the quality, accuracy, and reproducibility of laboratory data are:

1. Stress intensity (K) should be within ASTM criteria based on "flow" stress (average of yield and ultimate), which typically limits testing to K <40 - 45 ksi$\sqrt{in}$ for 1TCT specimens of common austenitic alloys. CT specimens should be side grooved, or the extent of crack branching and
out-of-plane cracking should be confirmed to be small. The pulsing of load from the ≈1 Hz operation of most high pressure pumps (which cause the system pressure, and therefore the load on the specimen, to vary) should be eliminated by using pulse dampeners (accumulators).

"Constant" active K testing (vs. wedge loaded) is strongly preferred, although use of constant displacement may be acceptable if it meets other criteria and less than 15% K (not load) relaxation has occurred during the test (perhaps 20% if modulus changes vs.

temperature are included), active crack monitoring is used, and active crack growth occurs. It should be clear whether tests were performed at constant load vs. constant K; in the latter case, the size of the change, and whether load is both increased and decreased to track apparent changes in crack length should be identified.

In practice, periodic unloading is not only acceptable but generally preferred because it helps maintain a straight crack front (crucial to sensible interpretation of dc potential drop measurements) and helps ensure continuous "active" crack growth, rather than intermittent or long-term "arrest" or retarded growth rates. Periodic unloading should be subtle enough to produce minimal enhancement in crack growth, yet not so subtle that it provides no benefit. Typically, use of R > 0.75 produces irregular benefits. R= 0 .7, frequencies of 0.01 or 0.001 Hz, and hold times (between unloading) of ≥9,000 s are recommended. It is always recommended that the effect of the periodic unloading on growth rate, which should be fairly small), is occasionally confirmed by increasing hold time and/or shifting to constant load.

2. Test preliminaries. Careful control and documentation of machining, surface condition (e.g., to obtain proper corrosion potentials), pre-cracking procedures, and pre-oxidation in high temperature water are important. Concerns include unintended surface cold work from machining, and unintended surface (mostly electrochemical) characteristics associated with electrodischarge machining (EDM), surface contamination, oxide films from heat treatment, etc. Final pre-cracking conditions and SCC loading procedure are particularly important, along with assurance that the crack was not contaminated by oils, cleaning solutions, etc. Pre-cracking is ideally performed in-situ, because in addition to preventing contamination it is possible to alter pre-cracking conditions so that the plastic zone size approaches that under constant load conditions (e.g., using R = 0.7 as a final phase), and assure a transition from a transgranular pre-crack to an intergranular stress corrosion crack (e.g., for austenitic materials). Pre-oxidation should be performed for at least several days (preferably two weeks), and the drift in the corrosion potential should be monitored and below about 10 mV/day.

3. Test temperature is most relevant between ≈274C (the BWR recirculation, bottom plenum, and core inlet temperature) and ≈290C (the BWR core exit temperature). Stability should be within ±0.5C, although ±1C may be adequate. The resolution of good dc potential drop systems is often controlled by the stability of the room temperature on power supplies and data acquisition instrumentation.

4. Inlet and outlet solution conductivity must be measured. Outlet conductivity should be <1.5X of the inlet, and is considered a better representation of the conditions to which the test specimen is exposed. Given modern BWR operation, tests in "high purity" water *require* that outlet conductivities <0.1 μS/cm be achieved, and <0.07 μS/cm at the outlet is both desirable and achievable for oxygen concentrations <2ppm. At higher oxygen concentrations (e.g., 42 ppm "oxygen saturated"), even achieving <0.1 μS/cm can be

difficult because of the large contribution of soluble chromate from the chromium-containing autoclave system materials. If intentional impurities are added, then the inlet conductivity (or measured concentration of the impurity) is equally important. Inlet conductivity is an excellent measure of ionic impurities, and can be used to accurately control impurity additions down to 10^{-8} M (Table 1) provided the inlet water is of theoretical purity (e.g., 0.055 μS/cm). It is crucial to identify the species added, since the conductivity of Na_2SO_4 vs. H_2SO_4 at the same sulfate level is very different (the anion activity generally controls SCC response).

The use of Ti parts (especially hot tubing) is helpful in minimizing the contribution of chromate. Operating the water system as a "closed loop" helps minimize organic and bacteria contamination; the autoclave outlet water must, of course, be treated by a well-conditioned mixed bed demineralizer followed up by sub-micron filter before re-use.

While current BWR operation puts severe restrictions on the meaning "pure water", studies of impurity effects require essentially the same level of control. It is not reasonable to study the effects of, e.g., sulfate if other impurities are present at 10 times higher concentration, and perhaps also vary with time. In most tests in "high purity water", the actual outlet conductivity is dramatically higher than the inlet, as a result of:

- chromate release by the autoclave materials;
- decomposition of organic species, resin fines, bacteria, plastics, greases, etc.;
- release of fluorine from Teflon or chloride from reference electrodes;
- in-leakage of carbon dioxide from the air (which raises the conductivity of pure water from 0.055 μS/cm to ≈1 μS/cm)
- other contaminants, such as copper, sulfur, lead, etc.

Table 1. Solution Conductivity vs. Species and Concentration

ppb Cl	0	3	10	30	100	300
μN	0	0.0846	0.282	0.846	2.82	8.46
μS/cm as NaCl	0.0549	0.0656	0.0906	0.162	0.412	1.125
μS/cm as HCl	0.0549	0.0725	0.110	0.367	1.205	3.609
ppb anion	0	3	10	30	100	300
μS/cm as HF	0.0549	0.0905	0.223	0.642	2.130	6.386
μS/cm as H_2SO_4	0.0549	0.0672	0.112	0.277	0.730	2.687
μS/cm as HNO_3	0.0549	0.0636	0.0942	0.215	0.683	2.040

5. Inlet and outlet oxygen and perhaps hydrogen should generally be measured, or there must be a very strong basis for accepting nominal values of oxygen for the inlet (e.g., based on gas mixtures and prior measurements / checks at that lab) and outlet (based on prior outlet measurements for known inlet oxygen in tests under essentially identical conditions - e.g., same autoclave, same flow rate, same conductivity, same autoclave & specimen materials, same oxygen/hydrogen gas mixtures, etc.). Dissolved hydrogen levels are

important because (1) hydrogen affects the corrosion potential whether oxygen is present or not, (2) hydrogen levels even below 100 ppb may have a significant effect on SCC of high nickel alloys below 300 C. In general, the outlet dissolved oxygen should be no less than 25% of the inlet. Sometimes special controls are necessary, such as maintaining low oxygen during heat up and cool down to avoid pitting in carbon and low alloy steels.

6. Corrosion potentials should be measured on the test specimen, since it is widely accepted that potential is a more fundamental parameter in SCC data than oxidant and reductant concentrations. The active tip of the reference electrode should be located close to the CT specimen (e.g., within 25 to 50 mm, and still closer if the specimen is not electrically isolated from the loading linkage. The accuracy and stability during testing of reference electrodes is very important, and should be verified in some (if not all) tests by comparisons with: (1) multiple reference electrodes of the same type; (2) reference electrodes of different types; (3) "blacked" Pt (e.g., in known concentrations of hydrogen-only or oxygen-only solutions); and/or (4) stainless steel in deaerated water of known hydrogen concentration (Pt is always better, but stainless steel should give a stable, known potential in hydrogen-deaerated water). These checks are ideally performed periodically during a test, if possible. Agreement within 25 mV is considered adequate because of current limitations in most reference electrodes, although it is clearly preferable to have an accuracy in corrosion potential measurements of <10 mV.

Controlling potentials via potentiostat is always less desirable because: (1) it is very difficult to correctly compensate for iR drops in high resistivity solutions (and it is difficult to be assured that highly conductive solutions are representative or relevant to BWRs); (2) it is almost impossible to maintain a uniform potential on a complex specimen geometry like a CT specimen (especially in the notch, which represents the majority of the "crack mouth"); and (3) there is a different distribution / separation of the anodes and cathodes on the specimen surface than exist under "free corrosion conditions", and significant and unrealistic shifts in pH can thus be induced by the potentiostat. Polarization can also lead to misleading conclusions when, for instance, cathodic polarization produces reduction of sulfate and sulfite to sulfide, which is known to increase crack growth rates markedly when present at >10 to 30 ppm. In such cases, many investigators are inclined to attribute cracking under cathodic polarization to "hydrogen embrittlement".

The possibility of interference in corrosion potential measurements from the dc potential drop crack length measurement needs to be evaluated. Interference most often results from the use of power supplies and other instrumentation that is not ground isolated, or from poor lead insulation through the autoclave seals. This should always be checked by measuring the corrosion potential while the current for the dc potential system is either reversing or being switched on and off.

7. Flow rate (especially in systems that employ high temperature recirculation pumps) should never be a "compromising" element of the test. High flow rates can retard crack

initiation and crack growth, particularly in carbon & low alloy steel where, e.g., the straight transgranular cracks make these materials susceptible to flushing of the crack tip chemistry, especially when flow is parallel to the crack mouth. These effects of high flow rate are not expected to play a large role in plant components, although the absence of any flow (i.e., in stagnant regions) are know to enhance SCC in plants. Thus, laboratory data under high flow rate conditions should automatically be viewed with caution / concern because the crack tip chemistry is much more readily flushed in three-side-open CT specimens than in the geometry of plant cracks. Because of the path tortuosity (from Lee James' data), flow is somewhat less of a concern where intergranular or interdendritical cracking occurs, but this should not be an automatic basis for dismissing this concern. In turn, the autoclave refresh rate should be high enough to control intentional (dissolved gases and ionic impurities) and minimizing unintentional contributions (usually ionic impurities) to water chemistry. This usually requires that the autoclave volume be refreshed >3 times per hour. The refresh flow rate (and high temperature recirculation rate, if any), autoclave volume, and location of inlet and outlet in the autoclave relative to the CT specimen should be reported.

8. Continuous crack monitoring is essential. Reversed dc potential drop is most commonly used, and good data requires a well-behaved crack extension of > ≈10 - 20X of the crack length resolution, or (for very low growth rates) times >300 - 1000 hours. Good crack length resolution in modern test facilities is a few microns on 1TCT specimens, and the error is typically <10% based on comparison between the *increment* in crack advance in hot water for dc potential drop vs. post-test fractographic measurement. The crack front of the fractured specimen should be confirmed to be relatively straight (varying by <0.05B, ideally <0.01B, where B = the (1-inch) thickness of a 1TCT). If there is a very uneven crack front or the agreement between potential drop and post-test fractography is off by > ≈50%, no post-test correction of crack growth rate data should generally be performed; however, with adequate justification special exceptions may be considered (this is because the crack length corrections cannot sensibly be applied "linearly" over the entire crack growth increment). Large corrections often occur with Alloy 182 weld metal, where much deeper cracking may occur along isolated weld dendrites; in these instances there are sometimes concerns for the contribution of pre-existing weld hot cracking (or perhaps simple corrosion of these boundaries) because there is no other sensible explanation for why cracks should grow faster and faster into a rapidly decreasing K field. In these instances there are many possible correction approaches that can be proposed, although they are never fully justified; if performed, the correction details and a "map" of the fracture surface should be provided.

The minimum acceptable crack increments need to be based partly on microstructural considerations; plastic zone size should also be considered for changes in loading condition. While a wide variety of microstructures are "sampled" across the width of a CT specimen, there are some concerns that small increments might still do a poor job of sampling and therefore exhibit anomalous behavior. This is a larger concern for carbon and low alloy steels, where the MnS distribution can be quite non-homogeneous, although there is some concern for materials like Alloy 182 weld metal, or heavily banded or lightly sensitized

stainless steel or Alloy 600. While there is some concern for increments below grain size dimensions, the best objective way to address this issue is to evaluate from available data whether there is any evidence of *depth-based* (not time-based) variations in the crack growth measurements.

If no growth is observed, or retarded (unusually low) growth rates are suspected, the use of periodic unloading or slow cycling, high load ratio, R – at least as a mechanism for reactivating the crack – is recommended.

Additionally, it should be verified that potential drop does not produce biasing of corrosion potential measurements (or polarization) of the CT specimens. This can be avoided by ground isolated instrumentation, and good electrical insulation of current and potential lead through the autoclave seal and in the autoclave. It can be verified by ensuring that the corrosion potential varies by <<10 mV as the dc current is reversed. It should also be recognized that changes in resistivity primarily of nickel alloys (esp. Alloy 600) occurs in the temperature regime of ≈310 to ≈450 C and can last >1000 h and account for many tenths of mm of *apparent* crack growth.

There is a laboratory that has shown that the use of reversing dc potential drop eliminates "high sulfur" behavior in low alloy steels in their "PWR" water. This is apparently associated with accelerated dissolution of MnS in the crack, and perhaps with enhanced transport of sulfur anions out of the crack. While these observations may be somewhat unique to the specific test conditions (very tight crack, conductive solutions, absence of oxidants, etc.) – and other laboratories have specifically not observed this effect – it highlights the need to ensure that the potential drop technique does not bias the environmental cracking response or other test measurements.

Demonstration of reproducibility of data under "standard conditions" using well defined, e.g., water chemistry conditions is valuable. For example, several changes during a given test to deaerated high purity water (or to, e.g., 2000 ppb O_2 high purity water) provide a valuable mechanism for validating the ability to reproduce a specific growth rate during a single test.

9. "No growth" data should be considered suspect (if not meaningless), except perhaps for very innocuous chemistry conditions (e.g., HWC) where the crack growth rate is, e.g., $<10^{-9}$ mm/s and the test is run for an appropriately long period of time (e.g., >1000 h). "No growth" should always be suspect (perhaps always rejected) for conditions where high growth rates (e.g., $>10^{-8}$ mm/s) have been commonly observed under nominally identical conditions. This is important because there are many reasons why some cracks do not start growing (or even sustain active growth), especially from a transgranular fatigue pre-crack. However, extensive experience has shown that most cracks will exhibit a finite, well-behaved crack growth rate if left long enough and/or if "encouraged" to grow (e.g., by short term exposure to very mild cyclic loading, which is recommended whenever there is reason

to suspect that the growth rates are too low). While we might ultimately want to know the fraction of cracks which start and continue to grow as a function of test condition, we first need to be able to achieve reproducible, consistent crack growth data from test-to-test and lab-to-lab. It should be recognized that there is a concern for the effects of transient loading on carbon and low alloy steels (more than ductile austenitic alloys), so special caution is recommended when using periodic unloading on these materials.

10. Material characteristics should be known, such as composition, crack orientation, yield strength/hardness, heat treatment conditions ("mill anneal" vs. lab anneal, sensitization, post weld vessel heat treatment, etc.), carbide/phase distribution (especially for nickel alloys and stainless steels), and "derived" parameters (such as N-bar). Composition (e.g., S, P, and some other elements) and welding conditions (heat inputs, etc.) are also valuable in discerning whether Alloy 182 weld metal is likely to have experienced hot cracking, since distinguishing hot cracking from SCC is essential even though both may contribute to through-wall penetration. Evaluation of other characteristics (e.g., degree of sensitization in stainless steels or nickel alloys) may need to be performed to adequately establish the nature of the material being tested. The nature and degree of sensitization is not well described or quantified in most studies. Electrochemical potentiokinetic repassivation (EPR) is a weak measure of sensitization, because if responds mostly to the width of the Cr profile (below about 15%) rather than the depth. For "blunt notch" CT tests, or other tests where cracks initiate from smooth surfaces, surface condition is extreme important to quantify and reproduce. Localized cold work, phase transformation, and sensitization (even below 400C in a few hours if cold work is present) are difficult to avoid on smooth surfaces of some materials.

11. Individual crack length vs. time response (along with conductivity (especially outlet), corrosion potential on the SCC specimen (and dissolved oxygen, especially outlet), and test temperature) should always be reported to ensure that data (a) meets resolution criteria, (b) meets "well behaved" criteria, (c) any selection of isolated portions of the data for determining crack growth rate are justified, and (d) there are no other anomalies of concern in the crack length or test parameters vs. time.

12. Accelerated testing and interpretation needs to be considered very carefully during test design through to data analysis. The use of highly conductive and/or aggressive solutions, potentiostatically controlled potentials, and other environmental "accelerants" must be viewed with great caution and preferable totally avoided to help ensure relevance of the test results to BWR conditions. In addition to serious anomalies in the data, there are complex interpretational issues, because the observed effect of any variables is often high affected by the values of all other variables in environment cracking. Similar concerns exist for "mechanical acceleration", since the "factor of improvement" observed, e.g., for changes in corrosion potential, water purity, or material characteristic will change with stress intensity. Of course, the interpretation of slow strain rate testing (e.g., what time

duration should be used to convert a crack length to a crack growth rate?) can also be complex.

* It is recognized that in most distributions (e.g., log-normal) the scatter (range) in the data is statistically related to both the standard deviation and the number of measurements (sample size). However, there is no guarantee that the crack growth measurements in hot water do obey a, e.g., log-normal distribution, and the scatter is often a good representation of the severity / extent of experimental problems and test anomalies.

Appendix B - Crack Growth Rate Data From All Laboratories

CONSTANT LOAD COMPARISON - ALL DATA 1E-10 = ZERO

Segment	Start h	ΔTime h	Growth mm	CG Rate mm/s	a/t Rate mm/s	a/W	K, MPa√m	O_2 ppb	SS mV_{she}	Pt mV_{she}	Outlet µS/cm	Constant Load	Changes / comments
ABB 39-2	195	145	0.05	1.40E-07	9.6E-08	0.481	33.2	2000	190		0.25	Y	
ABB 39-3	340	140	0	1.00E-10	0	0.481	33.2	500	170		0.15	Y	
ABB 39-4	480	262	0	1.00E-10	0	0.481	33.2	200	150		0.15	Y	
ABB 39-6	868	292	0	1.00E-10	0	0.492	33.5	500	165		0.33	Y	25 ppb SO4
ABB 39-8a	1240	340	0.026	2.10E-08	2.1E-08	0.494	33.5	500	165		0.33	Y	25 ppb SO4
ABB 39-8b	1580	420	0.33	2.29E-07	2.2E-07	0.498	33.8	500	165		0.33	Y	25 ppb SO4
ABB 43-2	195	145	0	1.00E-10	0	0.465	31.9	2000	190		0.25	Y	
ABB 43-3	340	140	0	1.00E-10	0	0.465	31.9	500	170		0.15	Y	
ABB 43-4	480	262	0	1.00E-10	0	0.465	31.9	200	150		0.15	Y	
ABB 43-6	868	292	0	1.00E-10	0	0.476	31.9	500	165		0.33	Y	25 ppb SO4
ABB 43-8	1240	760	0	1.00E-10	0	0.476	31.9	500	165		0.33	Y	25 ppb SO4
ABB 32-2	195	145	0.05	9.17E-08	9.6E-08	0.468	32.4	2000	190		0.25	Y	
ABB 32-3	340	140	0	1.00E-10	0	0.47	32.4	500	170		0.15	Y	
ABB 32-4	480	262	0	1.00E-10	0	0.47	32.4	200	150		0.15	Y	
ABB 32-6	868	292	0	1.00E-10	0	0.482	32.8	500	165		0.33	Y	25 ppb SO4
ABB 32-8	1240	760	0.19	7.64E-08	6.9E-08	0.486	32.8	500	165		0.33	Y	25 ppb SO4
ABB 37-5a	868	232	0	1.00E-10	0	0.512	33	500	165		0.33	Y	25 ppb SO4
ABB 37-5b	1100	570	0.16	6.25E-08	7.8E-08	0.523	33	500	165		0.33	Y	25 ppb SO4
ABB 44-5	868	802	0	1.00E-10	0	0.468	27.5	500	165		0.33	Y	25 ppb SO4
ABB 28-5	868	802	0.14	5.56E-08	4.8E-08	0.476	29.3	500	165		0.33	Y	25 ppb SO4
ABB 27-2	195	145	1.25	1.88E-06	2.4E-06	0.5	41	2000	190		0.25	Y	
ABB 27-3	340	140	0.03	4.60E-08	6E-08	0.5	41.5	500	170		0.15	Y	
ABB 27-4	480	262	0.04	4.60E-08	4.2E-08	0.5	41.5	200	150		0.15	Y	
ABB 27-7	868	1132	3.35	1.12E-06	8.2E-07	0.56	51.3	500	165		0.33	Y	25 ppb SO4, High K
ABB 33-2	195	145	0.43	7.22E-07	8.24E-07	0.48	39.1	2000	190		0.35	Y	
ABB 33-3	340	140	0.22	5.00E-07	4.4E-07	0.492	39.9	500	150		0.15	Y	
ABB 33-4	480	262	0.27	2.36E-07	2.9E-07	0.492	40.2	200	150		0.15	Y	
ABB 33-7a	868	712	0.65	5.15E-07	2.5E-07	0.54	45.8	500	165		0.33	Y	25 ppb SO4
ABB 33-7b	1580	420	2.2	1.66E-06	1.5E-06	0.54	45.8	500	165		0.33	Y	25 ppb SO4, High K
ABB 41-2	195	145	0.55	9.27E-07	1.05E-06	0.48	38.9	2000	190		0.35	Y	
ABB 41-3	340	140	0.08	1.35E-07	1.6E-07	0.492	39.4	500	150		0.15	Y	
ABB 41-4	480	262	0.11	8.47E-08	1.2E-07	0.492	39.5	200	150		0.15	Y	
ABB 41-7	868	1132	1.25	5.54E-07	3.1E-07	0.524	40.9	500	165		0.33	Y	25 ppb SO4

ABB 34-4	868	1132	0.66	1.24E-07	1.6E-07	0.47	32.9	500	165		0.33	Y	25 ppb SO4
ABB 31-4	868	1132	0.28	9.53E-08	6.9E-08	0.467	31.6	500	165		0.33	Y	25 ppb SO4
ABB 38-4a	868	532	0.31	1.99E-07	1.6E-07	0.47	32.2	500	165		0.33	Y	25 ppb SO4
ABB 38-4b	1400	600	0.18	9.72E-08	8.3E-08	0.476	32.2	500	165		0.33	Y	25 ppb SO4
AEA #1-2	359	51	0.011	5.00E-08	5.99E-08	0.4396	30.8	181	65		0.09	Y	
AEA #1-3	410	122	0	1.00E-10	0	0.4598	30.8	169	66		0.087	Y	
AEA #1-5	597	129	0.019	4.00E-08	4.09E-08	0.4402	30.9	227	100		0.084	Y	Pump restarted. Stable conditions at 640 hrs
AEA #1-6	728	144	0.008	2.00E-08	1.54E-08	0.4404	30.9	192	103		0.08	Y	
AEA #1-7	870	228	0.003	3.00E-09	3.65E-09	0.4405	30.9	182	96		0.094	Y	
AEA #2-1	0	514	0	1.00E-10	0	0.5734	33.7	494	63		0.275	Y	25ppb H2SO4
AEA #2-14	1300	150	0.06	1.10E-07	1.11E-07	0.617	42.1	520	33		0.257	Y	25ppb H2SO4, Rate slowed, then ↑ without changes
AEA #2-14b		341	0.03	2.00E-08	2.44E-08	0.617	42.1	520	33		0.257	Y	25ppb H2SO4, Rate slowed, then ↑ without changes
AEA #2-14c		450	0.2	1.30E-07	1.23E-07	0.617	42.1	520	33		0.257	Y	25ppb H2SO4, Rate slowed, then ↑ without changes
GE #1-3	310	1003.7	0	1.00E-10	0	0.4518	30.14	200	120	300	0.065	Y	
GE #1-7	1550	171.7	0.0117	4.70E-09	1.9E-08	0.4557	30.47	200	134	293	0.064	Y	
GE #1-10	2084.4	39.8	0.0075	1.00E-08	5.2E-08	0.456	30.5	200	139	291	0.063	Y	Too short to get growth rate
GE #1-14	2419	141.1	0.175	4.05E-07	3.4E-07	0.4574	30.62	2000	207	321	0.07	Y	
GE #1-15	2560	98.3	0.097	2.57E-07	2.7E-07	0.461	30.94	500	176	303	0.065	Y	
GE #1-16	2658	64.3	0.04	1.76E-07	1.7E-07	0.4628	31.1	325	164	297	0.064	Y	
GE #1-17a	2722	218.2	0.061	1.04E-07	7.8E-08	0.4636	31.17	200	149	289	0.064	Y	For #947-983, then slows down
GE #1-17b	2722	218.2	0.061	4.64E-08	7.8E-08	0.4636	31.17	200	149	289	0.064	Y	
GE #1-18	2940	119.1	0.029	8.80E-08	6.8E-08	0.4648	31.28	200	149	289	0.08	Y	After T/dcpd perturbation from flow
GE #1-19	3060	216.9	0.13	1.75E-07	1.7E-07	0.475	31.3	200	153	291	0.17	Y	Bypass demineralizers
GE #1-20	3276	129.2	0.06	4.20E-08	1.3E-07	0.4679	31.56	200	155	291	0.066	Y	Rate dropped only after ~100h
GE #2-8	168.8	604.8	0.007	1.00E-10	3.2E-09	0.5168	29.9	1960	192	322	0.06	Y	30 MPa/m constant load
GE #2-11	939.3	91.4	0	1.00E-10	0	0.5178	29.98	1980	202	317	0.059	Y	
GE #2-14	1196.3	121.7	0	1.00E-10	0	0.5185	30.04	1950	206	315	0.062	Y	
GE #2-19	1691	74.4	0.049	1.82E-07	1.8E-07	0.5212	30.33	2000	225	299	0.39	Y	
GE #2-20	1765.4	101.5	0.053	1.41E-07	1.5E-07	0.5222	30.4	2000	217	310	0.061	Y	
GE #2-21	1866.9	118.5	0.022	2.60E-08	5.2E-08	0.5232	30.5	500	187	292	0.06	Y	
GE #2-22a	1985.4	412.5	0.206	2.80E-07	1.4E-07	0.5236	30.54	500	190	298	0.241	Y	25 ppb H2SO4, #855-871
GE #2-22b	2397.9	470.4	0.096	5.42E-08	5.7E-08	0.5276	30.94	500	191	297	0.242	Y	Slowed down vs. time
GE #2-23	2868.3	151.7	0.032	3.63E-08	5.9E-08	0.5298	31.16	500	191	297	0.243	Y	After power interruptio
GE #3-7	94.4	332.3	0.01	1.00E-10	8.4E-09	0.4706	29.9	500	150	315	0.243	Y	30 MPa/m constant

GE #3-12	670.1	574.6	0.249	1.20E-07	1.2E-07	0.4732	30.12	500	180	305	0.241	Y	30 MPa/m constant
GE #3-13	1244.7	191.9	0.074	1.00E-07	1.1E-07	0.478	30.55	2000	207	314	0.061	Y	30 MPa/m constant, pure H2O
GE #3-14	1436.6	114.9	0.072	3.00E-08	1.7E-07	0.4806	30.79	2000	208	310	0.061	Y	30 MPa/m constant
GE #3-16	1598.9	30.4	0.0025	2.00E-08	2.3E-08	0.4819	30.91	2000	208	308	0.061	Y	30 (34.2) MPa/m constant
GE #3-21	1964.5	68.6	0.018	2.64E-07	7.3E-08	0.4847	31.17	2000	211	310	0.061	Y	34.2 MPa/m constant
Stud #1-1	0	1100	0.006	1.40E-09	1.52E-09	0.439	29.1	200	0		0.08	Y	-150 to +10 mVshe for CuO
Stud #2-2	1300	100	0.1	3.10E-07	2.8E-07	0.447	29.8	2000	90		0.18	Y	
Stud #2-4	2750	500	0.23	1.40E-07	1.3E-07	0.506	30.1	500	20		0.27	Y	25ppb H2SO4
Stud #2-5	3250	200	0.01	1.70E-08	1.4E-08	0.508	30.2	500	20		0.27	Y	After un/reload, 25ppb H2SO4
Stud #3-1	50	350	0.26	1.30E-07	2.1E-07	0.49	33.8	500	-20		0.24	Y	25ppb H2SO4
Stud #3-2	400	600	0.8	3.60E-07	3.7E-07	0.505	35	500	-20		0.24	Y	25ppb H2SO4
VTT #1-1	8	160	0	9.20E-09	0	0.442	29.1	200	60	230	0.2	Y	
VTT #1-3	239	1008	0	5.00E-10	0	0.454	29.8	200	100	260	0.1	Y	
VTT #1-5	1515	359	0	1.00E-10	0	0.456	29.8	200	100	260	0.08	Y	
VTT #1-8	2040	198	0.01	1.20E-08	1.40E-08	0.456	31	400	120	270	0.25	Y	Demin bypass
VTT #1-9	2238	150	0.09	2.20E-07	1.67E-07	0.456	30	600	136	276	0.2	Y	Demin bypass
VTT #1-10	2388	182	0.04	8.00E-08	6.11E-08	0.460	30	600	136	276	0.2	Y	Demin bypass
VTT #2-5	480	124	0	1.00E-10	0	0.498	29.5	2000	167	-50	0.32	Y	
VTT #2-8	960	318	0.03	1.00E-08	2.62E-08	0.500	29.5	2000	180	230	0.2	Y	
VTT #2-10	1463	656	0.01	1.00E-09	4.23E-09	0.506	29.8	2000	182	240	0.17	Y	
VTT #2-13	2355	285	0.01	3.70E-09	9.75E-09	0.511	30	2000	182	250	0.15	Y	
VTT #2-19	3051	803	0.1	3.10E-08	3.46E-08	0.525	29.9	500	127	242	0.28	Y	
VTT #3-7	220	67	0	1.00E-10	0	0.536	26.7	500	120	-65	0.43	Y	25ppb H2SO4
VTT #3-14	526	602	0.01	5.40E-10	4.61E-09	0.548	29.2	500	130	-50	0.36	Y	25ppb H2SO4
VTT #3-16	1490	191	0.01	6.20E-09	1.45E-08	0.551	29.5	500	150	265	0.3	Y	25ppb H2SO4
CYCLIC LOAD (e.g., <0.001 Hz) COMPARISON - ALL DATA													
ABB 39-1	68	127	0.13	2.50E-07	2.84E-07	0.48	33.2	2000	190		0.35	N	R=0.7, 0.001 Hz
ABB 39-7	1160	80	0.07	2.79E-07	2.4E-07	0.494	33.5	500	165		0.33	N	R=0.7, 0.001 Hz, 25 ppb SO4
ABB 43-1	68	127	0.09	1.31E-07	2E-07	0.464	31.9	2000	190		0.35	N	R=0.7, 0.001 Hz
ABB 43-7	1160	80	0.076	2.07E-07	2.6E-07	0.476	31.9	500	165		0.33	N	R=0.7, 0.001 Hz, 25 ppb SO4
ABB 32-1	68	127	0.18	4.11E-07	3.94E-07	0.466	32.3	2000	190		0.35	N	R=0.7, 0.001 Hz
ABB 32-7	1160	80	0.12	4.14E-07	4.2E-07	0.482	32.8	500	165		0.33	N	R=0.7, 0.001 Hz, 25 ppb SO4
ABB 37-1	68	272	0.02	1.40E-08	2.04E-08	0.488	28.7	2000	190		0.35	N	R=0.7, 0.001 Hz
ABB 37-2	340	140	0.019	1.40E-08	3.8E-08	0.488	28.7	500	170		0.15	N	R=0.7, 0.001 Hz
ABB 37-3	480	262	0.051	1.40E-08	5.4E-08	0.488	28.7	200	150		0.15	N	R=0.7, 0.001 Hz
ABB 44-1	68	272	0	1.00E-10	0	0.466	27.5	2000	190		0.35	N	R=0.7, 0.001 Hz
ABB 44-2	340	140	0	1.00E-10	0	0.466	27.5	500	170		0.15	N	R=0.7, 0.001 Hz

ABB 44-3	480	262	0	1.00E-10	0	0.466	27.5	200	150		0.15	N	R=0.7, 0.001 Hz
ABB 28-1	68	272	0.03	1.00E-10	3.06E-08	0.47	27.4	2000	190		0.35	N	R=0.7, 0.001 Hz
ABB 28-2	340	140	0	1.00E-10	0	0.47	27.4	500	170		0.15	N	R=0.7, 0.001 Hz
ABB 28-3	480	262	0	1.00E-10	0	0.47	27.4	200	150		0.15	N	R=0.7, 0.001 Hz
ABB 27-1	68	127	0.25	1.88E-06	5.47E-07	0.49	41	2000	190		0.35	N	R=0.7, 0.001 Hz
ABB 27-5	742	118	0.34	9.67E-07	8.00E-07	0.49	44.8	2000	190		0.35	N	R=0.7, 0.001 Hz
ABB 33-1	68	127	0.2	9.00E-07	4.37E-07	0.48	39.1	2000	190		0.35	N	R=0.7, 0.001 Hz
ABB 33-5	742	118	0.35	1.05E-06	8.24E-07	0.48	41	2000	190		0.35	N	R=0.7, 0.001 Hz
ABB 41-1	68	127	0.25	9.27E-07	5.47E-07	0.48	38.9	2000	190		0.35	N	R=0.7, 0.001 Hz
ABB 41-5	742	118	0.25	9.27E-07	5.89E-07	0.48	39.6	2000	190		0.35	N	R=0.7, 0.001 Hz
ABB 34-1	68	272	0.015	1.94E-08	1.53E-08	0.462	31.6	2000	170		0.35	N	R=0.62, 10X/day
ABB 34-2	340	140	0.01	1.94E-08	1.98E-08	0.462	31.7	500	170		0.35	N	R=0.62, 10X/day
ABB 34-3	480	388	0.03	1.94E-08	2.15E-08	0.462	31.7	200	170		0.35	N	R=0.62, 10X/day
ABB 31-1	68	272	0.01	2.00E-08	1.02E-08	0.463	31	2000	170		0.35	N	R=0.62, 10X/day
ABB 31-2	340	140	0.03	5.56E-08	5.95E-08	0.463	31	500	170		0.35	N	R=0.62, 10X/day
ABB 31-3	480	388	0.03	2.00E-08	2.15E-08	0.463	31.1	200	170		0.35	N	R=0.62, 10X/day
ABB 38-1	68	272	0.02	2.00E-08	2.04E-08	0.464	31	2000	170		0.35	N	R=0.62, 10X/day
ABB 38-2	340	140	0.015	2.50E-08	2.98E-08	0.464	31	500	170		0.35	N	R=0.62, 10X/day
ABB 38-3	480	288	0.03	2.50E-08	2.89E-08	0.464	31	200	170		0.35	N	R=0.62, 10X/day
AEA #2-2	514	138	0	1.00E-10	0	0.5734	33.7	489	38		0.266	N	R=0.7, 0.001 Hz, 25ppb H2SO4
GE #1-4	1314	49.1	0.046	2.60E-07	2.6E-07	0.4518	30.14	200	130	294	0.064	N	R=0.7, 0.001 Hz
GE #1-5	1363	70.7	0.013	5.00E-08	5.1E-08	0.4528	30.23	200	131	293	0.064	N	R=0.7, 0.0001 Hz
GE #1-6	1434	116.5	0.13	3.22E-07	3.1E-07	0.453	30.24	200	132	293	0.064	N	R=0.7, 0.001 Hz
GE #1-8	1722	217.8	0.002	2.00E-09	2.6E-09	0.4557	30.47	200	137	292	0.064	N	R=0.7, 24h rise - 3 cycles
GE #1-9	1940	144.1	0.01	2.13E-08	1.9E-08	0.4557	30.47	200	139	291	0.063	N	R=0.7, 9h rise continuous
GE #1-12	2317	70.6	0.053	2.34E-07	2.1E-07	0.457	30.5	2000	204	322	0.071	N	R=0.7, 0.9h rise continuous
GE #1-13	2388	30.7	0.016	2.00E-07	1.4E-07	0.4572	30.6	2000	205	321	0.071	N	R=0.8, 0.9h rise continuous
GE #2-9	773.6	94.8	0.038	1.04E-07	1.1E-07	0.5171	29.91	2000	199	322	0.059	N	R=0.7, 0.001 Hz
GE #2-10	868.4	70.9	0.004	1.60E-08	1.6E-08	0.5178	29.98	2000	202	320	0.059	N	R=0.7, 9h rise
GE #2-12	1030.7	77.7	0.005	1.00E-10	1.8E-08	0.5178	29.98	2000	205	319	0.059	N	R=0.7, 0.001 Hz for 1 day
GE #2-13	1108.4	87.9	0.032	1.33E-07	1E-07	0.5178	29.98	2000	205	318	0.061	N	R=0.7, 0.001 Hz
GE #2-15	1318	30.4	0.017	1.89E-07	1.6E-07	0.5185	30.04	2000	206	306	0.35	N	R=0.7, 0.001 Hz, bypass demin
GE #2-16	1348.4	156.7	0.044	1.00E-07	7.8E-08	0.5189	30.08	2000	217	301	0.35	N	R=0.7, 0.0001 Hz
GE #2-17	1505.1	121.5	0.032	7.20E-08	7.3E-08	0.5198	30.17	2000	222	296	0.46	N	R=0.7, 0.0001 Hz + 9000s hold
GE #2-18	1626.6	64.4	0.039	1.66E-07	1.7E-07	0.5204	30.23	2000	224	298	0.42	N	R=0.7, 0.0001 Hz + 76,400s hold
GE #3 -8	426.7	74.4	0	1.00E-10	0	0.4706	29.9	500	154	315	0.243	N	R=0.7, 1h dn 9h up
GE #3 -10	521.4	74.4	0.04	1.30E-07	1.5E-07	0.4718	30	500	160	310	0.242	N	R=0.7, 0.001 Hz
GE #3 -11	595.8	74.3	0.038	1.24E-07	1.4E-07	0.4726	30.07	500	164	310	0.242	N	R=0.7, 0.001 Hz + 900s hold
GE #3 -15	1551.5	47.4	0.052	3.00E-07	3E-07	0.481	30.83	2000	209	310	0.061	N	R=0.7, 0.001 Hz + 9000s hold

GE #3 -17	1629.3	145.4	0.017	3.00E-08	3.2E-08	0.482	30.92	2000	211	315	0.061	N	R=0.7, 0.001 Hz +9000s hold
GE #3 -18	1774.7	87.9	0.089	1.77E-07	2.8E-07	0.4823	31	2000	211	309	0.061	N	R=0.7, 0.001 Hz +9000s hold
GE #3 -19	1862.6	50.7	0.004	1.00E-08	2.2E-08	0.4837	31.03	2000	211	309	0.061	N	R=0.7, 0.001 Hz, 1/day
GE #3 -20	1913.3	51.2	0.071	1.67E-07	3.9E-07	0.4841	31.11	2000	211	309	0.061	N	R=0.7, 0.001 Hz, 1/day
Stud #2-3	2500	250	0.2	3.60E-07	2.2E-07	0.505	30.1	500	20		0.27	N	R=0.7, 0.001 Hz, 25ppb H2SO4
Stud #2-1	860	110	0.1	2.50E-07	2.5E-07	0.4438	29.7	2000	90		0.18	N	R=0.7, 0.001 Hz
VTT #1-4	1248	267	0.11	1.20E-07	1.14E-07	0.454	29.8	200	100	260	0.09	N	R=0.8, 0.01 Hz
VTT #1-6	1875	72	0.01	2.80E-09	3.86E-08	0.456	30	200	100	260	0.08	N	R=0.8, 0.01 Hz
VTT #1-7	1947	93	0.1	2.90E-07	2.99E-07	0.456	30	200	120	265	0.08	N	R=0.7, 0.001 Hz
VTT #2-6	604	217	0.06	1.70E-07	7.68E-08	0.498	30	2000	175	50	0.28	N	R=0.7, 0.001 Hz
VTT #2-7	821	130	0.1	2.10E-07	2.14E-07	0.499	30	2000	180	230	0.23	N	R=0.7, 0.001 Hz
VTT #2-9	1278	185	0.25	3.20E-07	3.75E-07	0.501	30	2000	180	235	0.18	N	R=0.7, 0.001 Hz
VTT #2-12	2256	99	0.03	1.30E-07	8.42E-08	0.511	30	2000	182	250	0.18	N	R=0.7, 0.001 Hz
VTT #2-15	2687	144	0.18	3.20E-07	3.47E-07	0.513	30	500	190	270	0.145	N	R=0.7, 0.001 Hz
VTT #3-15	1128	362	0.14	8.20E-08	1.07E-07	0.548	30	500	140	0	0.31	N	R=0.7, 0.001 Hz, 25ppb H2SO4

SKi

STATENS KÄRNKRAFTINSPEKTION
Swedish Nuclear Power Inspectorate

Postadress/Postal address	Telefon/Telephone	Telefax	Telex
SKI SE-106 58 Stockholm	Nat 08-698 84 00 Int +46 8 698 84 00	Nat 08-661 90 86 Int +46 8 661 90 86	11961 SWEATOM S